

Photocrosslinkable Polyimide and Poly(Imide Siloxane) Homo-
and Copolymers: Synthesis and Characterization

by

Eric S. Moyer

Dissertation submitted to the Faculty of the Virginia
Polytechnic Institute and State University in partial
fulfillment of the requirements for the degree of

Doctor in Philosophy

in

Chemistry

Approved:

~~_____~~
J.E. McGrath, Chairman

~~_____~~
L.T. Taylor, Co-chairman

~~_____~~
H.M. Bell

~~_____~~
J.G. Dillard

~~_____~~
J.R. Wolfe

November, 1989

Blacksburg, Virginia

**Photocrosslinkable Polyimide and Poly(Imide Siloxane) Homo-
and Copolymers: Synthesis and Characterization**

by

Eric S. Moyer

Committee Chairman: Dr. J.E. McGrath

Department of Chemistry

(ABSTRACT)

Novel, high molecular weight, high glass transition temperature, photocrosslinkable polyimide and poly(imide siloxane) homo- and segmented copolymers were prepared and characterized. The polyimides were synthesized by the classical two step method of first preparing soluble poly(amic acid) prepolymers by the reaction of various aromatic dianhydrides with aromatic diamines. The siloxane modified copolymers were synthesized by reacting single or mixed components of the aromatic dianhydrides with a mixture of aromatic amine and bis(3-aminopropyl) end blocked polydimethyl siloxane oligomers in a cosolvent system of tetrahydrofuran and N-methyl-2-pyrrolidinone. These difunctional aminopropyl terminated siloxane oligomers were prepared through an anionic ring opening equilibration polymerization of octamethylcyclotetrasiloxane with bis(3-aminopropyl) tetramethyldisiloxane in the presence of siloxanolate catalyst.

Soluble fully imidized polyimides were obtained by use of a solution imidization procedure which utilized a cosolvent system of N-methyl-2-pyrrolidinone and N-cyclohexyl-2-pyrrolidone at temperatures of approximately 170°C. The fully

imidized polyimides were soluble in a variety of solvents.

The homo- and copolymers have been characterized for compositional analysis by FT-IR and proton NMR spectroscopy. All polymers were characterized for their thermal properties by differential scanning calorimetry, dynamic mechanical thermal analysis and thermogravimetric analysis. All homo- and copolymers possessed excellent thermal characteristics and good mechanical properties.

The photosensitive properties of the polyimide and poly(imide siloxane) homo- and copolymers were investigated at the UV wavelengths of 313nm and 365nm. The photosensitivities were found to depend on both the amount of benzylic methyl substituted diamine incorporated into the polyimide backbone, and the amount of aromatic ketone concentration. High concentrations of fluorinated (6F) dianhydride were also desirable. Incorporation of the polydimethylsiloxane segments into the polyimide decreased the optical density without decreasing the photosensitivity and therefore desirably allowed thicker films to be crosslinked at lower exposure doses. The adhesion of the siloxane modified polyimides to the silicon wafers was increased with significantly increasing siloxane content and at 20 weight percent, eliminated the need for conventional coupling agents.

Dedication

The hours of research and work in preparing this dissertation are dedicated to my wife, _____, to my parents, _____ and to my brothers, _____ and _____ for their love and support throughout the entire pursuit of my education.

"Whatever you do, work at it with all your heart, as working for the Lord, not for men, since you know that you will receive an inheritance from the Lord as a reward. It is the Lord Christ you are serving."

Colossians 3:23 & 24 NIV

Acknowledgements

I would like to thank my advisor Dr. James E. McGrath for his guidance, support and encouragement, and for the opportunity to work in his research group. I would also like to extend my thanks to Dr. Larry T. Taylor for serving as co-chairman, and to my other committee members, Dr. H.M. Bell, Dr. J.G. Dillard, and Dr. J.F. Wolfe for serving on my committee and for helpful technical discussions and suggestions.

I would like to extend my sincere appreciation to _____ and _____ from the IBM-Thomas J. Watson Research Center for support of this project and for allowing me the opportunity to spend approximately three months at the IBM-Research Center to characterize the photosensitive polyimides for microelectronic applications.

I also would like to extend thanks to _____ for thermal analysis, _____ for intrinsic viscosity data, _____ for all of his help with the XPS surface analysis, and my fellow Graduate students for technical discussions and support. I would like to extend a special thanks to _____ for typing this dissertation.

Finally, I would like to thank my wife, _____, for many helpful technical discussions, and for her love, support, encouragement, patience, and prayers throughout graduate school; and my parents, _____ and _____, for providing me the valuable opportunity to pursue my education,

and for their love, understanding, encouragement and sacrifice.

Table of Contents

Chapter	Page
1.0 Introduction	1
2.0 Literature Review	4
2.1 Introduction	4
2.2 Photolithography	5
2.3 Polyimide use in Integrated Circuit Fabrication	9
2.4 Polyimide Properties for Electronic Applications	15
2.5 Polyimide Synthesis (Two-step Polycondensation)	22
2.5.1 Polyamic acid Synthesis	22
2.5.2 Imidization of Poly(amic acid)	29
2.6 Polyimide Patterning (Etching)	38
2.6.1 Wet Etching	38
2.6.2 Dry Etching	43
2.7 Photoimageable Polyimides	46
2.7.1 Photosensitive Poly(amic acids)	46
2.7.2 Photosensitive Soluble Polyimides	63
3.0 Experimental	85
3.1 Purification of Reagents and Solvents	85
3.1.1 Solvent Purification	85
3.1.2 Monomer Purification	85
3.2 Synthesis of monomers and amine terminated siloxane oligomers	92
3.2.1 Synthesis of 1,3-Bis (4-fluorobenzoyl) benzene	92
3.2.2 Synthesis of 1,3-Bis (3-aminophenoxy- 4'-benzoyl) benzene	92
3.2.3 Aminopropyl-terminated polydimethyl siloxane oligomers	94

Chapter	Page
3.3	Synthesis of high molecular weight polyimide homo- and copolymers 95
3.3.1	High molecular weight poly(amic acid) homopolymers 96
3.3.2	High molecular weight poly(amic acid) copolymers 98
3.3.2.1	Poly(amic acid) copolymers by varying the mole ratio of aromatic diamines 99
3.3.2.2	Poly(amic acid) copolymers by varying the mole ratio of aromatic dianhydrides 99
3.3.3	High temperature poly(amic acid) synthesis 100
3.3.4	Poly(amic acid siloxane) segmented copolymers 102
3.3.5	Imidization of poly(amic acid) prepolymers 104
3.3.5.1	Bulk thermal imidization 104
3.3.5.2	Solution imidization 105
3.4	Characterization of polymers and monomers 108
3.4.1	Titration of aminopropyl terminated siloxane oligomers 108
3.4.2	Intrinsic viscosities 109
3.4.3	Fourier Transform Infrared Spectroscopy 109
3.4.4	Proton Nuclear Magnetic Resonance 110
3.4.5	Ultraviolet and Visible Spectrophotometry 110
3.4.6	Profilometer film thickness measurements 111
3.4.7	Differential Scanning Calorimetry 111
3.4.8	Dynamic Mechanical Thermal Analysis 111
3.4.9	Thermogravimetric Analysis 112
3.4.10	X-Ray Photoelectron Spectroscopy 112
3.4.11	Photosensitivity and Contrast 113
4.0	Results and Discussions 118
4.1	Introduction 118
4.2	Synthesis of photoreactive polyimide homo- and copolymers 114
4.3	Characterization of the BTDA Dianhydride, and Bis-P and TMBis-P Diamine Based Polyimide Homo- and Copolymers 128

Chapter	Page
4.3.1	Intrinsic Viscosities and Glass Transition Temperatures 128
4.3.2	Polymer Solubility 132
4.3.3	Thermo-Oxidative Stability 134
4.3.4	Photosensitive Properties 137
4.4	Characterization of the BTDA Dianhydride and TMPDA and DKDEDA Diamine Based Polyimide Homo- and Copolymers 148
4.4.1	Synthesis of 1,3-Bis(3-Aminophenoxy-4' Benzoyl) Benzene (DKDEDA) 148
4.4.2	Intrinsic Viscosities and Glass Transition Temperatures 156
4.4.3	Polymer Solubility 162
4.4.4	Thermo-Oxidative Stability 162
4.4.5	Photosensitive Properties 164
4.5	Characterization of BTDA and 6FDA Dianhydride and TMPDA Diamine Based Polyimide Homo- and Copolymers 169
4.5.1	Intrinsic viscosities and glass transition temperatures 169
4.5.2	Polymer Solubility 173
4.5.3	Thermo-Oxidative Stability 175
4.5.4	Photosensitive Properties 177
4.6	Synthesis and Characterization of Poly(imide siloxane) Segmented Copolymers 185
4.6.1	Synthesis of Aminopropyl polydimethyl siloxane Oligomers 185
4.6.2	Synthesis of Poly(imide siloxane) Copolymers 187
4.7	Characterization of Poly(imide siloxane) copolymers 197
4.7.1	Intrinsic Viscosities and Glass Transition Temperatures 197
4.7.2	Polymer Solubility 202
4.7.3	Thermo-Oxidative Stability 202
4.7.4	XPS Surface Analysis 204
4.7.5	Photosensitive Properties 213
4.8	FT-IR Study of the Extent of Photocrosslinking 220

Chapter	Page
5.0 Conclusions	227
6.0 References	231
7.0 Vita	242

List of Schemes

Scheme		Page
2.5.1.1	Chemical structure of a polyimide repeat unit	22
2.5.1.2	Polycondensation reaction between an aromatic dianhydride and an aromatic diamine	25
2.5.1.3	Structure of DuPont's Kapton	24
2.5.1.4	Structure of Hitachi's PIQ	28
2.5.2.1	Imidization of Poly(amic acid)	30
2.5.2.2	Proposed Mechanism of Imidization	32
2.7.1.1	Preparation of the photoreactive polyimide precursor	48
2.7.1.2	Chemical principle and processing steps for direct production of polyimide relief patterns	50
2.7.1.3	Preparation of Merrem's photoreactive poly(amic acid)	53
2.7.1.4	Synthesis of photosensitive monomer's	58
2.7.1.5	Synthesis of photopositive poly(amic acid)	59
2.7.1.6	Schematic representation of 0-nitrobenzyl ester photorearrangement	62
2.7.2.1	Schematic representation of the formation triplet state of benzophenone upon UV irradiation	68
2.7.2.2	Schematic representation of a hydrogen abstraction reaction of the 1,2-diradical benzophenone from a hydrogen-donor molecule	69
2.7.2.3	Photocrosslinking reaction of tetramethyl bis-A polyarylene ether ketone	71
2.7.2.4	Synthesis of photoreactive fully imidized polyimide with pendent methacrylic ester groups	76
2.7.2.5	Synthesis of photopositive polyimide containing triarylsulfonium salts	80

Scheme		Page
2.7.2.6	Schematic representation of C-S bond cleavage during photolysis	82
4.2.1	Synthetic Process used for Polyimide Homo- and Copolymers where the Bis-P Diamine was Employed	121
4.2.2	Photocrosslinking Reaction of the Photosensitive Polyimides	129
4.4.1.1	Synthetic Process employed for 1,3-Bis (4-fluorobenzoyl) benzene	149
4.4.1.2	Synthetic Process employed for 1,3-Bis (3-aminophenoxy-4'-Benzoyl) benzene	153
4.6.1.1	Synthesis of Aminopropyl Terminated polydimethylsiloxane Oligomers	186
4.6.2.1	Synthesis of Poly(imide siloxane) copolymers	191

List of Tables

Table		Page
2.3.1	Criteria for an Organic Dielectric Insulator	14
2.4.1	Comparison Between Properties of PIQ and Some Inorganic Materials	16
2.4.2a	Comparison of Commercially Available Polyimide Physical Properties	19
2.4.2b	Comparison of Commercially Available Polyimide Electrical Properties	19
2.5.1.1	Solvents for Poly(amic acid) Synthesis	26
2.5.1.2	Known Monomers of Commercial Semiconductor Polyimides	27
2.5.2.1	Important Imide IR Bands	34
2.7.2.1	Polyimides with BTDA. Glass Transition Temperatures as a Function of the Methyl Substitution of the Diamine	65
2.7.2.2	Effect of Hydrogen Donor Content on Gel Dose	74
2.7.2.3	Structure and Properties of Sixef Hydroxy Polyimide	84
4.2.1	Monomers Employed in Homo- and Copolymerization Studies	120
4.2.2	FT-IR Assignments for the BTDA/TMBis-P Homopolymer	127
4.3.1.1	Intrinsic Viscosities and Glass Transition Temperatures of BTDA, TMBis-P and Bis-P based homo- and copolymers	131
4.3.2.1	Solubilities of BTDA/TMBis-P/Bis-P Based Homo- and Copolymers	133
4.3.4.1	Effect of Amount of Tetramethyl Diamine Incorporation on Photosensitivity and Contrast	147
4.4.1.1	FT-IR Assignments for 1,3-Bis(3-Aminophenoxy-4'-Benzoyl) Benzene	149

Table	Page
4.4.2.1 Intrinsic Viscosities and Glass Transition Temperatures of BTDA, TMPDA and DKDEDA based Homo- and Copolymers	160
4.4.3.1 Solubilities of BTDA/TMPDA/DKDEDA Based Homo- and Copolymers	163
4.4.5.1 Optical densities of BTDA/TMPDA/DKDEDA Based Homo- and Copolymers	166
4.4.5.2 Photosensitive Properties of BTDA/TMPDA/DKDEDA Based Homo- and Copolymers	168
4.5.1.1 Intrinsic viscosities and glass transition temperatures of BTDA, 6FDA and TMPDA based homo- and copolymers	171
4.5.2.1 Solubilities of BTDA/6FDA/TMPDA based Homo- and Copolymers	174
4.5.4.1 Photosensitive Properties of BTDA/6FDA/TMPDA Based homo- and copolymers (exposed at 365nm)	181
4.5.4.2 Photosensitive Properties of BTDA/6FDA/TMPDA Based homo- and copolymers (exposed at 313nm)	184
4.6.1.1 FTIR assignments for an Aminopropyl terminated polydimethyl siloxane oligomer	189
4.6.2.1 FTIR assignments for BTDA/TMPDA based poly(imide siloxane) copolymer	195
4.6.2.2 Amount of polydimethyl siloxane incorporated into the polyimide copolymers determined by Proton NMR	198
4.7.1.1 Intrinsic Viscosities and Glass Transition Temperatures for the BTDA and TMPDA based poly(imide siloxane) copolymers	200
4.7.2.1 Solubilities of Poly(imide siloxane) Copolymers based on BTDA and TMPDA	203
4.7.4.1 XPS Surface Analysis of Siloxane Modified Polyimide Thin Films (BTDA/TMPDA based)	209
4.7.4.2 Binding Energies of Poly(imide Siloxane) copolymers: XPS results (BTDA/TMPDA based)	210

Table		Page
4.7.4.3	XPS Surface Analysis of Siloxane Modified Polyimide Thin Films on the glass side (BTDA/TMPDA based)	214
4.7.4.4	Binding Energies of Poly(imide Siloxane) copolymers: XPS results on glass side (BTDA/TMPDA based)	215
4.7.5.1	Optical Densities of BTDA/TMPDA based poly(imide siloxane) copolymers	216
4.7.5.2	Photosensitive Properties of BTDA/TMPDA based poly(imide siloxane) copolymers	218
4.8.1	FT-IR Assignments for a BTDA/TMPDA based polyimide homopolymer	222

List of Figures

Figure		Page
2.2.1	Schematic representation of the photolithographic process sequence	7
2.2.2	High pressure Mercury-Xe-arc spectrum	10
2.4.1	Structure for Hitachi's PIQ	17
2.4.2	Schematic cross sections of metal lines isolated by dielectrics. (a) inorganic dielectric (b) polyimide	20
2.4.3	Weight loss as a function of time for polyimide	23
2.5.2.1	Dissipation factor D at 1 MHz vs. time at a specified temperature for a 1 micron thick polyimide film	36
2.5.2.2	Tan delta vs. time for polyimide films	37
2.6.1.1	PMDA-ODA polyimide etch behavior at three different levels of cure. Etched with 0.23 M KOH	41
2.6.1.2	Schematic of polyimide wet etch processes using (a) positive resist and (b) negative resist	42
2.6.2.1	Schematic of a polyimide dry etch process using a photoresist mask	45
2.7.1.1	TGA-curve of the photocrosslinked polyimide precursor	51
2.7.1.2	Structures of synthesized photoreactive 6F containing polyimide precursors	55
2.7.1.3	Change in IR spectra of photopositive polyamic acid after irradiation	60
2.7.2.1	Structural unit of fully imidized solvent-soluble polyimides	64
2.7.2.2	Structures of the model compound and photo-excited intermediates and products	72
3.1.1	Apparatus used for the distillation of solvents	86

Figure	Page
3.2.2.1 Apparatus used for diamine synthesis	93
3.3.1 Apparatus used for poly(amic acid) synthesis	97
3.3.5.2.1 Apparatus used for solution imidization	107
3.4.11.1 Photosensitive response plot for a negative photoresist	114
3.4.11.2 Quartz wafer used in sensitivity studies	117
4.2.1 FT-IR Spectrum of a fully imidized polyimide (BTDA/TMBis-P Based)	126
4.3.3.1 Thermogravimetric Analysis of BTDA/TMBis-P/Bis-P Based Homo- and Copolymers	136
4.3.4.1 UV Absorption Spectrum of the BTDA/TMBis-P Polyimide Homopolymer	138
4.3.4.2 Photosensitive Response Plot for the BTDA/TMBis-P Homopolymer at the 313nm wavelength	140
4.3.4.3 Contrast Plot for the BTDA/TMBis-P Based Homopolymer at the 313nm wavelength	141
4.3.4.4 Photosensitive Response Plot for the BTDA/TMBis-P Based Homopolymer at the 365nm wavelength	142
4.3.4.5 Contrast Plot for the BTDA/TMBis-P Homopolymer at the 365nm wavelength	143
4.3.4.6 Comparison of the Photosensitive Response Plots for a low molecular weight BTDA/TMBis-P Homopolymer at the 313nm and 365nm wavelengths	145
4.4.1.1 FTIR Spectrum of 1,3-Bis(4-Fluorobenzoyl) benzene	150
4.4.1.2 Proton NMR Spectrum of 1,3-Bis(4-Fluorobenzoyl) benzene	152
4.4.1.3 FTIR Spectrum of 1,3-Bis(3-Aminophenoxy-4'-Benzoyl) benzene	154
4.4.1.4 Proton NMR Spectrum of 1,3-Bis(3-Aminophenoxy-4'-Benzoyl) benzene (0 to 10 ppm)	157

Figure	Page
4.4.1.5 Proton NMR Spectrum of 1,3-Bis(3-Aminophenoxy-4'-Benzoyl) benzene (6.0 ppm to 8.5 ppm)	158
4.4.2.1 Dynamic Mechanical Thermal Analysis, Tan delta damping peak for the BTDA/TMPDA based Homopolymer	161
4.4.4.1 Thermogravimetric Analysis of BTDA/TMPDA/DKDEDA based Homo- and Copolymers	165
4.5.3.1 Thermogravimetric Analysis of BTDA/6FDA/TMPDA based Homo- and Copolymers	176
4.5.4.1 Optical densities as a function of the mole percent 6FDA incorporation at the 365nm wavelength	178
4.5.4.2 Optical Densities as a function of the mole percent 6FDA incorporation at the 313nm wavelength	180
4.6.1.1 FTIR spectrum of an Aminopropyl Terminated polydimethyl siloxane oligomer (Mn = 2,500 g/mole)	188
4.6.2.1 FTIR spectrum of a BTDA/TMPDA based poly(imide siloxane) copolymer	194
4.6.2.2 Proton NMR spectrum of a BTDA/TMPDA based poly(imide siloxane) copolymer with 20 weight percent siloxane incorporation (PSX: Mn = 2,465 g/mole)	196
4.7.1.1 Tan delta damping curves for the homopolymer and 20 weight percent polydimethyl siloxane modified copolymer	201
4.7.3.1 Thermogravimetric Analysis of BTDA/TMPDA based Poly(imide siloxane) copolymers	205
4.7.4.1 XPS Wide Scan Spectrum of a Siloxane Modified Polyimide; Siloxane Content - 20 wt %; Siloxane Mn = 2,465 g/mole (90° take-off angle)	208
4.7.5.1 Working energy required to crosslink various film thicknesses of a 20 weight percent siloxane modified polyimide copolymer (BTDA/TMPDA based)	219

Figure		Page
4.8.1	FTIR Spectrum of a one micron thick film of a BTDA/TMPDA based homopolymer	221
4.8.2	FTIR Spectrum of a one micron thick film of a BTDA/TMPDA based homopolymer after a 440 mJ/cm ² exposure dose at the 365nm wavelength	224
4.8.3	FTIR Spectrum of a one micron thick film of a BTDA/TMPDA based homopolymer after a 2,640 mJ/cm ² exposure dose at the 365nm wavelength	225
4.8.4	FTIR Spectrum of a one micron thick film of a BTDA/TMPDA based homopolymer after a 12,540 mJ/cm ² exposure dose at the 365nm wavelength	226

Chapter I

1.0 Introduction

Polyimides are becoming increasingly important in the microelectronic industry for the manufacturing of integrated circuits. They are currently being used in a variety of applications such as interlayer dielectrics (1), passivation coatings, alpha particle barriers (2) and in a variety of other applications as insulating layers (3). However, due to the number of processing steps required in patterning polyimide coatings, numerous investigations on the development of photoimageable polyimides have been motivated. A photosensitive polyimide could be patterned like a photoresist and remain as a permanent part of the electronic device due to its excellent thermal and mechanical stability.

Perhaps the first method of designing a photosensitive polyimide was to incorporate photosensitive groups into the backbone of the polyimide precursor. One of the first groups to take this approach was Kervin and Goldrick of Bell Telephone Laboratories as early as 1971 (4). They added potassium dichromate to the polyamic acid, yielding a photosensitive polyimide prepolymer that could be patterned and subsequently imidized during a post cure step. Another approach was to incorporate methacrylic groups into the polyamic acid by an esterification reaction (5). Other similar systems were presented in 1982 at the First

International Conference on Polyimides (6-9). All of these systems suffered from problems such as poor shelf life and shrinking during the imidization step, which was a required step after exposure and pattern development. Distorted images were generally observed.

Pfeifer and Rohde recently reported a fully imidized, solvent-soluble polyimide system that can be directly patternable (10). The fact that it was a soluble polyimide overcame many of the problems that existed in previous polyamic acid systems. Thus, there was no post cure step needed and therefore the shrinkage was eliminated. The polymer system was based on the benzophenone-moiety and alkyl substituted aromatics incorporated into the polymer backbone. The mechanism is thought to proceed through hydrogen abstraction by the photoexcited triplet benzophenone and the subsequent combining of radicals formed. However, the statement was made by Pfeifer and Rohde that "although the benzophenone-moiety is known for its photosensitizing properties in a variety of chemical systems, it is unknown how photocrosslinking between this group and neighboring polymer chains occurs." (10). Intermolecular hydrogen-atom abstraction from polymers involving the photoexcited triplet state of the aromatic carbonyl group has been known for sometime (11,12). It has also been reported that benzophenone is able to crosslink vinyl polymers during UV exposure (13). Mohanty et al. showed that polymers such as tetramethyl Bis-

A polyaryl ether ketones with aromatic keto and alkyl substituted aromatic groups incorporated into the polymer backbone were photocrosslinkable, and an "intermolecular hydrogen-atom abstraction" mechanism was proposed (14-16). Further evidence concerning the mechanism of photocrosslinking benzophenone containing polyimides has been recently reported by novel approaches (17-19).

The objectives of this research were to study the synthesis and characterization of novel, high glass transition temperature, soluble, photoimageable polyimide homo-, copolymers, and siloxane modified segmented copolymers for microelectronic applications. The experimental approach was to synthesize polyimide homo-, and copolymers containing the benzophenone-moiety and methyl substituted aromatic groups incorporated into the polymer backbone. Benzophenone tetracarboxylic acid dianhydride was used as the aromatic keto containing monomer responsible for absorbing UV radiation to form the photoexcited triplet benzophenone-moiety. The methyl substituted diamines were used as hydrogen donating groups to allow the free radical crosslinking reaction to take place. A series of homo- and copolymers was synthesized and characterized for their photosensitive properties with respect to their polymer backbone structure and other important variables.

Chapter II

2.0 Literature Review

This chapter contains a general review of the synthesis and properties of polyimides used in the electronic industry. Emphasis was placed on the homo- and copolymers with photosensitive properties pertinent to the research described herein. Consequently, photosensitive polyamic acids and polyimides will receive substantial attention.

2.1 Introduction

Since the mid-1950's microelectronics has become a dominant influence in our lives. This integrated circuit revolution was driven by the need for very small and lightweight electronic circuits for computer, military and aerospace applications. After development of the first transistor and later, the integrated circuit, the microelectronic industry has now grown into a multi-billion dollar industry. Integrated circuit miniaturization has progressed from small-scale, medium scale, and large scale integration (SSI, MSI and LSI) to VLSI, or very large scale integration with 10^5 or more components per chip.

The basic building block in microelectronics is the integrated circuit, which is simply interconnected components such as resistors, transistors, diodes and capacitors fabricated directly onto silicon wafer substrates. In cross-

section an integrated circuit is a sandwich of many layers, the number being dependent on the complexity and density of the devices. Some of these layers lie within the silicon and some are stacked on top. Each layer is a unique detailed pattern composed of either silicon, inorganic oxides, metal, metal oxides or polymeric materials. When these layers are precisely stacked one on top of another and interconnected, these layers form the three-dimensional network structure of the integrated circuit. The success of a given circuit design depends on the formation of this precise sequence of layers to achieve the necessary internal composition. The individual chips or integrated circuits are then packaged in order to link them with one another to allow them to communicate with the outside world.

Polymers are important building blocks used in the microelectronic industry. For example photosensitive polymers called photoresist and polyimides are used in the fabrication of ICs. Polyesters and polyimides are employed in flexible circuit board manufacturing. IC encapsulating, packaging and die attach adhesive materials are also primarily polymers. Each of these polymers is used in these applications due to their unique properties.

2.2 Photolithography

Photolithography is the backbone of semiconductor microlithography and supplies the microelectronic industry

with high density, low cost chips. The principle of photolithography is based on radiation-induced structural degradation, or alteration of photosensitive polymers called photoresists. Many photoresists used in semiconductor manufacturing were originally developed for the printing industry (20). Refinements have been made over the years enabling patterning of device dimensions to within a couple of microns.

The basic steps of the photolithographic process are outlined in Figure 2.2.1 (21). In a typical process, the photoresist is applied onto the silicon wafer by spin coating to form a thin uniform film. With a quartz plate called a "mask" coated with an opaque material (usually chrome) bearing an array of circuit design patterns, selected areas of the photoresists are irradiated. The exposed regions of the polymer exhibit different solubilities, in certain developing solvents, resulting in the formation of a relief image of the mask. Depending on the chemical nature of the photoresist, either a positive or negative relief image of the original mask is formed (Figure 2.2.1). Resists which produce negative images generally undergo crosslinking upon exposure to UV light, rendering them insoluble in the developer solvent and are called negative resists. On the other hand, positive resists experience molecular changes such as chain scission or changes in polarity rendering the exposed regions more soluble.

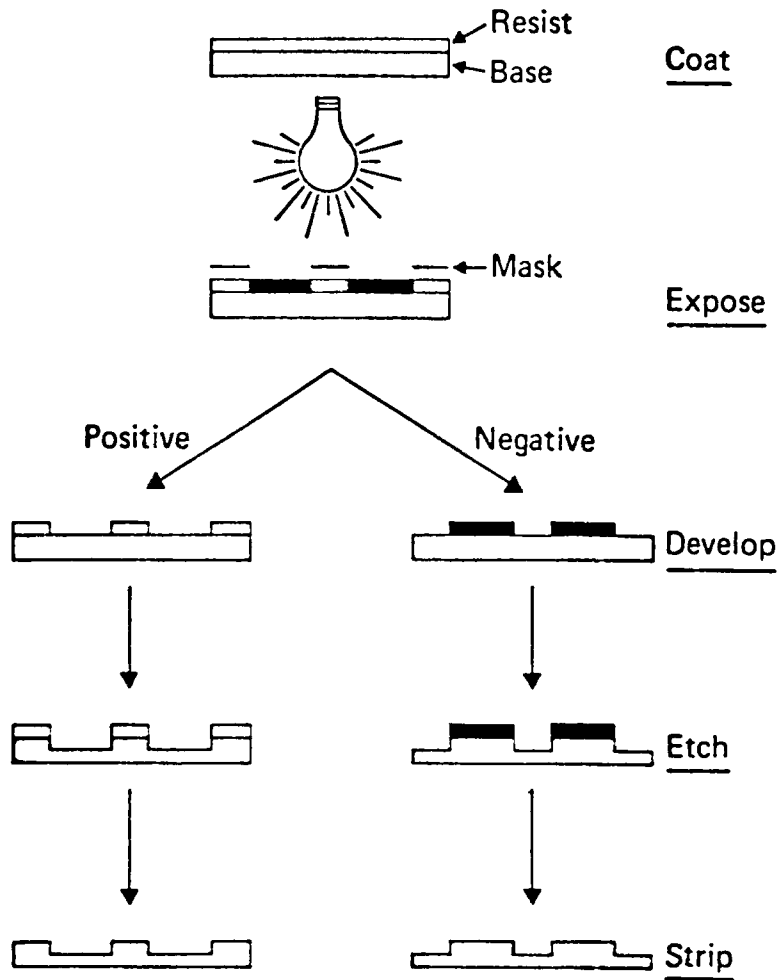


Figure 2.2.1. Schematic representation of the photolithographic process sequence (21).

The developed areas that remain are used to mask the underlying substrate for subsequent etching or other transfer steps. For example, if the underlying substrate were silicon dioxide, immersion of the wafer into an etchant such as buffered hydrofluoric acid would result in selective etching of the SiO_2 in those areas that are exposed during the development step. The photoresist "resists" the etchant and prevents it from attacking the underlying substrate in those areas covered by the resist material. The name resist evolved as a description of the ability of these materials to resist etchants (21). As the last step, the resist is stripped by wet chemical or plasma methods. This photolithography procedure is repeated for every patterned circuit layer on the integrated circuit device. Manufacturing of semi-conductor devices requires the generation of many sequential photoresist images that define the diffusion, insulator and conductor lines that make up the device.

Resist materials used in this application must meet stringent requirements. It must not only have high sensitivity and the ability to resolve small features, but also must possess excellent film-forming properties that will adhere well to a variety of substrates ranging from semi-conductor, metals and insulators. It must also have durability to withstand the highly corrosive chemicals, plasma treatments, and temperature changes encountered during substrate etching, doping and deposition processes.

Photoresists have been designed to respond to the output of simple high pressure mercury arc lamps, whose spectrum is shown in Figure 2.2.2 (21). This spectrum is arbitrarily divided into three regions that correspond to the resist system and the exposure tools used. The region comprising the 366 to 438nm wavelength mercury lines is referred to as the "near UV" region. The region from 313 to 365nm is the "mid-UV" region, and below 300nm is designated as the "deep UV" region. It is currently impractical to use the wavelength below 200nm because of the absorption of air, and of the quartz masks and lens systems of optical printers in this region. Polymers exposed to wavelengths between 200nm and 300nm can undergo crosslinking and chain scission because the energy ($>100\text{kcal/mole}$) is greater than the bond energy of organic carbon-carbon bonds. In the UV range between 300nm to 438nm, where less energy is available, chromophores are incorporated into the polymer backbone to enhance crosslinking efficiency or to create a differential solubility between the exposed and unexposed areas.

2.3 Polyimide use in integrated circuit fabrication

Very large scale integrated circuits (VLSI) require multilevel structures consisting of alternating metal and dielectric layers to achieve high density interconnection. The function of the interlayer dielectric in this multilevel structure can be broken down into three requirements: 1. it

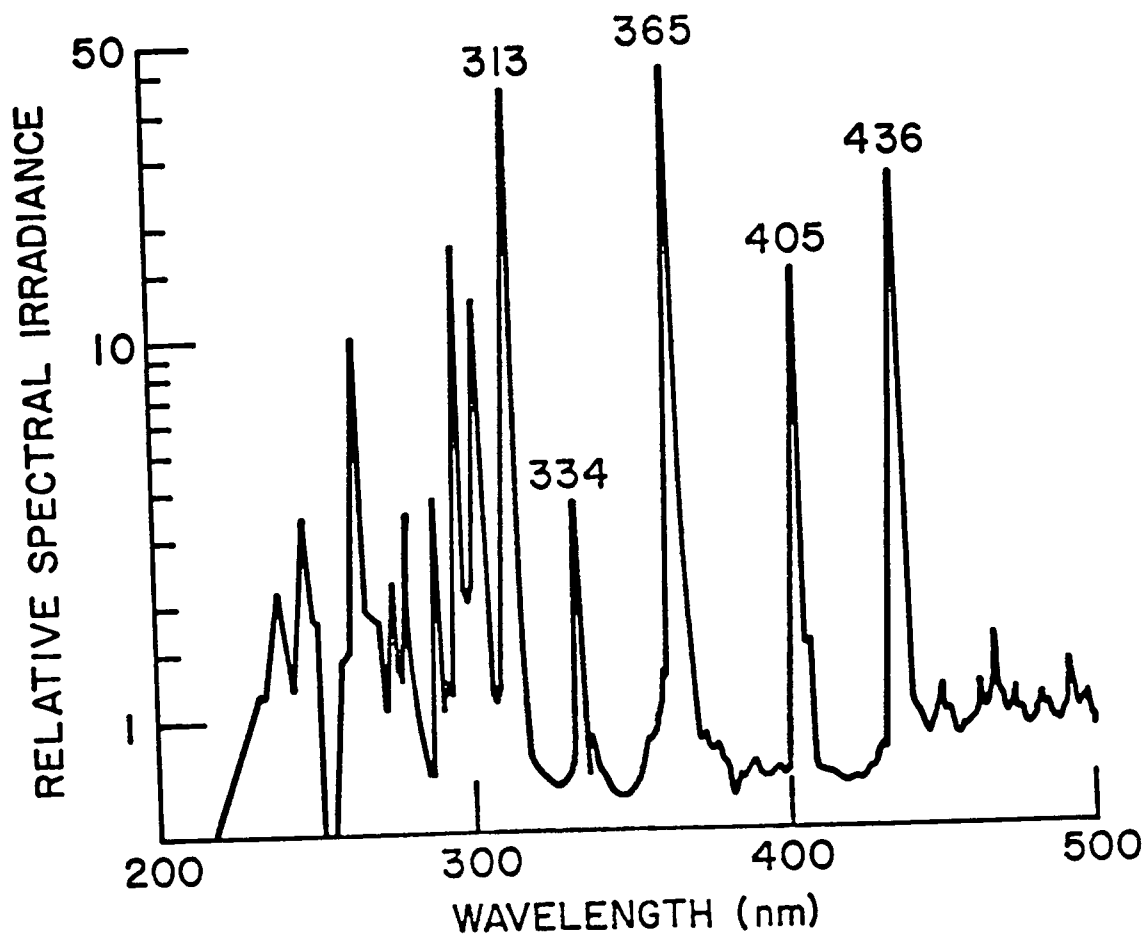


Figure 2.2.2. High pressure Mercury-Xe-arc spectrum (21).

must provide planarization of underlying topography while allowing high resolution patterning of "via" holes needed for contact between metal layers, 2. it must provide insulation integrity, and 3. it must contribute minimally to device capacitance (22).

Insulating or dielectric layers of the metal interconnect system are generally referred to as "intermetallic dielectrics." These materials are traditionally inorganic silicon-based materials such as silicon dioxide, polycrystalline silicon, or silicon nitride, 1-2 microns thick (23-25). The layers are deposited by sputtering, evaporation, or by a chemical vapor deposition (CVD) process which uses high temperatures or plasmas to decompose selected gases. The product is a thin conformal film of insulating material deposited on the substrate.

The top or passivation layer of an integrated circuit, also a dielectric material, is a protective coating masked and etched by lithographic techniques to define openings through which the exposed metal can be attached to the chip package by metal wires or leads. This overcoat serves to protect the chip against mechanical damage and against moisture and ionic contaminants which can gain access to the circuit metallization via the bonding pad openings or defect sites, which could lead to corrosion of the internal metallization and metal leads. A variety of inorganic thin films have also been used as passivation overcoats by the semiconductor

industry including silicon dioxide, quartz, and silicon nitride deposited by sputtering or CVD (24,25).

Inorganic dielectric materials which are deposited conformally often have many inherent problems, both from the standpoint of deposition and of photolithography. Film thicknesses of inorganic films are limited to two microns or less. These films tend to reproduce the topography of the underlying substrate since they lack any planarizing properties. Problems that are typically encountered are poor step coverage and thinning of the coating over sharp surface structures. Thicker inorganic films are prone to cracking. Poor step coverage of these films ultimately leads to poor linewidth resolution and long-term reliability problems stemming from cracks and discontinuities in the conducting and insulating layers (26).

The ability to planarize topographical features has become a crucially important property of the interconnect dielectric layers. New materials which would enable planarization of the individual interconnect layers have recently become the subject of intensive research. Organic polymers which previously have never been used as a permanent, embedded dielectric layer within the IC structure are now being investigated because of their superior planarity over inorganic dielectrics (40).

Organic polymers must meet the same requirements imposed on inorganic materials in order to be used as a dielectric

layer. For example, the polymers must have minimal outgassing of residual solvent or moisture. Stability up to 400°C without volatile by-products is necessary for the subsequent metal sinter step required in IC manufacturing. The glass transition temperature of the polymer must be higher than any of the other processing temperatures including packaging and soldering steps, which range from 200-400°C, in order to avoid structural deformation in the interconnect device. The desired material properties have been summarized and translated into structural features listed in Table 2.3.1 (27). Based on these criteria polyimide homo- and copolymers appear promising.

Polyimides as a class of polymers have been known for quite some time. One of the first attempts to prepare a polyimide is believed to have been as early as 1908 (28). Polyimides have been used in the electronic industry for some time as polymer insulation materials because of their excellent electrical and mechanical properties at elevated temperatures (29). One of the first commercially available resins for electrical insulation was marketed by DuPont in the 1960s under the trade name Pyre-ML (30). Early in the 1970s the semiconductor industry began evaluating this resin as a spin-coated thin film dielectric. This same polymer was already established as a planar insulating material in other branches of electronics in the form of a cured film marketed by DuPont under the tradename of Kapton. The initial work in

**Table 2.3.1. Criteria for an Organic Dielectric Insulator
(27).**

Desire Property	Structural Feature
Planarizability	*LowMolecularWeight Prepolymer (viscous flow before cure)
No Microporosity	*Cured by Addition Reaction
Thermal Stability (400°C)	*Incorporate Aromatic Units
No Moisture Pick-up	*Eliminate H₂O Adsorbing Groups
Low Dielectric Constant	*Eliminate Polar Groups
Lithographic Sensitivity	*Photosensitive Prepolymer
High Mechanical Properties	*Optimize Molecular Weight and Network Structure

the area of polyimide as a multilevel interconnect dielectric was published by Hitachi Central Research Laboratories in 1973 (31,32). Use of polyimide as a final passivant layer was also reported (33). Since then the literature found on the use of polyimides in the microelectronic industry has proliferated. Today many polyimide manufactures have an entire line of "semiconductor grade" polyimide products which vary in their viscosity, percent solids, and chemical structure to achieve the desired effect.

2.4 Polyimide Properties for Electronic Applications

Properties which make polyimides suitable substitutes for inorganic dielectrics are listed in Table 2.4.1, which compares a commercially available polyimide called PIQ polyimide marketed by Hitachi (see Figure 2.4.1) with other inorganic materials typically used in IC manufacturing (26). An important feature of the polyimide is its relatively low dielectric constant, below 3.5, which is typical for many organic polymers. As can be seen in Table 2.4.1 this dielectric constant is somewhat comparable to that of silicon dioxide but significantly lower than that of silicon nitride and silicon. The dielectric break-down strength and volume resistivity also closely resemble those of silicon dioxide and other inorganic insulators (34-36). In addition to the electrical properties some physical properties are also listed in Table 2.4.1. Even though polyimides are not as thermally

Table 2.4.1. Comparison Between Properties of PIQ and Some Inorganic Materials (26).

Material	Coefficient of thermal expansion $\times 10^6$ ($^{\circ}\text{C}^{-2}$)	Young's modulus (gf cm^{-2})	Tensile strength $\times 10^6$ (gf cm^{-2})	Thermal conductivity (mcal $\text{cm}^{-1}\text{s}^{-1}\text{ }^{\circ}\text{C}^{-1}$)	Melting point ($^{\circ}\text{C}$)	Dielectric constant	Dielectric breakdown strength (V cm^{-1})	Volume resistivity (cm)
PIQ	20-70	300	1.7 ^a	0.4	450-500 ^b	3.5-3.8	106	1016
Si	2.3	1.6	120	72-340	1420	11.7-12	105	---
SiO ₂	0.3-0.5	0.7	1.4	5	1710	3.5-4.0	106-107	1016
Si ₃ N ₄	2.5-3	1.6	6.4	28	1900	7-10	106-107	1012
Al ₂ O ₃	9	3.7	28	78	2050	7-9	105	1014
Al	25	70	0.7-1.4	570	660	---	---	2.5 $\times 10^{-6}$

a Limit of tensile strength

b Temperature of decomposition

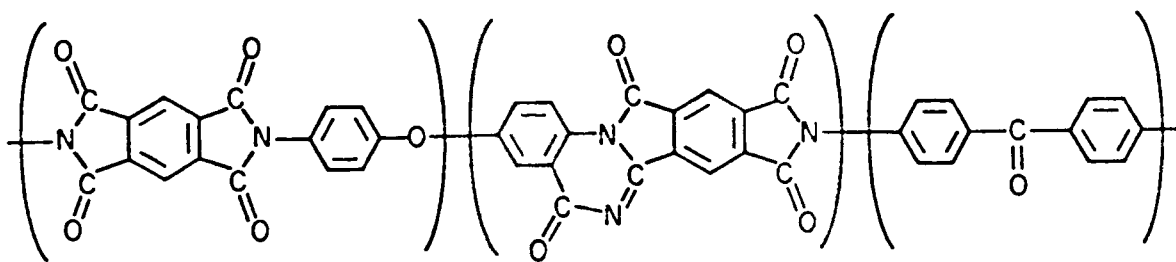


Figure 2.4.1. Structure for Hitachi's PIQ (polyimide and isoindoloquinazolinedione).

stable as the inorganic isolators, their thermal stability is high enough to allow them to be used in computer chips with a decomposition temperature of 450-500°C. Less desirable features of polyimides are the high coefficient of thermal expansion and low thermal conductivity. Stresses in polyimide films due to the coefficient of thermal expansion mismatch between polyimide and substrate, drying, and curing have been studied (37). Regardless of their high coefficient of thermal expansion, polyimides exhibit less residual stresses than inorganic dielectrics (37). Good mechanical stability of the polyimide is indicated by a high Young's modulus, elongation at break and high tensile strength. Other properties which make polyimide suitable for dielectric and passivation application are their excellent chemical resistance and radiation resistance. A list of physical and electrical properties for DuPont's commercially available polyimides PI 2540 and PI 2550 and Hitachi's polyimide PIQ are shown in Tables 2.4.2a and 2.4.2b (33,38-39).

The single most important property which make polyimides particularly attractive as an interlevel insulator is the ability to planarize underlying topography. Figure 2.4.2 schematically shows the difference in planarization ability between an inorganic dielectric such as silicon dioxide with the organic polyimide dielectric (40). In Figure 2.4.3a "steps" are formed in the inorganic dielectric material due to underlying topographical features on the substrate (40).

Table 2.4.2a. Comparison of Commercially Available Polyimide Physical Properties (39).

	PI 2540 (PI 2545)	PI 2550 (PI 2555)	PIQ
Tensile Strength (ultimate)	17,000 psi	19,000 psi	14,500 psi
Elongation	25%	10%	9.5%
Density	1.42 gm/cc	1.39 gm/cc	1.4 gm/cc
Refractive Index	1.78	1.70	1.62
Flexibility	180° bend no cracks (same for all polyimide types)		

Table 2.4.2b. Comparison of Commercially Available Polyimide Electrical Properties (39).

	PI 2540 (PI 2545)	PI 2550 (PI 2555)	PIQ
Dissipation Factor (1kHz)	.002	.002	.002
Dielectric Strength	4000v/mil	4000v/mil	8890v/mil
Volume Resistivity	10^{16} ohm-cm	10^{16} ohm-cm	2×10^{17} ohm-cm
Surface Resistivity	10^{15} ohms	10^{15}	---
Dielectric Constant (1KHz)	3.5	3.5	3.45
(1MHz)	3.75	3.75	3.8

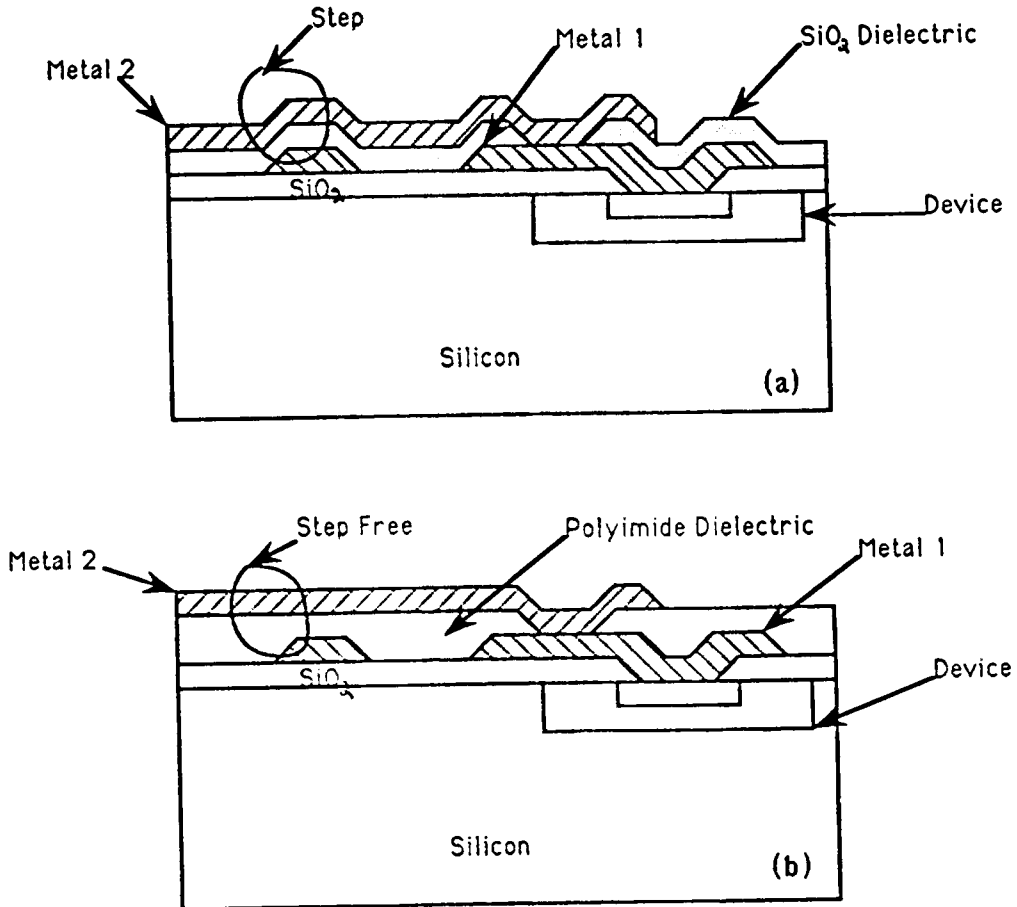


Figure 2.4.2. Schematic cross sections of metal lines isolated by dielectrics. (a) inorganic dielectric (b) polyimide (40).

However, these steps are eliminated with the use of a polyimide insulator (Figure 2.4.3b), thus making a planar layer for subsequent metal line deposition. Many papers have been published on the use of polyimides in microelectronics because of their ability to planarize underlying topography (41-49).

Even though the critical advantage of organic polymers over inorganics as an intermetallic dielectric is the planarizing ability, this feature alone does not enable polyimides to become the choice alternative. Another significant property of polyimides is their high thermal stability. Materials used must be thermally stable to 400°C since certain process steps such as deposition, sputtering and bonding operations are done at or below this temperature. Many commercial polyimides claim initial weight loss above 450°C.

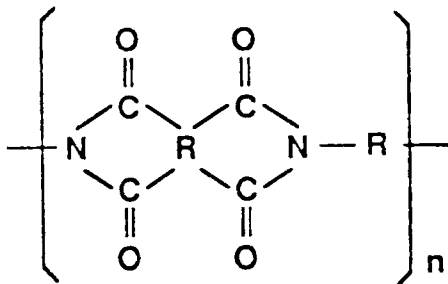
Polyimide thermal stability can be determined by thermogravimetric analysis (TGA) in a variety of atmospheres such as air or nitrogen, and by monitoring mechanical property changes as a function of thermal aging. Lee et al. proposed a mechanism of thermal degradation of polyimides in standard atmospheres based on three degradative reactions (47). The first is deterioration in air which can be attributed to radical-initiated oxidation. A hydrolysis mechanism is predominant at moderate temperatures and high humidity. In an inert atmosphere, polyimides degrade through a pyrolytic

reaction yielding carbon monoxide and carbon dioxide as the major decomposition products. Lee et al. also found that substrate materials in contact with polyimide exert an influence on the decomposition rate in an air environment (47). For example, polyimide on aluminum at 500°C in air has less weight loss than the neat polyimide film at the same temperature (see Figure 2.4.3) (47). They hypothesized that the improved thermal stability of polyimide on Al is due to the preferential reaction of oxygen with aluminum at 500°C, therefore reducing the concentration available to attack the polyimide.

2.5 Polyimide Synthesis (Two-step polycondensation)

2.5.1 Poly(amic acid) synthesis

Polyimides are heterocyclic chain polymers which are characterized by the presence of the imide functionality, a cyclic nitrogen bound to two carbonyl groups (Scheme 2.5.1.1), and may contain either aliphatic or aromatic groups in the polymer backbone.



Scheme 2.5.1.1

Typically, synthesis of polyimides occurs by a two-step

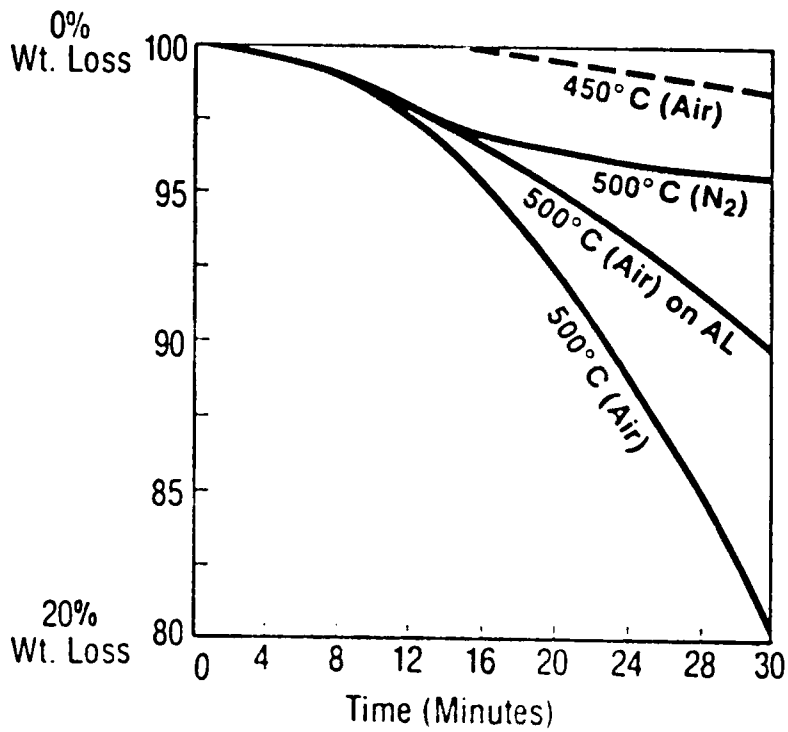
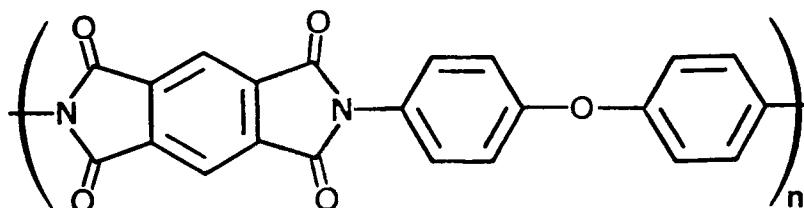


Figure 2.4.3. Weight loss as a function of time for polyimide (pyromellitic dianhydride and 4,4'-diamino diphenyl ether) (47).

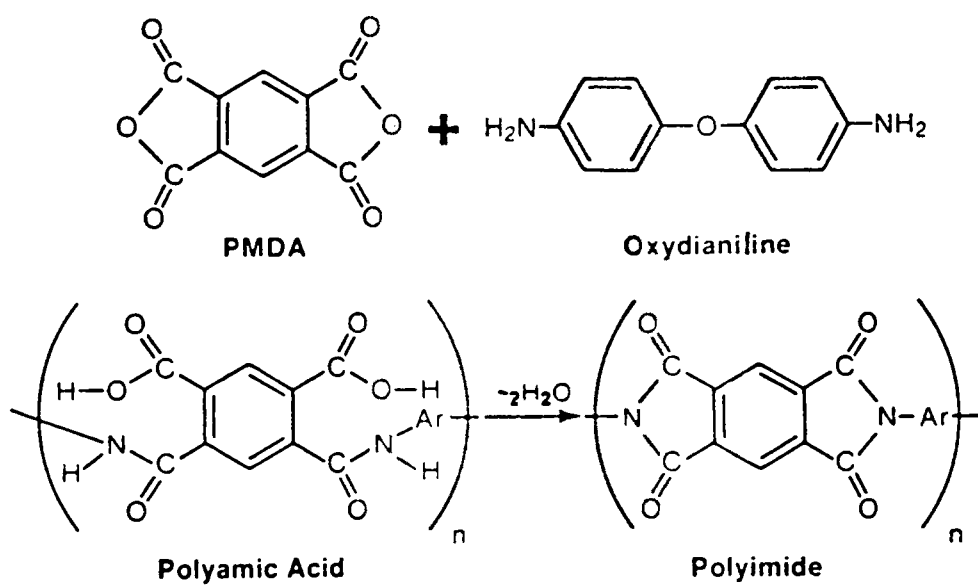
method. This method was first disclosed by workers at DuPont in the mid 1950s (50,51). The first stage of this reaction, shown in Scheme 2.5.1.2 involves the formation of the polyimide precursor polymer, polyamic acid, by a polycondensation reaction of an acid dianhydride with a difunctional amine. This reaction is usually carried out at ambient temperatures in dipolar aprotic solvents such as the solvents listed in Table 2.5.1.1 (52).

Over the years a large number of polyamic acids have been prepared from various aliphatic and aromatic dianhydrides and diamines, but aromatic constituents are primarily used in the preparation of polyamic acids for use in IC (52). Table 2.5.1.2 lists some known monomers of commercial semiconductor polyimides prepared by this two step method (26). Perhaps the best documented of these are the aromatic monomers pyromellitic dianhydride (PMDA) and 4-4'-diamino diphenyl ether (DADPE), otherwise known as oxydianiline (ODA), which are the monomers used in DuPont's Kapton film (Scheme 2.5.1.3).



Scheme 2.5.1.3

Hitachi's PIQ consists of isoindoloquinazolinedione and ordinary polyimide shown in Scheme 2.5.1.4.



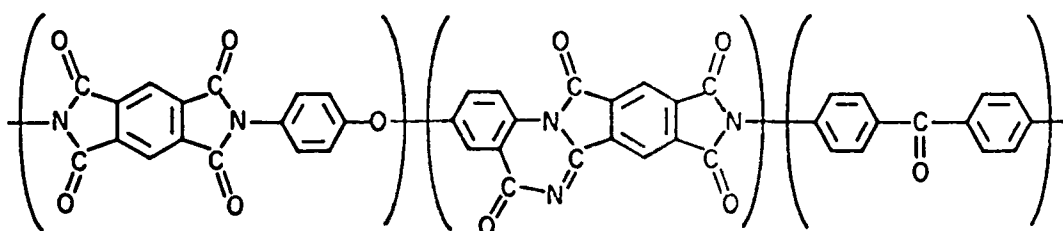
Scheme 2.5.1.2. Polycondensation reaction between an aromatic dianhydride and an aromatic diamine (47).

Table 2.5.1.1. Solvents for Poly(amic acid) Synthesis (52).

N,N-dimethyl formamide	N-methyl-2-pyrrolidone
N,N-dimethyl acetamide	pyridine
N,N-diethyl formamide	dimethyl sulfone
N-methyl caprolactam	tetramethylene sulfone
N,N-dimethylmethoxyacetamide	hexamethylphosphoramide
Dimethyl sulfoxide	N-acetyl-2-pyrrolidone

Table 2.5.1.1.2. Known Monomers of Commercial Semiconductor Polyimides (26).

Manufacturer	Resin	R'	Anhydride	R''	Base
DuPont	PI2545 ¹⁹	50 mol %	Pyromellitic dianhydride (PMDA)	50 mol %	4,4'-Diamino-diphenyl ether (DADPE)
	PI2540 RC5057 PYRE ML	50 mol %		50 mol %	
Hitachi	PIQ ¹⁰	25 mol %	PMDA	45 mol %	DADPE
		25 mol %		5 mol %	
CIBA-Geigy	XU218 ¹³ PI3N	50 mol %	BPTCA	50 mol %	5(6)-Amino-1-(4'-amino phenyl)-1,3,3-trimethylindane (DAPI)
		50 mol %		5 mol %	



Scheme 2.5.1.4

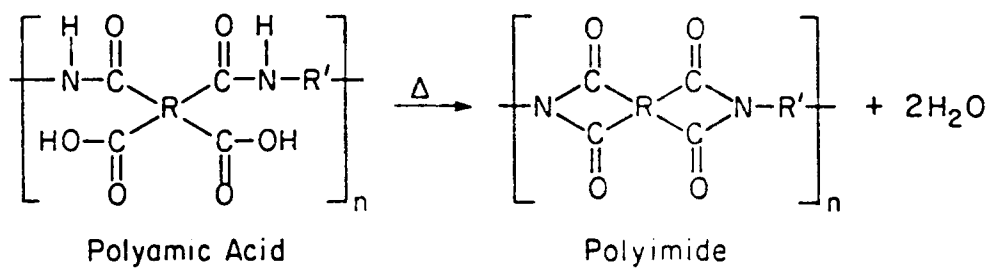
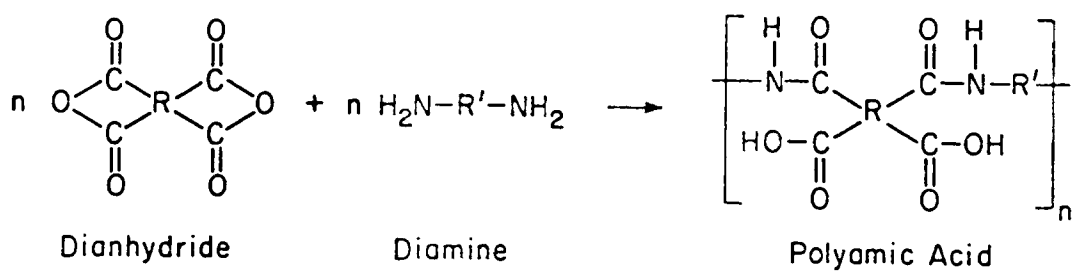
This structure is said to have greater thermal stability due to the addition of an extra ring (32).

The success in achieving high molecular weight poly(amic acid) is dependent on the reaction conditions. These conditions include the use of extremely pure monomers, which are greater than 99 percent pure, exclusion of moisture, choice of solvent, and low to moderate reaction temperature (53,54). At higher temperatures above 50°C possible side reactions may occur which would limit molecular weight. These side reactions are as follows: (1) partial conversion of the polyamic acid to polyimide causing the release of water that could hydrolyze the poly(amic acid); and (2) extensive conversion to polyimide which could result in precipitation of low molecular weight polymer from the reaction-solvent. Another important parameter in making high molecular weight polymer is the order of monomer addition. Typically poly(amic acid) are synthesized by the addition of the dry dianhydride crystals to a rapidly stirring diamine solution at room temperature (55). This order of addition yields higher molecular weights when compared to the reverse order of addition. This has been explained in two ways. First, the

dianhydride is moisture sensitive and could react with residual water in the solvent before the diamine is added, causing an upset in the 1:1 stoichiometry, resulting in a lower molecular weight polymer. Another reason could be the partial complexation of the dianhydride with the solvent. Poly(amic acids) are highly soluble polymers, but are hydrolytically unstable in this form. They are typically stored in their reaction solutions under an inert atmosphere to protect them from moisture. Even under these storing conditions, poly(amic acids) have a limited shelf-life due to their sensitivity to temperature, concentration, and moisture (52). Concentrated solutions are more stable than dilute solutions, and can be stored for longer periods of time at low temperatures (below 0°C in the absence of moisture).

2.5.2 Imidization of Poly(amic acid)

The poly(amic acid) may be converted to the polyimide by a thermal treatment of thin solution cast films (53,54,56-58). This heat treatment, known as "curing," typically is administered in a step-wise fashion to remove most of the solvent and cause cyclodehydration. The curing process involves three different actions: (1) removal of solvent; (2) covalent bond formation in a two-step ring closure; and (3) the release of two molecules of water per polymer repeat unit (Scheme 2.5.2.1). A typical curing cycle might be as follows:

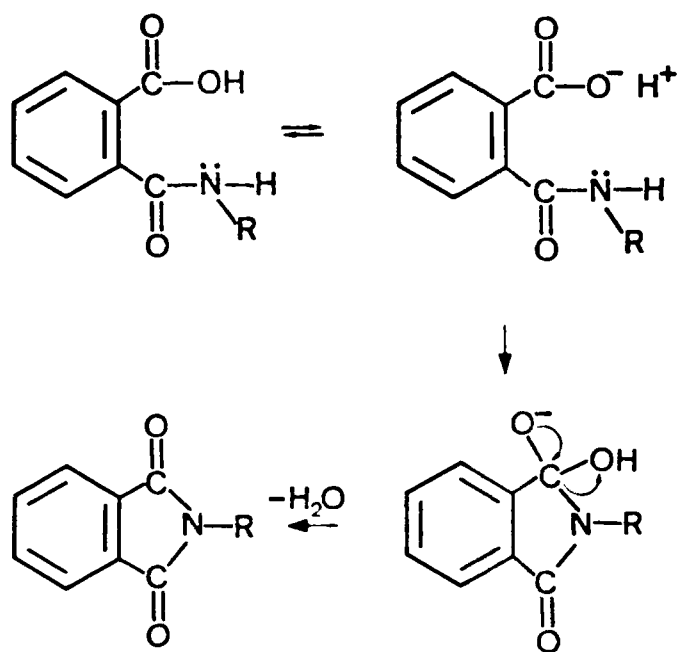


- 2) One hour at 100°C
- 3) One hour at 200°C
- 4) One hour at 300°C
- 5) Cool down to room temperature.

Temperatures higher than 300°C may be required in order to complete the imidization process, depending on the final glass transition temperature of the polyimide formed. However, a majority of the imidization occurs in the temperature range of 150°C to 200°C, but there is not adequate chain mobility for complete conversion of the polyamic acid to the polyimide at these temperatures. It has been reported that two polyimide moieties within the polymer chain can hydrogen-bond up to seven water molecules which are difficult to remove, especially in the rigid, fully imidized chain network (59-61). Because of this, some users of polyimides in microelectronic applications employ an additional quick, superhot (420-450°C) bake to remove water.

One proposed mechanism of imidization involves the equilibrium of the ortho carboxylate anion with the amide hydrogen which affords an easy ring closure route releasing a molecule of water (62). This mechanism is shown in Scheme 2.5.2.2 (62).

A number of methods to monitor thermal imidization have been described in the literature. One of the earliest methods cited is IR spectroscopy which gives semi-quantitative data on the polyimide cure by monitoring the disappearance of the



Scheme 2.5.2.2. Proposed Mechanism of Imidization (62).

N-H band at 3247 cm^{-1} and the appearance of characteristic imide bands at 1770 cm^{-1} and 725 cm^{-1} (47,63). Other researchers have synthesized model compounds and polymers and have identified important imide band regions listed in Table 2.5.2.1 (64-68).

Kinetic studies of the imidization using IR techniques have been reported by Kruez et al. on solvent cast films of poly(amic acids) (62). Imidization was found to proceed by a two-step ring closure through a fast step (activation energy $\Delta E = 26 \pm 3$ kcal/mole, entropy of activation $\Delta S = -10$ e.u.) and a slow step (activation energy $\Delta E = 23 \pm 7$ kcal/mole, entropy of activation $\Delta S = -24$ e.u.). The difference in the two values of activation energy is not significant but the differences in the entropy of activation indicates that the control of the rates resides in the frequency factor. The slower rate of the second ring closure is due to the more negative entropy of activation associated with a steric restriction factor. As imidization proceeds, the glass transition temperature increases and the polymer chains become more rigid, inhibiting alignment of the reactive groups (68). Other IR studies have shown that the rate of imidization is dependent on other parameters such as imidization temperature (62,65,68,69-73) chemical structure (71,79), casting solvent (65,69,71) and film thickness (75).

Another very sensitive method of monitoring the imidization of a poly(amic acid) is the measurement of the

Table 2.5.2.1. Important Imide IR Bands.

Imide I	1780-1770 cm^{-1} and 1730-1720 cm^{-1}
Imide II	1400-1340 cm^{-1}
Imide III	1140-1100 cm^{-1}
Imide IV	740-710 cm^{-1}
amide band	1540-1550 cm^{-1}

dielectric dissipation factor (22,47,76). The dissipation factor decreases with increasing cure temperature until full cure is reached. It appears to proceed in discrete stages (Figure 2.5.2.1). This technique detects both the temperature at which maximum cure is obtained and the rate of achieving it (22). Not only is the series of curves shown in Figure 2.5.2.1 unique for a particular polyimide chemistry, but also for a given film thickness. The Tan delta versus time curve in Figure 2.5.2.2 also illustrates the two distinct phases of time evolution reflecting the two stage nature of the imidization process (47).

Thermal imidization of polyamic acids in solution has also been studied. One of the first attempts to imidize poly(amic acids) in solution was performed in refluxing NMP at 200°C (77). High molecular weight polyimide was not obtained possibly because of one of two reasons. One reason was the water released during imidization remained in the solvent to cause hydrolytic degradation of the poly(amic acid). Another more likely reason was premature precipitation of the polyimide formed during imidization.

In a more recent study it was demonstrated that hydrolysis of the poly(amic acid) could be avoided if the imidization in solution was carried out in the presence of "azeotroping agents" capable of removing the water of imidization (78). Polyetherimides were successfully solution imidized in solvents such as phenols and cresols used along

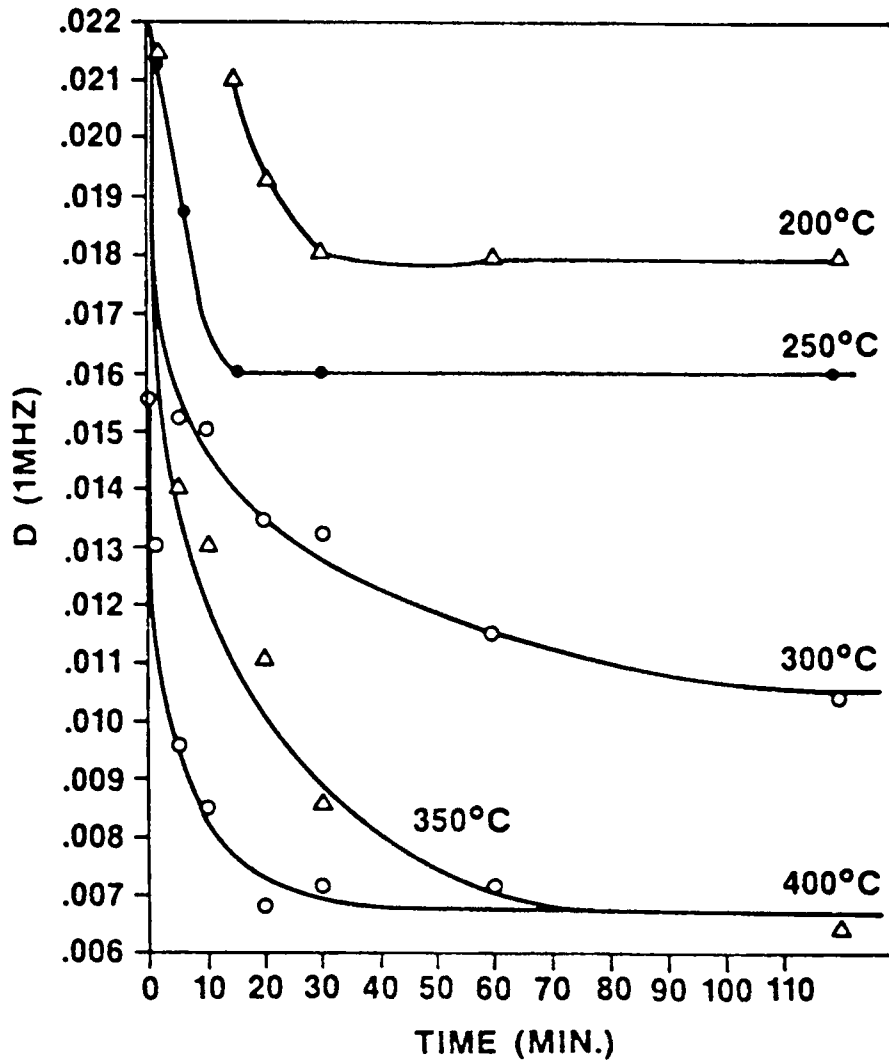


Figure 2.5.2.1. Dissipation factor D at 1MHz vs. time at a specified temperature for a 1 micron thick polyimide film (22).

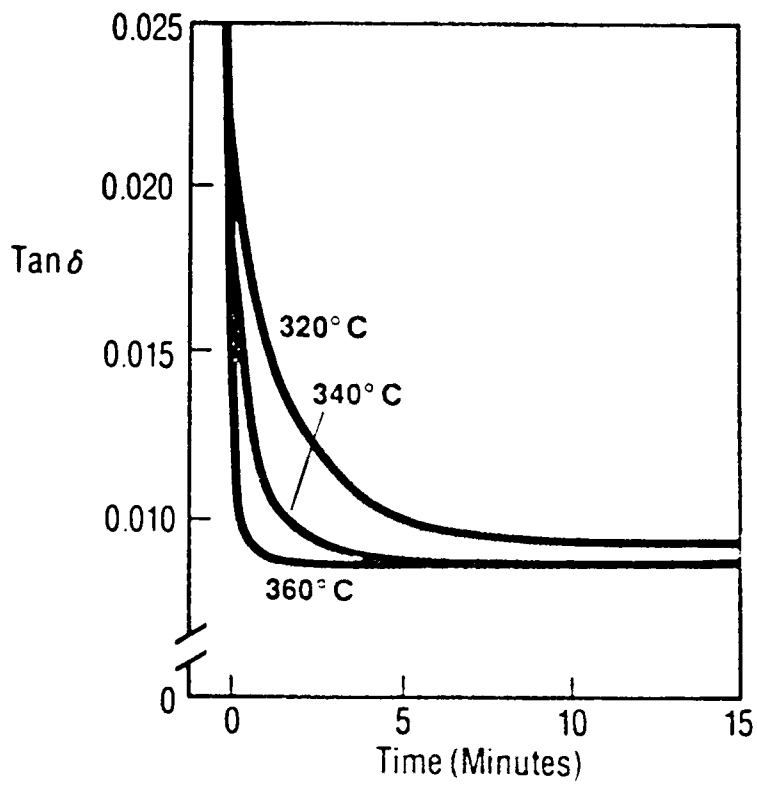


Figure 2.5.2.2. Tan delta vs. time for polyimide films (47).

with azeotroping solvents such as toluene or chlorobenzene at temperatures in the 160°C to 180°C range. Quantitative imidization was possible at temperatures below the glass transition because the polymer was solubilized during imidization, allowing adequate mobility of the polymer chain for quantitative ring closure.

Alternative routes to obtain polyimides such as from a disocyanate reaction (79-90), a nitro displacement reaction (91,92), and a Diels-Alder reaction (93,94) have been previously reported. Since polyimides used in microelectronic applications are almost exclusively synthesized by the classical two-step method of reacting a diamine with a dianhydride, these other routes to polyimides will not be discussed here.

2.6 Polyimide patterning (Etching)

2.6.1 Wet Etching

Polyimides used as interlayer dielectrics must be patterned to open "via" holes for metal contacts in integrated circuits. Patterning of polyimides is also required when they are used as a passivation overcoat to form a bonding pad location for packaging. Polyimides are typically patterned by either a wet-etch or dry etch technique using photoresists as an etching mask to transfer the developed pattern.

Historically, Japanese workers at Hitachi were the first to implement wet-etching when they developed a hydrazine-based etchant (95) capable of patterning fully cured polyimides (96,97). The process they developed used a photoresist polymer spin-coated on top of the polyimide layer, which was then exposed and developed to produce the desired pattern. The pattern was transferred to the polyimide by dipping the silicon wafer into hydrazine hydrate to selectively etch the unmasked areas of the polyimide. The etchant left the masking material, a negative photoresist intact. The resist material was stripped in a subsequent step. A hydrazine-based etchant which contains an amine compound, ethylenediamine, developed by Hitachi has a linear etch rate (1,98). Since hydrazine-hydrate is highly toxic and because of the availability of safer procedures, hydrazine-based etchants are not commonly used in United States.

A partially cured polyimide with carboxylic acid moieties along the polymer backbone can react with strong bases. This reaction results in a high-charge ratio of carboxylate groups which makes the polymer chain soluble in aqueous base and other polar solvents (99). Typical commercial positive resist developers such as 0.05-0.5N solutions of tetralkyl ammonium hydroxide, sodium hydroxide, and potassium hydroxide can attack and remove unprotected polyimide areas masked with negative or positive resist (100). The etch rate of uncured poly(amic acid) is approximately five microns per minute,

which is too rapid to control. Therefore, the polyamic acid is partially imidized by a heat treatment prior to the etching process. The degree of imidization and the amount of solvent remaining after bake determine the etch rate of the polyimide. Careful control of the temperature, time, and conditions of the initial poly(amic acid) bake determines the degree of imidization and etch rate (101). Figure 2.6.1.1 shows the variation in etch rate as a function of degree of polyimide cure (101).

Typical wet etch processes using positive or negative resists are given in Figure 2.6.1.2. First the poly(amic acid) is applied to the silicon wafer and soft baked. The photoresist is then spin-coated on top of the partially cured polyimide, prebaked aligned and exposed, and developed to give the relief pattern. The major difference between the two processes is the addition of a separate step required in the negative process. In the negative resist process the resist must be developed with negative resist developers such as xylene which will not etch the underlying polyimide. After the resist is patterned, the polyimide is etched with an aqueous base solution (102). However, in the positive resist process, the two steps of resist development and polyimide etch are combined into one. Once the base developer penetrates the resist layer, it begins to etch the exposed underlying polyimide. The resist can then be removed using commercial resist strippers which are organic solvents that

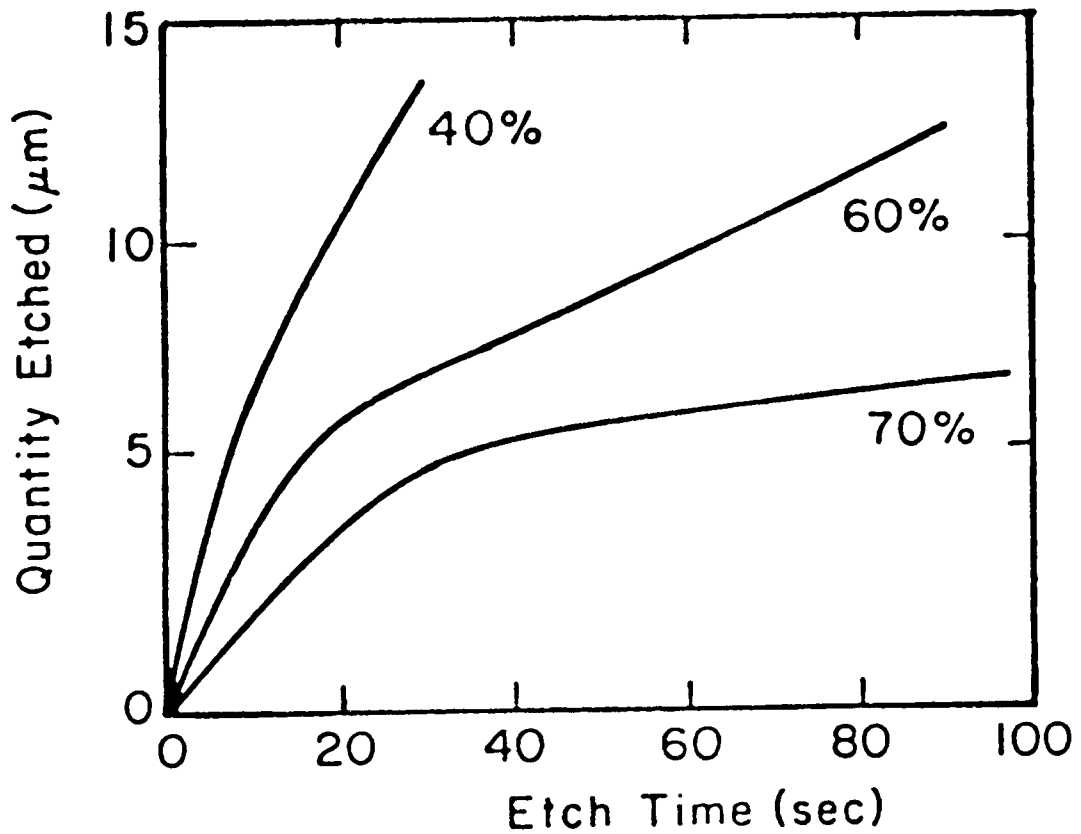
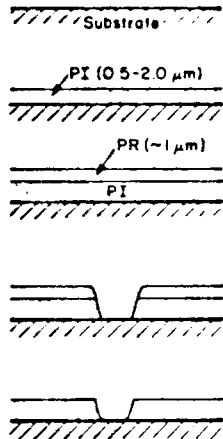


Figure 2.6.1.1. PMDA-ODA polyimide etch behavior at three different levels of cure. Etched with 0.23 M KOH (101).

(a) Polyimide Wet Etch Process Using Positive Photoresist

1. Apply adhesion promoter by spinning
2. Apply polyimide by spinning and soft bake $<140^{\circ}\text{C}$
3. Apply positive photoresist by spinning and soft bake $<140^{\circ}\text{C}$
4. Expose and develop photoresist in standard aqueous base developer. Etch polyimide simultaneously
5. Strip photoresist and cure polyimide

**(b) Polyimide Wet Etch Process Using Negative Photoresist**

1. Apply adhesion promoter by spinning
2. Apply polyimide by spinning and soft bake $<140^{\circ}\text{C}$
3. Apply negative photoresist by spinning and soft bake $<140^{\circ}\text{C}$
4. Expose and develop photoresist in organic solvent developer
5. Etch polyimide in aqueous base (optional. Neutralize with HOAC)
6. Strip resist in stripper and cure polyimide

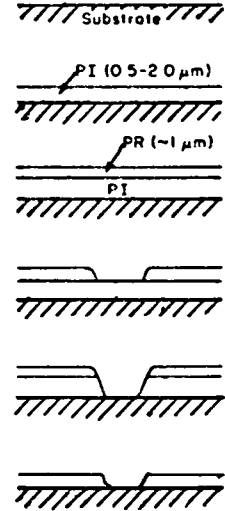


Figure 2.6.1.2. Schematic of polyimide wet etch processes using (a) positive resist and (b) negative resist.

do not affect the patterned polyimide. Using positive photoresists is the method of choice among wet etching processes because they are developed in aqueous base which does not swell the patterns formed.

2.6.2 Dry Etching

Polyimide etching by plasma is more desirable than wet etch methods because it gives superior resolution and uniformity. Oxygen and oxygen mixed with small amounts of fluorine containing gases such as CF_4 and SF_6 are used in plasma etching of polyimides (103). The etch rate of the plasma is a function of all the parameters which include plasma reactor type, power, pressure, temperature, time, and gas composition. Polyimides and photoresists etch at different rates depending on their chemical composition. However, a one-to-one etch ratio of aromatic resist to polyimide is usually assumed. Therefore, the photoresist is approximately twice as thick as the polyimide in order to serve as an etch mask.

Reactive ion etching (RIE) and reactive ion milling (RIM) can also be used to pattern polyimides as a dry technique (34). These techniques are more directional and can achieve higher resolution and vertical sidewalls required in some IC applications. RIE and RIM are usually used in conjunction with more complicated masking techniques than plasma etching. Generally, "hard" or "non-erodible" inorganic masks are used

which etch at a lower rate in oxygen or oxygen/fluorine mixture RIE than polyimide. Various metals and inorganic insulators have been used for this purpose such as Al (104), Mo (104), Cu, silicone-nitride, and silicon dioxide (34).

Oxygen plasma etching degrades the polyimide both by oxidative attack and UV degradation. In plasmas where oxygen and CF_4 gases are mixed X-ray photoelectron spectroscopy (XPS) has shown that polyimides first incorporate fluorine into the polymer matrix as a mixture of CF_x -type compounds and then undergo enhanced oxidative degradation (105). However, the presence of excess amounts of fluorine atoms inhibits plasma etching (106).

Figure 2.6.2.1 shows schematically the simplest process of polyimide oxygen plasma etching using a photoresist mask. In all dry etch method techniques the polyamic acid is applied to the silicon wafer and fully cured before the photoresist is applied on top. The photoresist which is approximately twice as thick as the underlying fully cured polyimide, is spun, exposed, and developed using standard photolithographic procedures. After the developed patterned is formed in the photoresist, the pattern is transferred to the polyimide by plasma etching. The resist is also being etched along with the polyimide. The remaining resist can be chemically stripped or if the process is adjusted precisely all the resist can be stripped during the plasma etch cycle. Since the photoresist mask isotropically erodes away at about the

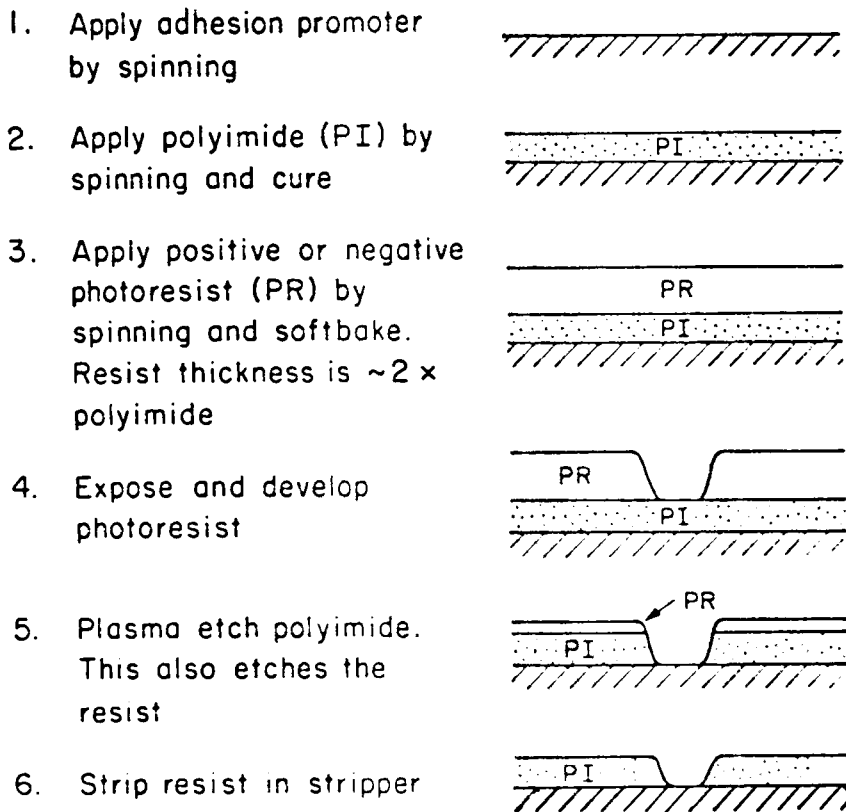


Figure 2.6.2.1. Schematic of a polyimide dry etch process using a photoresist mask.

same rate as the polyimide, the final dimensions of the polyimide via holes is the same size or larger than the printed relief image. In production of IC the practical limitation on the resolution are about 5 x 5 micron via holes for a 1-2 micron thick film. The etch techniques and photoresist system determine the wall slope, resolution limit, and dimensional control. The general criteria used to select a dry etch process are resolution requirements, desired etch profile, polyimide thickness, and equipment available. The slightest process variation often produces significant differences in the final product.

2.7 Photoimageable Poly(imides)

2.7.1 Photosensitive Poly(amic acids)

Due to the number of processing steps required in patterning polyimides by the wet or dry etch methods numerous investigations on the development of photoimageable polyimides have been motivated. Photosensitive polyimides could be patterned like a photoresist eliminating the etching processes, and they could remain incorporated as a permanent part of the electronic device due to their thermal and mechanical stability.

The first method of designing a photosensitive polyimide was to incorporate photosensitive functional groups into the backbone of the polyamic acid. Kervin and Goldrick of Bell

Telephone Laboratories took this approach as early as 1971 (4). They added potassium dichromate to the polyamic acid, yielding a photosensitive polyamic acid. The polyamic acid that they used in their study was a commercially available polymer sold by DuPont under the trade name of Pyre-ML, which is a 13% solids solution in N-methyl-2-pyrrolidone made from the monomers pyromellitic dianhydride with 4,4-diaminodiphenylether. The potassium dichromate used as the photochemically active crosslinking agent was added to the polymer solution just prior to use due to the unstable solution formed. The modified polyamic solution could be spun onto the silicon substrate and exposed and developed to form the relief image, then subsequently heated above 250°C in order to convert the polyamic acid to the polyimide. The two major problems with this approach were that relief images formed would shrink during the polyimide cure cycle giving poor line width control and adhesion to the substrate, and the presence of the dichromate salts would decrease the thermal stability of the polyimide formed.

Another approach in forming a photosensitive polyamic acid was to incorporate photosensitive organic functional groups, instead of inorganic crosslinking agents, into the polymer backbone. Rubner et al. incorporated methacrylic groups into the polyamic acid by an ester type reaction (5,6). The reaction scheme used is shown in Scheme 2.7.1.1 (5). First the pyromellitic acid dianhydride was converted into the

corresponding pyromellitic acid diesters by adding β -oxyethylmethacrylate at room temperature (Scheme 2.7.1.1a). The diester was then reacted with thionyl chloride to form the acid chlorides (Scheme 2.7.1.1b). The last step was to add the diaminodiphenylether to form the high molecular weight poly(amic acid) with the pendant photosensitive methacrylic groups (Scheme 2.7.1.1c).

The method of processing the photoreactive prepolymer is illustrated in Scheme 2.7.1.2 (6). Like conventional photoresists, the ester-like bound photoreactive groups can be crosslinked to form patterns simply by selective UV-exposure and subsequent development. Because of their structure, the crosslinked polyamic acid patterns can be chemically converted into polyimide patterns by curing at high temperatures. During cyclodehydration, the remaining photoreactive groups and the crosslinked bridges are volatilized in the form of alcohols and polyalcohols. A characteristic weight-loss curve is shown in Figure 2.7.1.1 (5). The steep initial slope at 275°C is due to the rapid cyclization and evaporation of the β -oxyethylmethacrylate. At 400°C further weight loss is shown by the volatilization of the former crosslinking bridges. This volatilization and split-off of photoreactive compounds and crosslinking bridges causes a 30-50% decrease in film thickness.

Other similar photosensitive polyamic acid systems were presented in 1982 at the First International Conference on

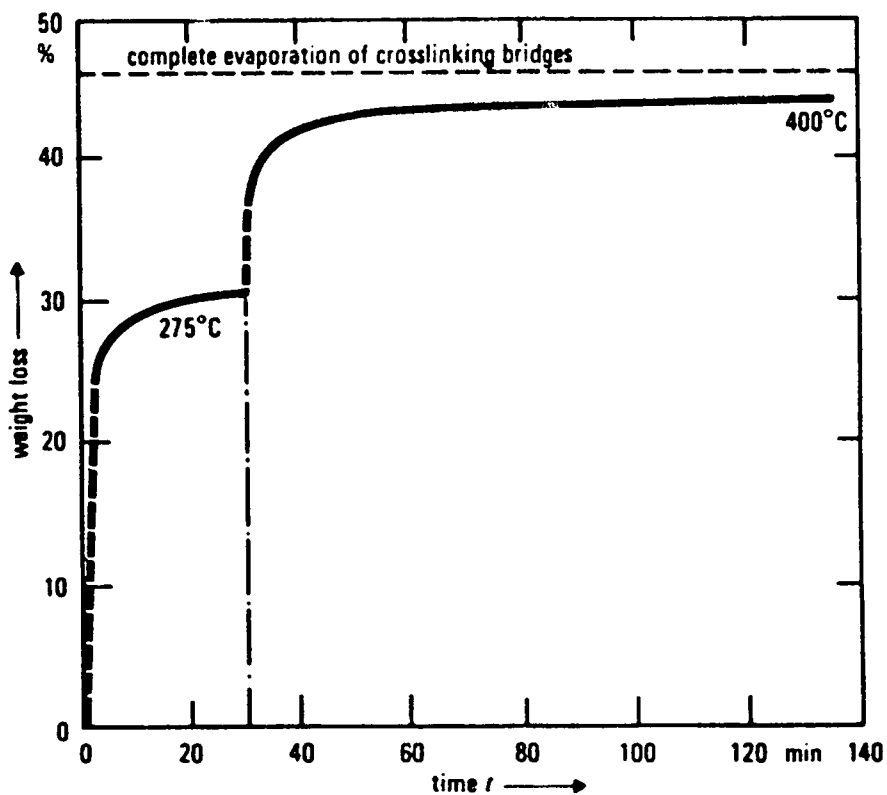
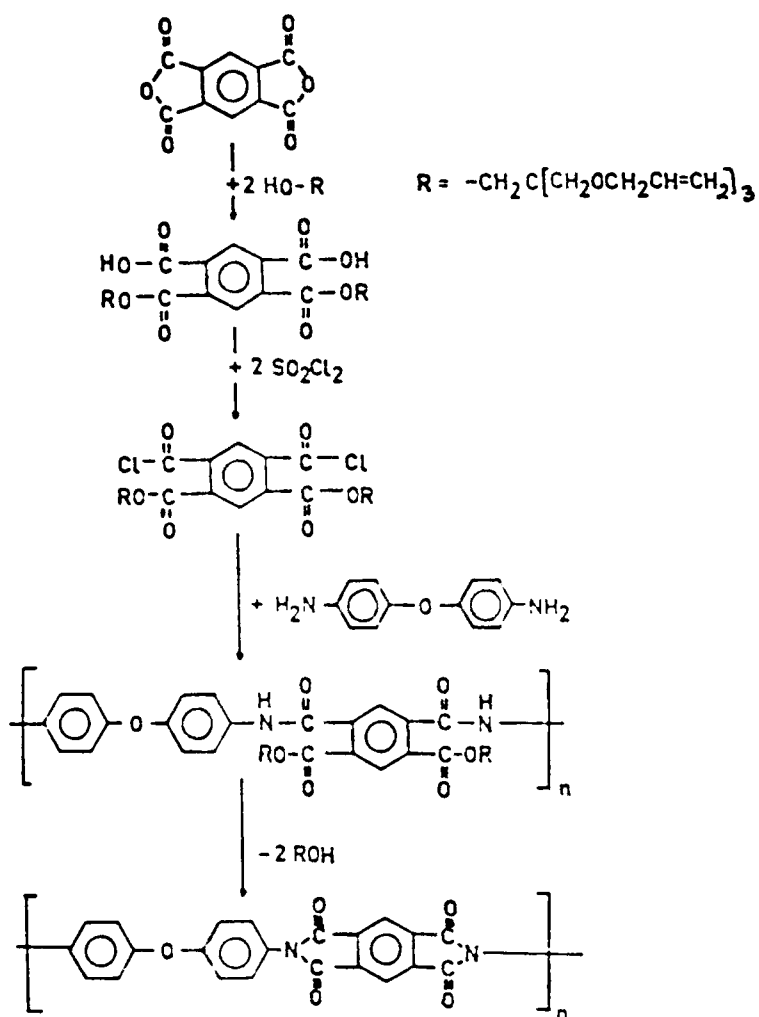


Figure 2.7.1.1. TGA-curve of the photocrosslinked polyimide precursor (5).

Polyimides (6-9). H.J. Merrem and coworkers demonstrated that a more photosensitive polyamic acid could be synthesized by using a different light sensitive compound such as pentaerythritriallylether instead of the methacrylic groups (7). Their photosensitive polyamic acid was synthesized in a similar manner as Rubner's system and is outlined in Scheme 2.7.1.3 (7). A second method used by Merrem to increase the sensitivity was the addition of monomeric polyfunctional crosslinkable systems to the poly(amide acid ester) such as 2,4,5-trisallyloxy-1,3,5-triazin, along with a comonomer such as maleimide, and a photoinitiator such as Michler's ketone. By addition of these sensitivity enhancers the sensitivity increased to 120-130 mJ/cm² from 650-700 mJ/cm² as previously reported by Rubner for a one micron thick film. Two other photosensitive polyamic acid systems were reported at the First International Conference on Polyimides claiming to have increased sensitivity compared to Rubner's polyamic acid system. However, the chemical structure and reaction of the photosensitive group used to synthesize the polyamic acid ester were not discussed.

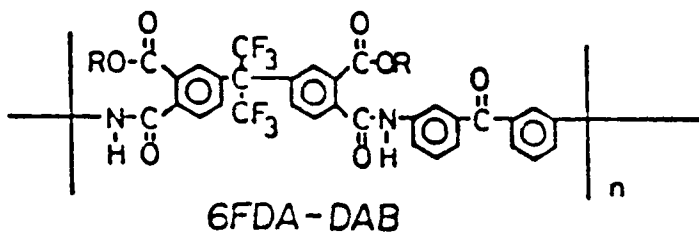
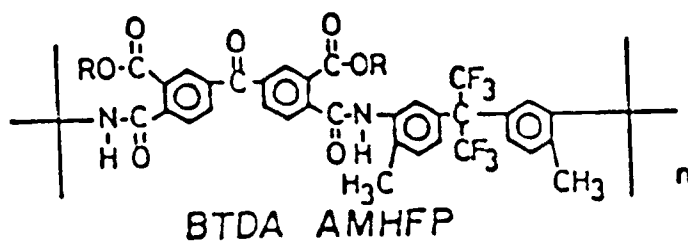
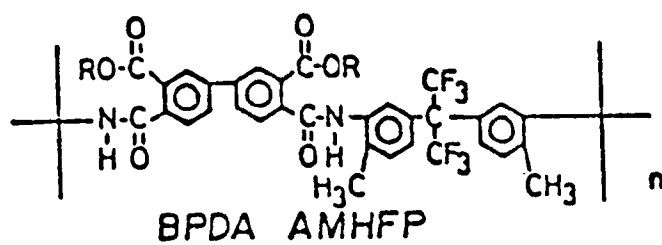
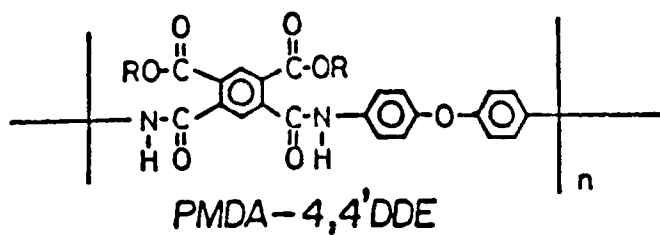
Companies like DuPont (107) and Ciba-Geigy (108) have commercially available photosensitive polyamic acids based on the pioneering work of Rubner et al. of Siemens Company (5,6, 109). Ciba-Geigy corporation added novel sensitizers to the poly(amic acid ester) in order to make a more photosensitive system tailored to the exposure wave length of 365nm and



Scheme 2.7.1.3. Preparation of Merrem's photoreactive poly(amic acid) (7).

marketed under the trade name of Probimide 300 (108). Film thicknesses up to 70 microns thick have been patterned using this system. DuPont Company has patented a similar photosensitive polyamic acid using the dianhydride, 2,3,-bis (3,4-carboxyphenyl)-hexafluoropropane dianhydride, instead of the commonly used pyromellitic dianhydride, reacted with 4,4-diaminodiphenylether (107). Unlike Rubner and coworkers, workers at DuPont reacted the diamine and dianhydride to first form the poly(amic acid) and subsequently reacted the carboxylic acid groups along the polymer chains with monoepoxides to form the esterlike photosensitive groups. The two olefinically unsaturated monoepoxides used were the unsaturated epoxides glycidyl acrylate and glycidial methacrylate. A polyfunctional acrylate compound and a photoinitiator system comprising hydrogen donor initiator and aromatic bimidazole were added to the polymer to increase the photosensitivity of the system (107).

Another more recent study by T. Omote and coworkers reported the synthesis and characterization of novel fluorine-containing photoreactive polyimide precursors (110). The polyamic acid was first synthesized by the polycondensation of diamines with tetracarboxylic acid dianhydrides, followed by esterification by addition of 2-hydroxyethyl (metha) acrylate. The structures of the photoreactive polyamic acids are shown in Figure 2.7.1.2 (110). The polymers containing the benzophenone moiety along the polymer backbone were more



R: β -oxyethyl methacrylate

Figure 2.7.1.2. Structures of synthesized photoreactive 6F containing polyimide precursors (110).

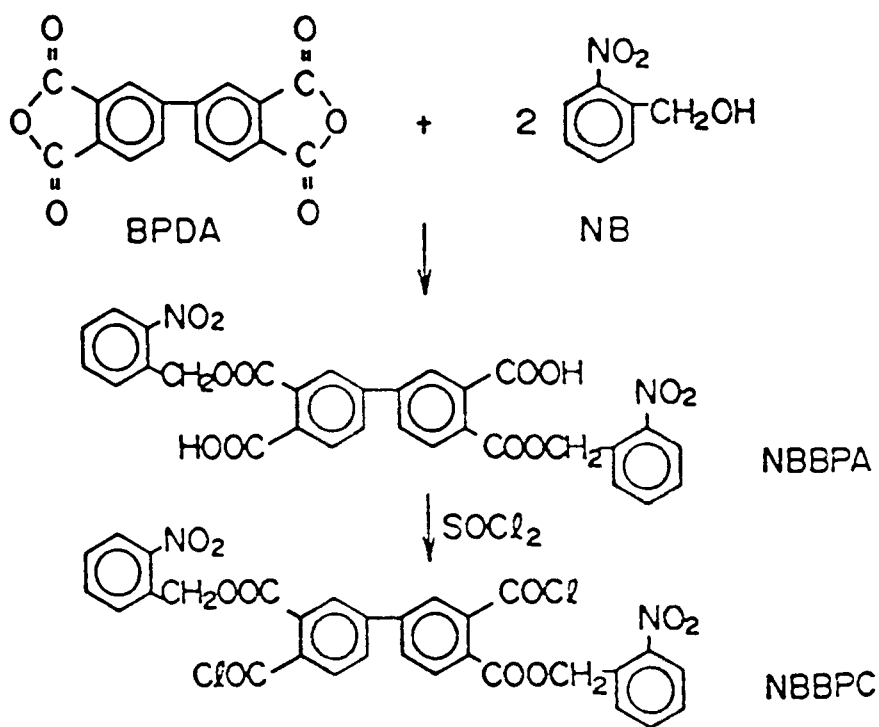
photosensitive than the other polymers at the 365nm exposure wavelength. The benzophenone moiety was thought to act as a photosensitizer to allow the crosslinking reaction to take place more efficiently. However, the fluorine containing polymers had the advantage of being less optically dense at 365nm, and therefore more transparent to the UV light.

Poly(amic acid siloxane) segmented copolymers were also reported to be made photoreactive by workers at General Electric Company (111,112). Methods similar to Rubner's were used to incorporate photoreactive groups into the polymer backbone. Polydimethyl siloxane oligomers with either anhydride or amine end groups were reacted with the appropriate aromatic diamine or dianhydride to yield high molecular weight poly(amic acid siloxane) copolymers. A monoepoxide containing either a photoreactive acrylate, cinnamate or 2,3-diphenylcyclopropenol ester functional group was reacted with the pendent carboxylic acid groups on the poly(amic acid siloxane) to yield a photosensitive prepolymer. In some cases acryloyl chloride, and isocyanatoethyl methacrylate were used to incorporate photoreactive functional groups into the polymer chain (111). Bis-maleimide terminated siloxane oligomers and photosensitizers were added to the poly(amic acids) to enhance the sensitivity to UV light. Bis-maleimide terminated oligomers can also be photolytically crosslinked with the poly(amic acid) having pendent aromatic groups via a 1,2-cycloaddition reaction forming a bridge

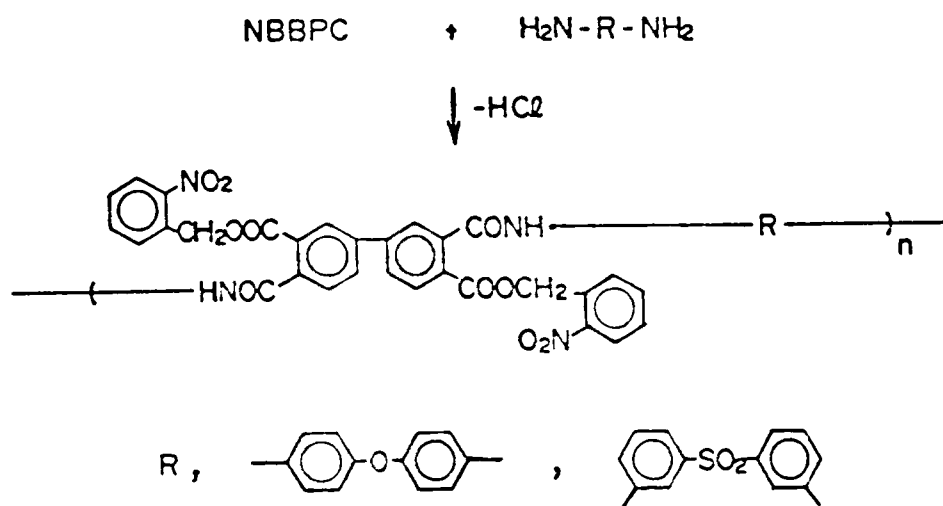
between two polymer chains (112).

Novel positive photoreactive poly(amic acids) containing α -[2-nitrophenyl] ethyl ester side chains have been reported by S. Kubota, et al. (113,114,115). Unlike previously discussed photosensitive polyamic acid systems which undergo crosslinking when irradiated by UV light, these systems undergo a photochemical rearrangement rendering them soluble in aqueous bases. The monomers containing the photosensitive groups were prepared by a two step synthesis procedure outlined in Scheme 2.7.1.4 (115). Both biphenyl-tetracarboxylic acid dianhydride and pyromellitic dianhydride were used in these studies. The synthesis of the photoreactive monomers was carried out with the reaction of the dianhydride and o-nitrobenzyl alcohol in toluene. The acid chlorination was carried out by the use of thionyl chloride in the presence of dimethylformamide as a catalyst. The polyamic acids were synthesized from the diacid chlorides and diamines by means of a solution polymerization in N,N'-dimethylacetamide at an ice bath temperature as shown in Scheme 2.7.1.5 (115). Various molecular weight poly(amic acids) were obtained by adjusting the stoichiometry of the monomers with an excess of diacid chloride.

The o-nitrobenzyl ester groups introduced into the poly(amic acid) chain undergo an intramolecular photoarrangement by UV irradiation. Figure 2.7.1.3 shows the change in IR absorption spectra of a polyamic acid film upon



Scheme 2.7.1.4. Synthesis of photosensitive monomers (115).



Scheme 2.7.1.5. Synthesis of photopositive poly(amic acid) (115).

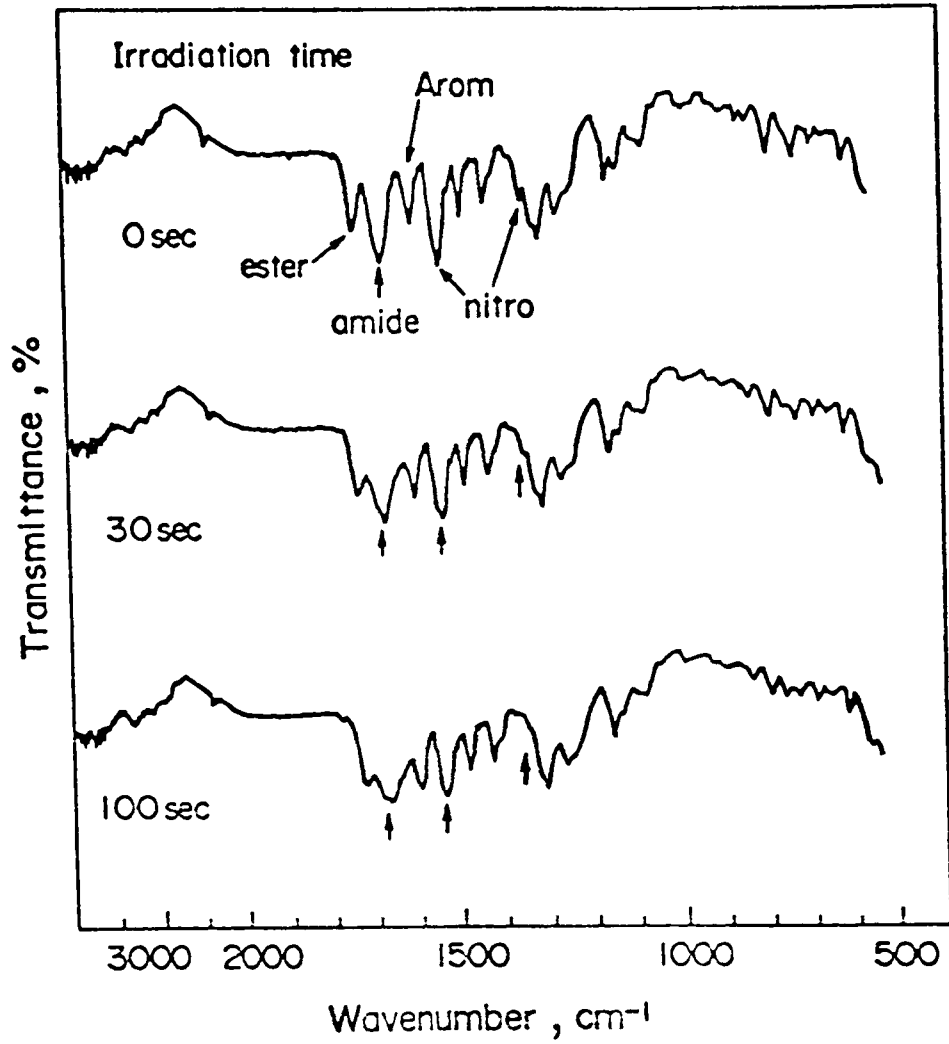
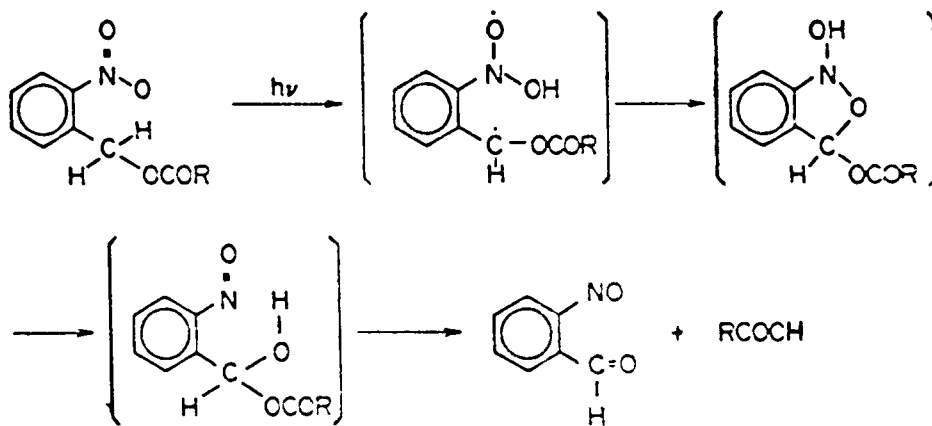


Figure 2.7.1.3. Change in IR spectra of photopositive polyamic acid after irradiation (115).

irradiation. There is a decrease in the intensity of the nitro group peak at both 1520 and 1340 cm^{-1} . The rearrangement reaction that is believed to occur is shown in Scheme 2.7.1.6 (115). The exposed areas of the film were soluble in aqueous base developer. Unlike other positive photoresist systems, the sensitivity of the poly(amic acid) decreased with increased molecular weight. The reason for this difference was explained by the fact that most positive resist systems undergo chain scission making the difference rate of dissolution in developer greater for high molecular weight material. However, in this system the functional groups causing the polymer to be more soluble are formed by irradiation without main chain scission of the polymer chain. Therefore, their solubilities are determined by their molecular chain length. Increasing molecular weight results in reduced sensitivity in these photoreactive polyamic acid systems.

All the photoreactive poly(amic acids) discussed here suffer from two major problems. The first is poor shelf life of the polyamic acid when stored at room temperature. The other disadvantage is shrinking of the pattern during the imidization step, which is a required step after exposure and pattern development. Shrinkage of greater than 40 percent was seen in most of the poly(amic acid) systems, generally resulting in distorted images and patterns.



Scheme 2.7.1.6. Schematic representation of 0-nitrobenzyl ester photorearrangement (115).

2.7.2 Photosensitive Soluble Polyimides

Pfeifer and Rohde of Ciba-Geigy Corporation recently reported a fully imidized, solvent-soluble polyimide system that can be directly patterned like a photoresist (10). The fact that it was a soluble fully imidized polyimide overcame many of the problems that existed in previous photoreactive polyamic acid systems. Since a post cure step is not required the shrinkage was eliminated. The basic structural unit for the fully imidized solvent-soluble polyimides is shown in Figure 2.7.2.1 (10). Pfeifer and coworkers found that many polyimides with this structure are soluble and inherently photosensitive. The authors realized that these polyimides were photosensitive when they were investigating solvent-soluble polyimides and observed that the polyimides would turn insoluble when exposed to filtered sunlight. The authors studied a variety of polyimides formed by reacting benzophenone tetracarboxylic dianhydride (BTDA) with the diamines listed in Table 2.7.2.1 (10). All polyimides formed were soluble except the homopolymer obtained from 2,4-diaminotoluene (I).

The photosensitive properties of these polyimides were found to be governed by their chemical structure. Soluble polyimides with the alkyl substituents in the ortho-position relative to the amino group were more photosensitive than the polyimides with the alkyl substituents in the meta-position. Also, as the number of ortho-substituents increased the

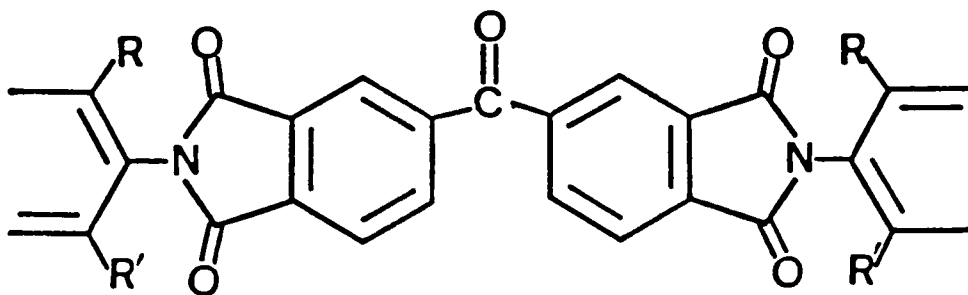
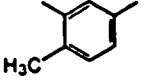
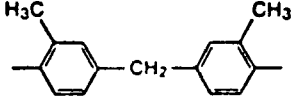
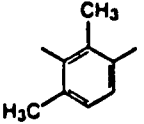
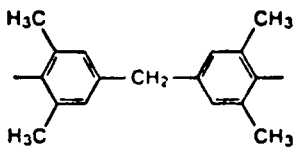
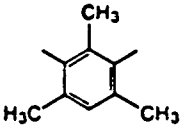
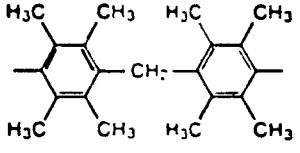
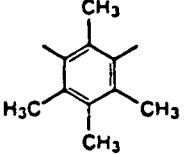
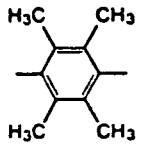


Figure 2.7.2.1. Structural unit of fully imidized solvent-soluble polyimides (10).

Table 2.7.2.1. Polyimides with BTDA. Glass Transition Temperatures as a Function of the Methyl Substitution of the Diamine (10).

	Diamine	T_g ($^{\circ}\text{C}$)	Diamine	T_g ($^{\circ}\text{C}$)
(I)		315		285 (VI)
(II)		384		309 (VII)
(III)		398		373 (VIII)
(IV)		429		
(V)		439		

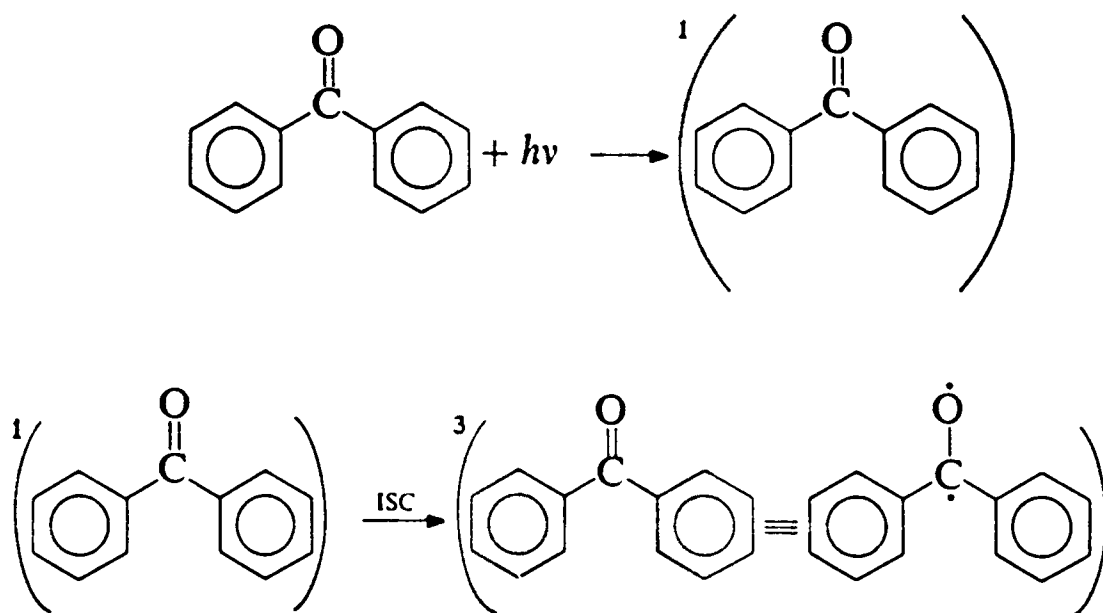
sensitivity of the polyimides was shown to increase. Another property found to influence the photosensitivity was the chemical nature of the ortho-substituted alkyl substituent. An isopropyl alkyl substituent containing polyimide was found to be more photosensitive than a polyimide with an ethyl substituent which in turn was found to be more sensitive than a polyimide with a methyl substituent.

A 1.5 micron thick film of photosensitive polyimide was reported to require an exposure dose of 270 mJ/cm^2 in order to render it totally insoluble. 3.0 micron spaces were resolved for a 1.5 micron thick film, corresponding to an aspect ratio of 0.5, when patterned through a mask. The authors found that if a thin film was heated above 350°C for ten minutes that it would also render the film insoluble even before UV exposure. Since the polymer was already imidized no volatiles were given off, other than residual solvent, when heated to high temperatures. Therefore, the thickness retention was found to be 91-95% rather than approximately 50% for photosensitive polyamic acids.

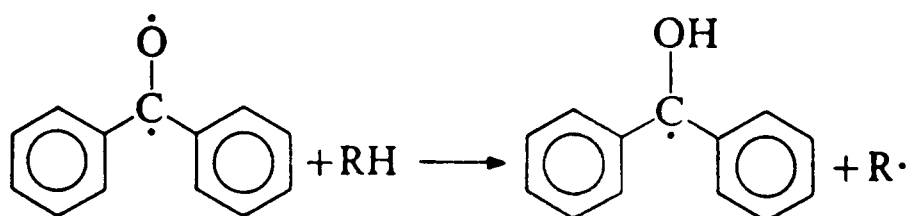
Even though the workers at Ciba-Geigy had studied the photosensitive properties of the soluble polyimides, they did not know the mechanism of UV initiated crosslinking. The statement was made by Pfeifer and Rohde that "Although this novel photocrosslinking mechanism works quite effectively, its chemical pathway is still completely unknown" (10). The mechanism is thought to proceed through a hydrogen abstraction

by the photoexcited triplet benzophenone moiety and the subsequent combining of the radicals formed. In fact, hydrogen-atom abstraction involving the photoexcited triplet state of benzophenone and an appropriate hydrogen donating molecule has been the subject of extensive research.

Irradiation of benzophenone with UV light excites the benzophenone molecule to the excited singlet state $S_1(n, \pi^*)$ or $S_2(\pi, \pi^*)$, respectively. The intersystem crossing (ISC) from $S_1(n, \pi^*)$ to the triplet state $T_1(n, \pi^*)$ occurs very efficiently forming the chemically active triplet state $T_1(n, \pi^*)$ (see Scheme 2.7.2.1 (116,117)). During this excitation of the carbonyl group, the π bond is broken and the triplet state T_1 of the benzophenone can be considered as a 1,2 diradical. Conjugation of the carbonyl group with the benzene rings lower the carbonyl π -bond energy and the resulting 1,2-diradical is resonance-stabilized. The 1,2-diradical formed in the triplet state of benzophenone has been shown to abstract hydrogen from hydrogen-donor molecules (RH) such as hydrocarbons, alcohols, ethers, amines, thiols, sulphides, phenols, and even from macromolecules and produce a benzophenone ketyl radical, also called a diphenylhydroxymethyl radical or semipinacol radical (118-129) (see Scheme 2.7.2.2) (117). Intermolecular hydrogen-atom abstraction from polymers involving the photoexcited triplet state of the aromatic carbonyl group has been known for some time (11,12). It has also been reported that



Scheme 2.7.2.1. Schematic representation of the formation triplet state of benzophenone upon UV irradiation (117).



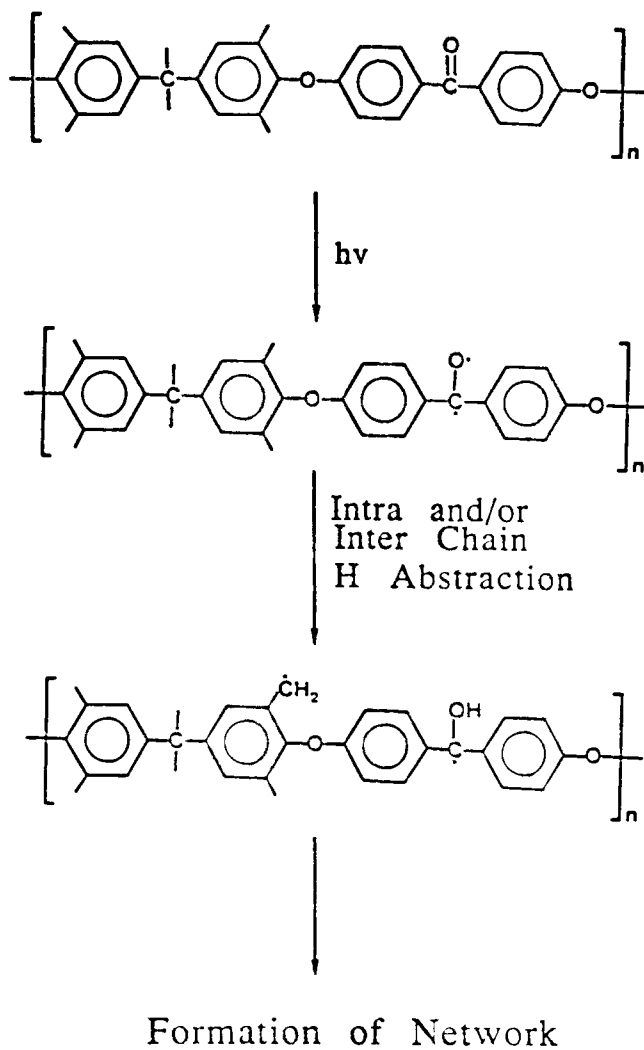
Scheme 2.7.2.2. Schematic representation of a hydrogen abstraction reaction of the 1,2-diradical benzophenone from a hydrogen-donor molecule (117).

benzophenone is able to crosslink vinyl polymers by a hydrogen abstraction reaction (13).

Mohanty et al. showed that polymers such as tetramethyl Bis-A polyaryl ether ketones, with aromatic keto and alkyl substituted aromatic groups incorporated into the polymer backbone, were photocrosslinkable, and an "intermolecular hydrogen-atom abstraction" mechanism was proposed (14,15,16). Scheme 2.7.2.3 shows the reaction sequence proposed for this polymer system.

Recently Scaiano and coworkers studied the mechanisms of crosslinking of the inherently photosensitive polyimides containing a benzophenone moiety by using phosphorescence techniques (18,19,130). The phosphorescence study was performed on a model compound shown in Figure 2.7.2.2A (18,19,130). Irradiation of a solution of the model compound in NMP with the 365nm mercury line was found to lead almost entirely to the photoreduced benzhydrol system shown in Figure 2.7.2.2C. The formation of the photoreduced system is thought first to go through the ketyl radical shown in Figure 2.7.2.2B produced in the photoreduction of the triplet state of A.

Their results indicated that the triplet state of A behaves like a highly reactive benzophenone and undergoes photoreduction quite readily. The authors wanted to determine if the phthalimide carbonyl groups were involved in the photocrosslinking reaction. They thought that species shown in Figure 2.7.2.2D could be involved which could undergo ring



Scheme 2.7.2.3. Photocrosslinking reaction of tetramethyl bis-A polyarylene ether ketone (14,15,16).

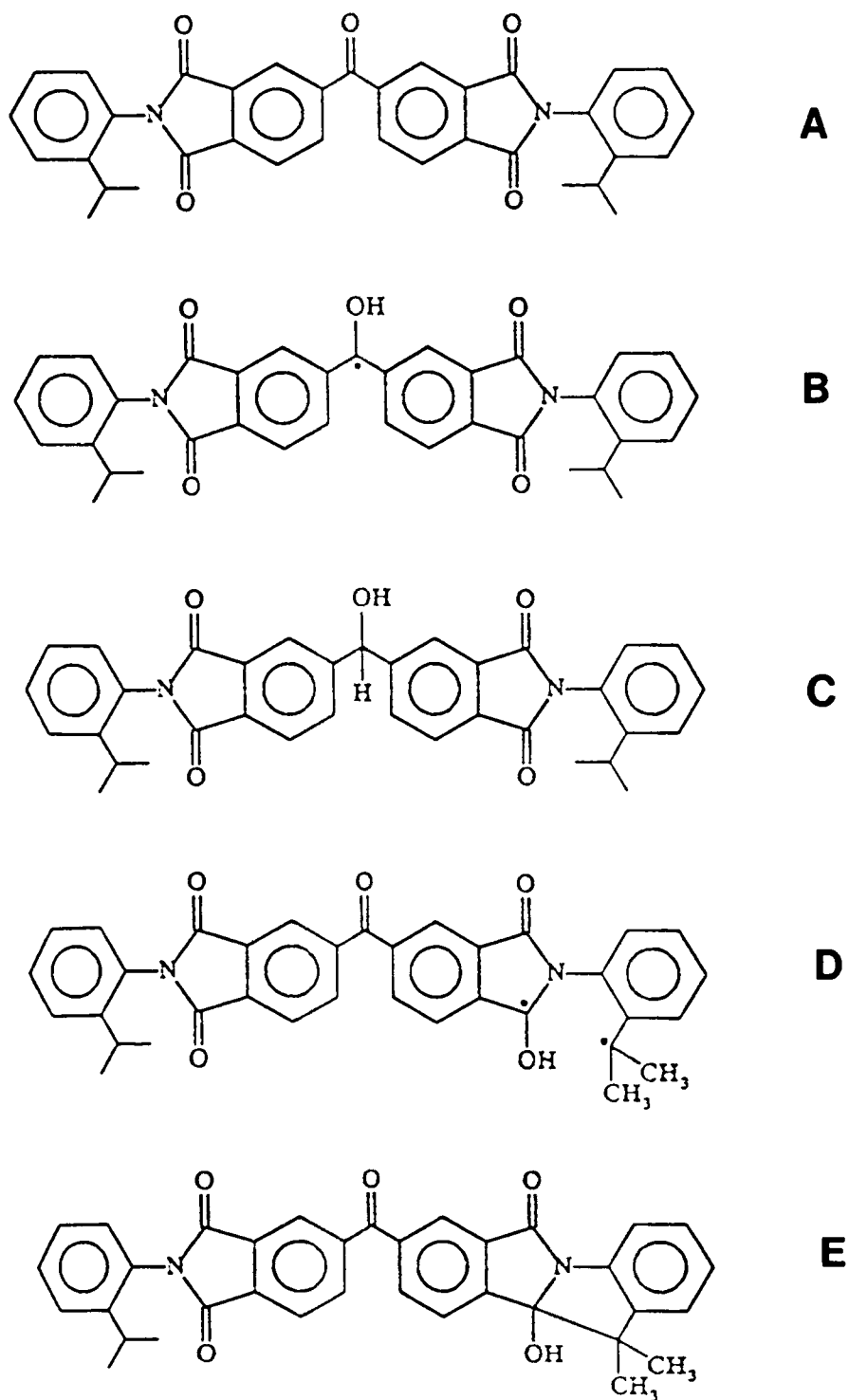


Figure 2.7.2.2. Structures of the model compound and photo-excited intermediates and products (130).

closure to form an alcohol as shown in Figure 2.7.2.2E. However, all their evidence suggested that D and E were not involved at all, indicating that the excitation energy remains largely localized in the benzophenone-like moiety.

Scaiano and coworkers concluded that the photosensitive polyimides are photosensitive due to the benzophenone-like behavior of their triplet state. The photocrosslinking reaction results from the reaction of the intermediate ketyl following hydrogen abstraction from the alkyl substituents and crosslinking occurs by the combination of radicals formed.

Another study on the photocrosslinking mechanism of benzophenone containing polyimides was performed by Lin and coworkers on polymeric systems rather than model compounds (17). To investigate the involvement of benzophenone and of the hydrogen donors in the cross-linking of the polyimides they prepared a series of copolymers using benzophenone tetracarboxylic dianhydride (BTDA), tetraethylmethylenedianiline (TEMDA), and 1,3-Bis (aminopropyl) tetramethylsiloxane (BADs). A series of copolymers using different ratios of TEMDA to BADs was prepared in order to see how the amount of hydrogen donor species, in this case ethyl substituents, affects the photosensitivity of the copolymers formed. As indicated in Table 2.7.2.2 the less TEMDA incorporated into the polymer backbone the more exposure dose is required to cause crosslinking (17), indicating that the photosensitivity of polymers with the same benzophenone

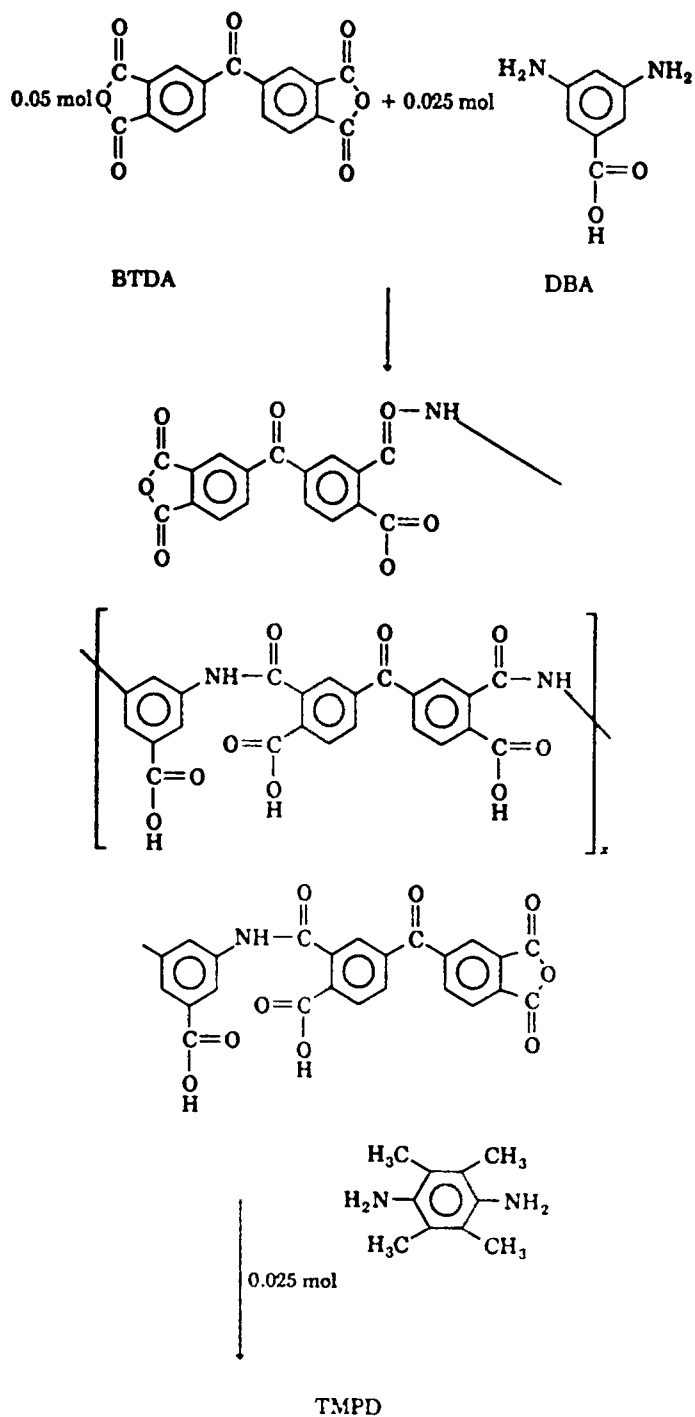
Table 2.7.2.2. Effect of Hydrogen Donor Content on Gel Dose (17).

polymer	TEMDA:BADs	gel dose, mJ/cm ²		
		air	nitrogen	oxygen
II	100:0	26.0	23.2	34.7
III	80:20	34.7	26.0	40.8
IV	50:50	66.5	60.7	75.2
IV	50:50	75.2	72.2	81.0
V	20:80	150	148	159
VI	0:100			

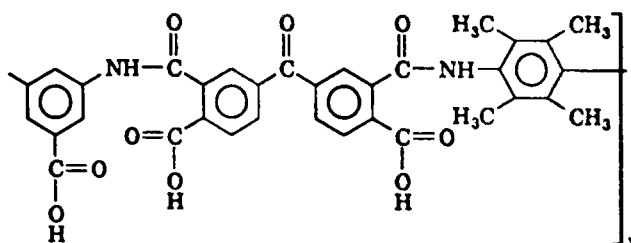
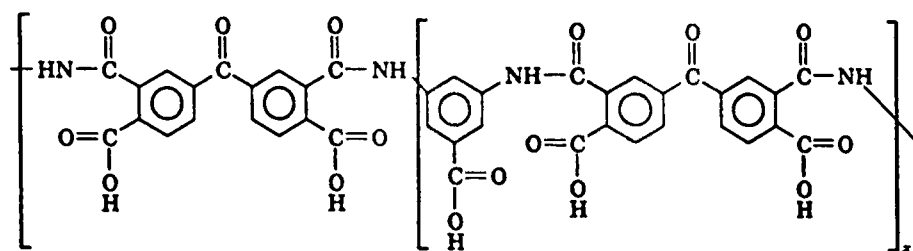
content is proportional to the content of hydrogen donors in the polymer.

A homopolymer using the dianhydride biphenyl-3,4;3',4'-tetracarboxylic dianhydride (BPDA) instead of BTDA was made using TEMDA as the diamine in order to determine the effects of the phthalimide carbonyls on the crosslinking mechanism. The homopolymer that did not contain the benzophenone moiety did not crosslink even after prolonged exposure to UV light indicating that the phthalimide carbonyls are not involved in the crosslinking reaction. Like the model study by Scaiano and coworkers, they concluded that the benzophenone moiety is needed in order to cause crosslinking, and crosslinking is brought about through hydrogen abstraction by the excited benzophenone moiety and subsequent radical coupling.

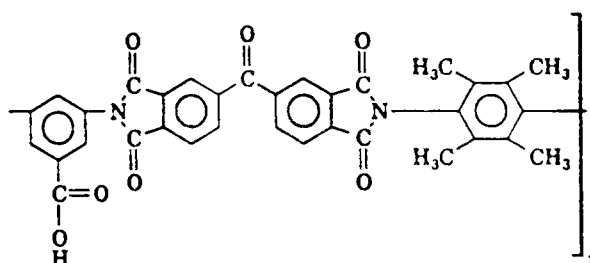
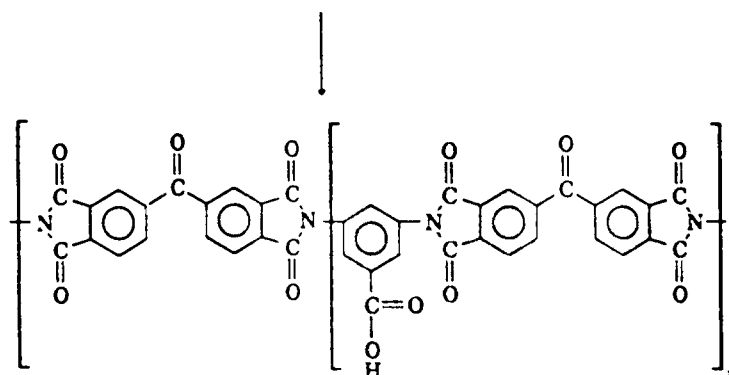
A novel photosensitive copolyimide based on Rubner's photocrosslinking reaction with methacrylic ester groups pendent to the polymer backbone was synthesized and characterized by Lee and coworkers (131). The synthesis of the photosensitive fully imidized polymer is shown in Scheme 2.7.2.4 (131). The copolyimide was synthesized from benzophenone tetracarboxylic dianhydride, 3,5-diaminobenzoic acid, and 2,3,5,6-tetramethyl-p-phenylene diamine. After complete imidization of the polyamic acid the monoepoxide, methacrylic acid glycidyl ether was added to the polyimide solution in order to react with the pendent carboxylic acid



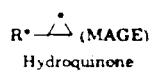
Scheme 2.7.2.4. Synthesis of photoreactive fully imidized polyimide with pendent methacrylic ester groups (131).



Polyamic acid



OSC

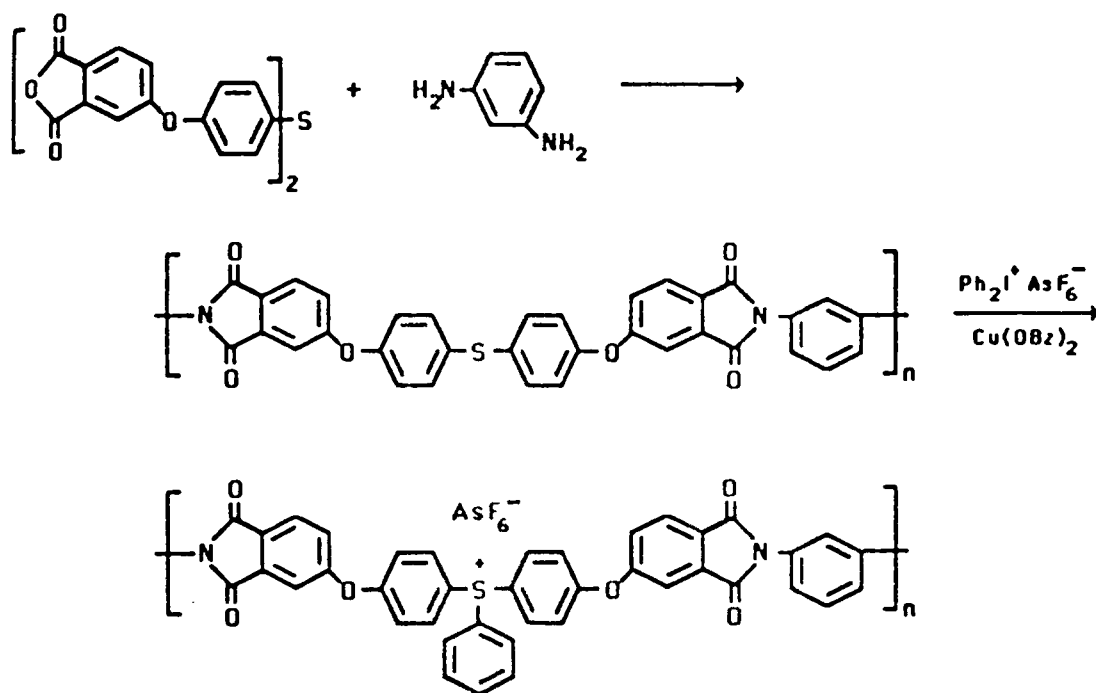


Scheme 2.7.2.4 (continued).

groups in the polyimide to form pendent methacrylic acid ester groups, responsible for the photocrosslinking. The copolyimide formed was demonstrated to be photosensitive and became insoluble after UV light exposure. Michler's ketone was added to the polyimide to act as a photosensitizer in the crosslinking reaction.

The major drawback of this type of photosensitive copolyimide is that the methacrylic ester groups pendent to the polymer backbone are cleaved and volatilized after heating above three hundred degrees C, causing shrinkage of about 20% in the formed polyimide pattern (131). Even though the shrinkage is not as great as in photoreactive polyamic acid systems ($> 40\%$), the shrinkage in the copolyimide is significant compared to the photosensitive polyimides reported by Pfeifer and Rohde, which only have a 5% shrinkage after being heated above 400°C (10).

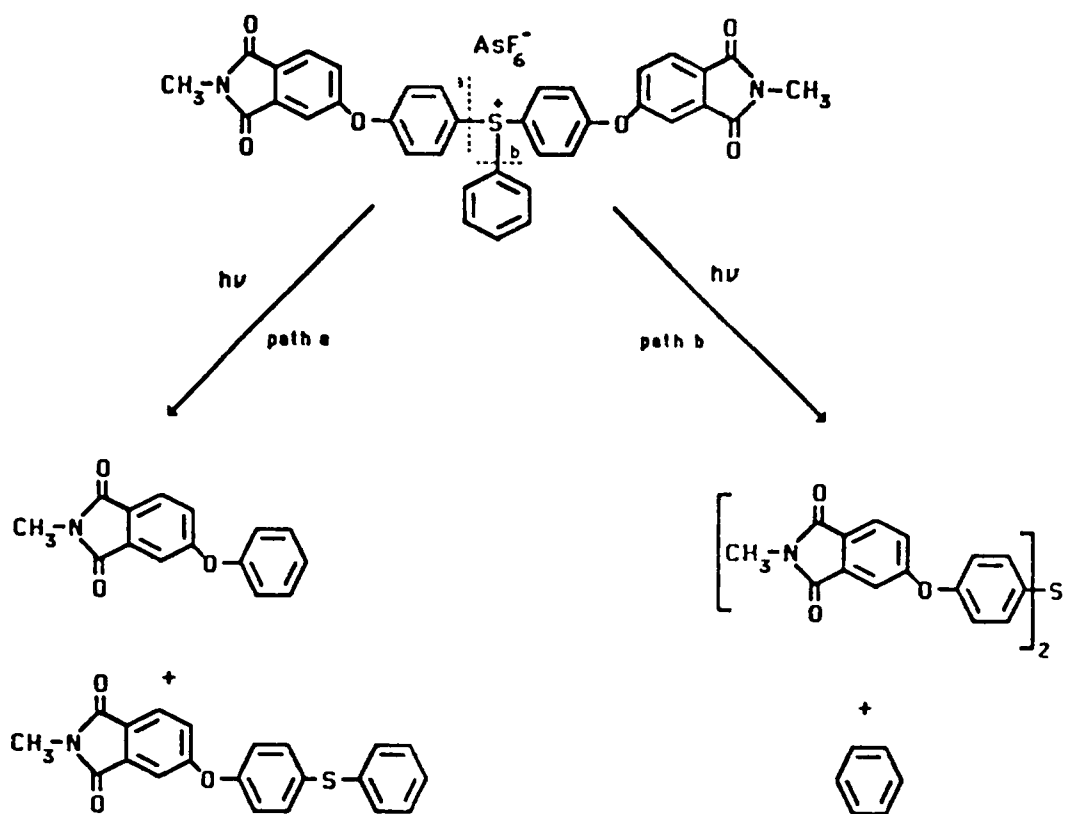
Novel photopositive polyimide systems were also recently investigated for use in microelectronic applications (132,133,134). J.V. Crivello and coworkers at General Electric Company synthesized all aromatic polyimides having diarylsulfide linkages in the main chain which were then subsequently phenylated with diphenyl iodonium salts to convert the diarylsulfide groups to triarylsulfonium salts. The photosensitive polyimides were synthesized according to the reaction pathway shown in Scheme 2.7.2.5 (132). Phenylation of the two sulfur containing polyimides was



Scheme 2.7.2.5. Synthesis of photopositive polyimide containing triarylsulfonium salts (132).

carried out at 125-130°C using diphenyliodonium hexafluorophosphates catalyzed by copper salts. The arylated polymers were soluble in dipolar aprotic solvents such as N-methylpyrrolidone, and dimethylformamide. The resulting photosensitive polyimide was shown to undergo main chain cleavage during photolysis using UV light. This cleavage of the triarylsulfonium salts is shown in Scheme 2.7.2.6 (132). The only UV study performed on these polymers was carried out in a solution of N-methylpyrrolidone using perylene as a photosensitizer. The molecular weight of the polyimides decreased during exposure to UV light caused from photolytic chain cleavage and followed by measuring the reduced viscosity as a function of exposure time. The authors found that there was a marked decrease in molecular weight of the polymer early in the photolysis. The rate of decrease in molecular weight slowed as the photolysis proceeded. The resulting increase in solubility which occurs as a result of the decrease in molecular weight on UV exposure can serve as a mechanism for photoimaging. These polyimides could be candidates for positive working, high temperature photoresist materials. However, only preliminary photoimaging studies were performed.

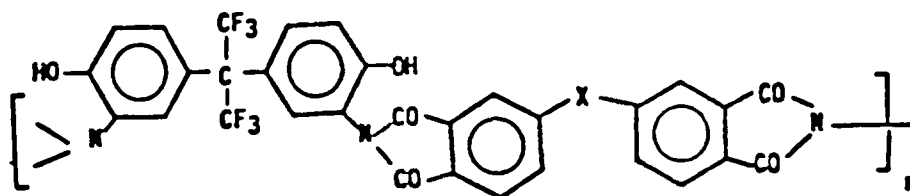
Khanna and coworkers from Hoechst Celanese Corporation recently reported new high temperature stable positive photoresist systems based on hydroxyl polyimide and polyimides containing the hexafluoroisopropylidene linking groups along the polymer backbone (133,134). The hydroxy polyimides were



Scheme 2.7.2.6. Schematic representation of C-S bond cleavage during photolysis (132).

synthesized by a high temperature solution condensation method. Table 2.7.2.3 shows the inherent viscosity and glass transition temperatures of the three hydroxy polyimides formed (133). The glass transition temperatures ranged from 250 to 300°C, and were stable at 350°C in air. The weight loss of 5 percent took place between 450 to 470°C. When these hydroxyl polyimides were formulated with a diazonaphthoquinone sensitizer a positive photoresist, which can be processed similar to conventional positive photoresists, was formed. The sensitivity of the polyimide resist was about 100 mJ/cm² with a contrast in the range of 1.5 to 2.0 (133). Photosensitive hydroxy polyamides that can be converted to polybenzoxazoles upon heating were also reported in these two papers. However, they will not be discussed here since they are not polyimides.

Table 2.7.2.3. Structure and Properties of Sixef Hydroxy Polyimide (133).



Where "X" is:	Inherent Viscosity ^a η inh (dl/g)	T_g^b (°C)	Temp. at 5 Percent Wt. Loss ^c (°C)
$\begin{array}{c} \text{CF}_3 \\ \\ -\text{C}- \\ \\ \text{CF}_3 \end{array}$	0.50	306	470
$-\text{O}-$	0.50	251	460
$\begin{array}{c} \text{O} \\ \\ -\text{C}- \end{array}$	0.51	259	450

^a Inherent viscosity at 25°C, 0.5 percent concentration in dimethylacetamide.

^b Glass transition temperature (T_g) using DSC at 20°C/min.

^c Thermal analysis using TGA in air at 20°C/min.

Chapter III

3.0 Experimental

3.1 Purification of Reagents and Solvents

In order to obtain high molecular weight photoreactive polyimide homo- and copolymers, it was important to start with extremely pure monomers and solvents and to maintain anhydrous conditions throughout the synthetic procedures. Therefore, monomers and reagents were carefully purified and solvents were distilled from drying agents using the apparatus shown in Figure 3.1.1. This apparatus allowed reduced pressure distillations and refluxing over drying agents prior to solvent collection. The distilled solvents were collected in round bottomed flasks and sealed with a rubber septum prior to use. The dried solvents were stored under nitrogen and were handled using syringe techniques to minimize moisture exposure.

3.1.1. Solvents Purification

3.1.1.2. N-Methyl-2-Pyrrolidone (NMP: Fisher) was dried for at least 12 hours by stirring over phosphorus pentoxide. Phosphorus pentoxide was used in order to remove amine impurities (135). The solvent was then distilled under reduced pressure generated by a mechanical vacuum pump (55°C)

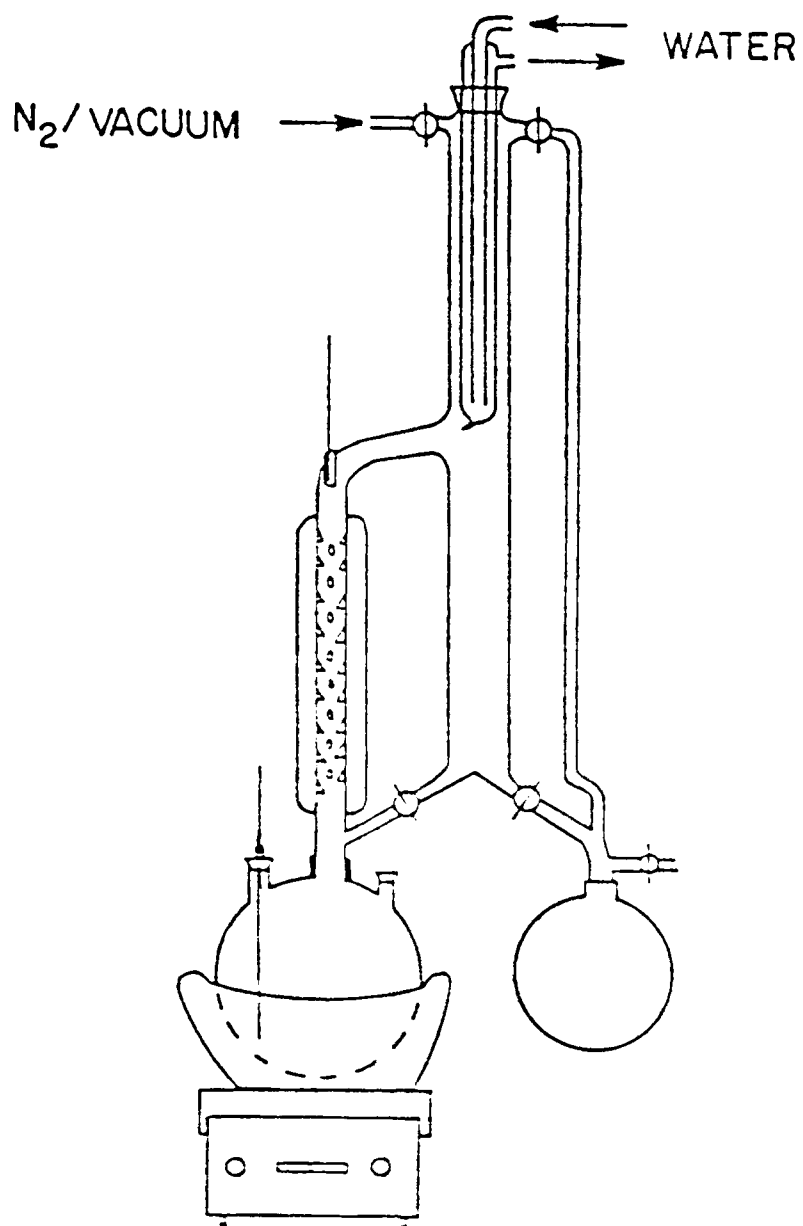


Figure 3.1.1. Apparatus used for the distillation of solvents.

(b.p. 205°C; at atmospheric pressure).

3.1.1.3 N-Cyclohexyl-2-Pyrrolidone (CHP: GAF) was dried for at least 12 hours by stirring over crushed calcium hydride. The solvent was then distilled under reduced pressure generated by a mechanical vacuum pump (b.p. 290°C).

3.1.1.4. Tetrahydrofuran (THF: Fisher) was dried for at least 12 hours by stirring over crushed calcium hydride. The solvent was then distilled at atmospheric pressure under a nitrogen gas purge (b.p. 76°C).

3.1.1.5. Toluene (Fisher) was dried for at least 12 hours by stirring over crushed calcium hydride. The solvent was then distilled at atmospheric pressure under a nitrogen gas purge (b.p. 110°C).

3.1.2. Monomer Purification

3.1.2.1 3,3',4,4'-Benzophenone Tetracarboxylic Acid Dianhydride (BTDA: Allco Company) was obtained as a white crystalline solid of ultra pure monomer grade. A thermal treatment served to form anhydride moieties from any remaining diacid functionalities (136). It was placed in a forced air convection oven at 150°C for 12 hours prior to use (mp = 224-226°C, lit. = 225-226.5°C; Allco Company communication).

3.1.2.2. 2,2-Bis (3,4-Dicarboxyphenyl) Hexafluoropropane Dianhydride (6FDA: Hoechst Celanese Corp.) was obtained as an electronic grade material (99 + % purity) and was essentially of monomer purity. It was placed in a forced air convection oven at 150°C for 12 hours prior to use in order to form anhydride moieties from any remaining diacid functionalities (mp = 245-246°C, lit. = 245-246.5°C; Hoechst Celanese Corp. Communication).

3.1.2.3. [4,4' - [1,4-Phenylene (1-Methylethylidene)] bisbenzenamine (Bis-P: Air Products Company) was obtained as a fine white powder (99% pure). Recrystallization from deoxygenated ethanol was chosen as the method for purification. Ethanol was deoxygenated by heating it to 35°C in an erlenmeyer flask and bubbling nitrogen through it for three hours. Bis-P was added to the deoxygenated ethanol until the solution became supersaturated. More ethanol was added until the solution became clear again. The heat was removed and the solution was cooled to room temperature. To further induce crystallization the flask was placed in the freezer for several hours. The white flake-like crystals of Bis-P were then isolated via filtration, dried in a vacuum oven for at least 8 hours at 60°C, and stored in a desiccator until needed (mp = 165-166°C, lit = 165°C; Air Products Communication).

3.1.2.4. [4,4'-[1,4-phenylene(1-methylethylidene)]bis(2,6-dimethylbenzenamine)] (TM Bis-P: Shell Chemical Company) was obtained as crude gray solid (88% pure). Recrystallization from anhydrous diethyl ether was chosen as the method for purification. 500 ml of diethyl ether was placed in a 1 liter Erlenmeyer flask and heated in a water bath to 30°C. TM Bis-P was added to the diethyl ether until the solution became supersaturated. More diethyl ether was added until the solution became clear again. 3 grams of activated charcoal was added to the warm solution. The dark colored solution was allowed to stand for 5 minutes and filtered through celite in order to completely remove the charcoal. The clear tan colored solution was then placed in a freezer to induce crystallization. The tan needle-like crystals of TM Bis-P were isolated via filtration. The recrystallization procedure was repeated twice more to further purify the TM Bis-P. After the third recrystallization, the white needle-like crystals were isolated via filtration, dried in a vacuum oven for at least 8 hours at 60°C, and stored in a desiccator until needed (mp = 154-155°C, lit = 150.5-154°C; Shell Chemical Company Communication).

3.1.2.5. 1,4 Phenylene Diamine (PDA: Aldrich) was obtained as a white crystalline material (99 + % pure) of monomer grade purity and was used as received without further purification (mp = 144-145°C, lit = 143-145°C; Aldrich Catalog).

3.1.2.6. 2,3,5,6 Tetramethyl-1,4-Phenylene Diamine (TMPDA: Pfaltz and Bauer) was obtained as a tan crystalline solid (97% pure). Recrystallization from anhydrous diethyl ether was chosen as the method of purification. 500 ml of anhydrous diethyl ether was placed in a 1 liter Erlenmeyer flask and heated in a water bath to 30°C. TMPDA was added to the diethyl ether until a supersaturated solution was obtained. More diethyl ether was added to the solution until it became clear again. 3 grams of activated charcoal was added to the warm solution. The black colored solution was allowed to stand for 5 minutes and then it was filtered through celite in order to completely remove the charcoal. The filtered solution was placed in a freezer for more than three hours to induce crystallization. The tan needle-like crystals of TMPDA were isolated via filtration. The recrystallization procedure was repeated twice more to further purify the TMPDA. After the third recrystallization, the light tan needle-like crystals were isolated via filtration, dried in a vacuum oven for at least 8 hours at 60°C, and stored in a desiccator until needed (mp = 150-151°C, lit = 149-150°C; Pfaltz and Bauer Catalog).

3.1.2.7. Bis(3-aminopropyl) tetramethyl disiloxane (DSX: Petrarch Systems Inc.) was obtained in monomer grade purity and was used without further purification (bp = 132°C, lit. = 132°C; Petrarch Systems Inc. Communication).

3.1.2.8. Octamethylcyclotetrasiloxane (D4: Union Carbide or Petrarch System Inc.) was obtained as a clear colorless liquid of high purity and was used without further purification (bp = 174°C, lit = 175-176°C; Petrarch Systems Inc. Communication).

3.1.2.9. m-Aminophenol (Aldrich) was obtained as a fine white powder (98% pure). Sublimation was chosen as the method of purification. The meta-aminophenol was placed in the bottom of the sublimator and the cold finger was filled with a dry ice and acetone mixture. A mechanical vacuum pump was used to insure that an adequate vacuum was obtained. The sublimator was heated by an oil bath to 110°C. After the white crystals formed on the cold finger, the crystals were collected into a jar and placed in the desiccator until needed (mp. 125-126°C, lit. = 124-126°C; Aldrich Catalog).

3.1.2.10. Isophthaloyl dichloride (Aldrich) was obtained as a fine white powder (98% pure). Sublimation was chosen as the method of purification. The isophthaloyl dichloride was placed in the bottom of the sublimator and the cold finger was filled with a dry ice and acetone mixture. A mechanical vacuum pump was used to ensure an adequate vacuum was obtained. The sublimator was heated to 35°C in a water bath. After white crystals formed on the cold finger, they were collected in a bottle, sealed with Teflon tape and placed in

a dessicator until needed (mp = 43-44°C, lit. = 43-44°C; Aldrich Catalog).

3.2 Synthesis of monomers and amine terminated siloxane oligomers

3.2.1. Synthesis of 1,3-Bis (4-fluorobenzoyl) benzene 1,3-Bis(4-fluorobenzoyl) benzene was synthesized by a Friedel-Crafts acylation of fluorobenzene with isophthaloyl chloride using anhydrous aluminum chloride as the Lewis acid. The reaction was run at 80°C for five hours in 100% excess fluorobenzene. The crude product was recrystallized from toluene, isolated via filtration, and dried in the vacuum oven at 80°C for 48 hours. The white flake-like crystals were stored in a desiccator until needed (mp = 179-180°C, lit. = 177.5-178.5°C (137)). Anal. Calcd for C₂₀H₁₂O₂F₂: C, 74.53; H, 3.75. Found: C, 74.63; H, 3.75.

3.2.2. Synthesis of 1,3-Bis (3-Aminophenoxy-4'-Benzoyl) benzene.

1,3-Bis (4-fluorobenzoyl) benzene (50.0000g, 0.1551 moles) 3-aminophenol (35.5508g, 0.3258 moles), anhydrous potassium carbonate (51.4556g, 0.3723 moles), DMAc (270 ml), and toluene (130 ml) were placed in a 500 ml four-necked round bottom flask equipped with a Dean-Stark trap, condenser with drying tube, nitrogen gas inlet, thermometer and a mechanical

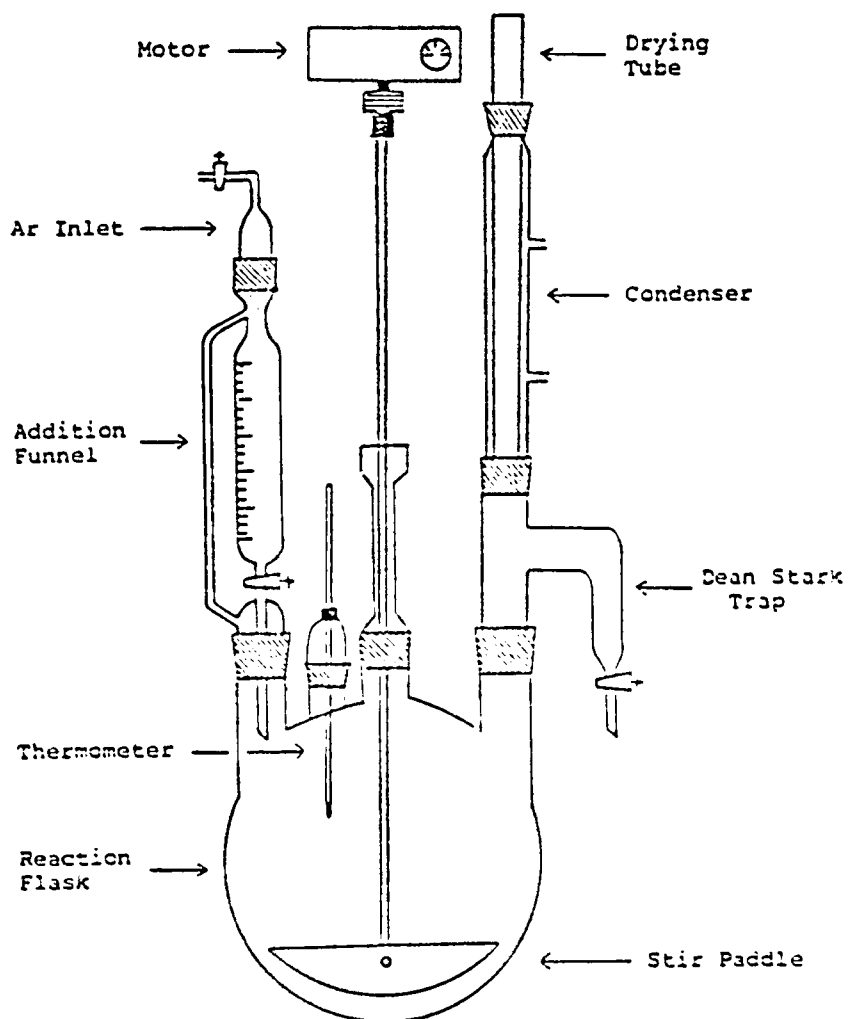


Figure 3.2.2.1. Apparatus used for diamine synthesis.

stirrer (see Figure 3.2.2.1). The reaction solution was heated to 130°C using an oil bath and the reaction mixture was stirred for 19 hours at 130°C under a nitrogen gas purge. Water was removed by azeotropic distillation with toluene. After 19 hours at 130°C, the temperature was increased to 145°C for 5 hours to insure that the reaction was complete. The reaction solution was allowed to cool to room temperature and subsequently added to hot deoxygenated water to precipitate a solid which was isolated by filtration, and dried in a vacuum oven at 80°C for 8 hours. The crude product was further purified by two recrystallizations from toluene. The purified product was isolated via filtration and dried at 80°C for two days in a vacuum oven. The pale yellow solid was obtained in 66% yield after the two recrystallizations and stored in a desiccator until needed (mp = 140-142°C, lit. = 142-144°C (138)). Anal. Calcd for C₃₂H₂₄O₄N₂: C, 76.79; H, 4.83; N, 5.60. Found: C, 76.66; H, 4.85; N, 5.52.

3.2.3. Aminopropyl-Terminated Polydimethylsiloxane Oligomers.

The siloxane oligomer was synthesized in bulk via an anionic ring opening equilibration reaction involving aminopropyl disiloxane and the cyclic tetramer commonly known as D₄ (139). The polymerization was carried out in a 500ml three-necked round bottom flask equipped with a nitrogen gas inlet thermometer, condenser, drying tube and mechanical

stirrer. In order to synthesize a 2,500 g/mole aminopropyl terminated polydimethylsiloxane oligomer, 30.0000g (0.1207 moles) of bis (3-aminopropyl) disiloxane along with 271.8109g (0.9164 moles) of D_4 were placed into the round bottom flask. The flask was heated to 80°C by an oil bath and 3.0181g (1.0 wt%) of tetramethylammonium siloxanolate was added to the stirring solution.

The reaction was allowed to proceed for 48 hours at 80°C under a dry nitrogen gas purge to insure that the equilibration was achieved. After the 48 hours, the reaction temperature was raised to 150°C for 3 hours to decompose and volatilize the catalyst. The solution was then cooled to room temperature and transferred to a vacuum distillation apparatus and the cyclics formed were removed via vacuum stripping. The final molecular weight of the aminopropyl-terminated siloxane oligomer was determined by potentiometric titration of the amine end groups with 0.1 N alcoholic HCl and was found to be 2465 g/mole. The siloxane oligomer was placed in a glass jar and stored in a desiccator until needed.

3.3. Synthesis of high molecular weight polyimide homo- and copolymers.

High molecular weight photoreactive polyimide homo- and copolymers and siloxane modified polyimide segmented copolymers were synthesized by the classical two-step method. The first step was the synthesis of soluble poly(amic acid)

precursors by the reaction of aromatic diamines with aromatic dianhydrides in a dipolar aprotic solvent. The prepolymers were then cyclodehydrated by two different thermal methods to form the polyimides.

The poly(amic acids) were synthesized in a 250ml three necked round bottom flask equipped with a nitrogen gas inlet, thermometer, drying tube, overhead stirrer and in the case of poly(amic acid siloxanes) an addition funnel was used as shown in Figure 3.3.1. The apparatus was flamed just prior to use via a Bunsen burner while under a nitrogen gas purge in order to remove any residual moisture from the glassware. Five representative synthetic procedures will be outlined to synthesize various poly(amic acids). One general synthetic procedure for poly(amic acid) homopolymers, another procedure for copolymers with varying ratios of different aromatic diamines, another for copolymers with varying ratios of different aromatic dianhydrides, still another modified procedure for synthesizing homo- and copolymers with the Bis-P diamine, and finally a synthetic procedure for poly(amic acid siloxane) segmented copolymers will be discussed.

3.3.1. High Molecular Weight Poly(amic acid) Homopolymers

A typical high molecular weight poly(amic acid) homopolymer is synthesized by a solution condensation reaction with aromatic diamines and dianhydrides at room temperature in the dipolar aprotic solvent N-methyl pyrrolidone. The

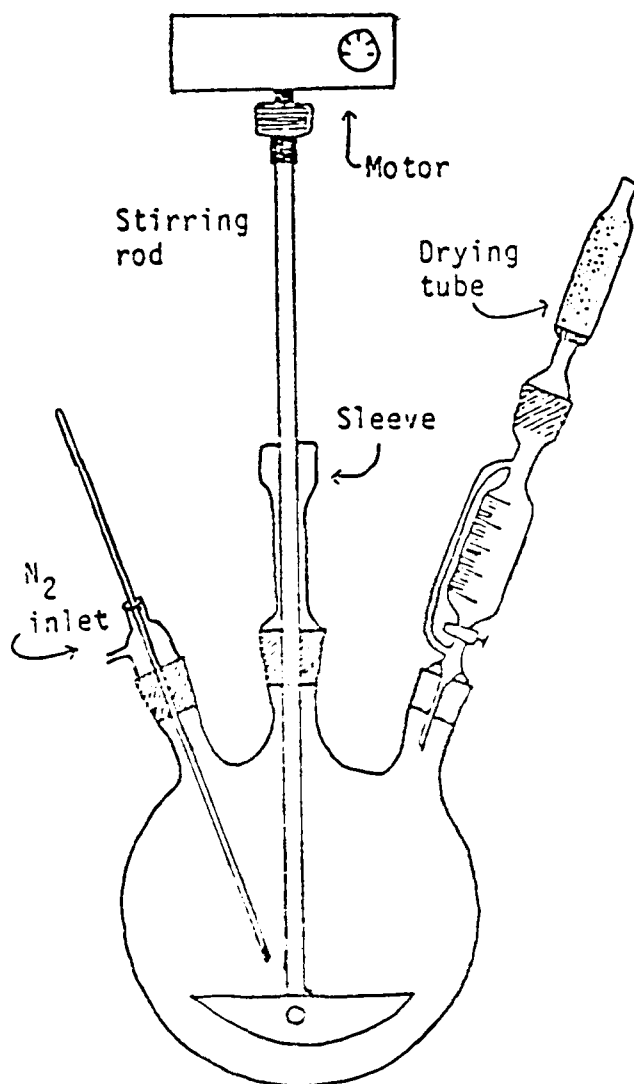


Figure 3.3.1. Apparatus used for poly(amic acid) synthesis.

following is a representative poly(amic acid) homopolymer polymerization procedure. 8.6654g of TMPDA (0.05276 moles) was dissolved in 75 ml of distilled NMP in a 250ml round bottom flask equipped as shown in Figure 3.3.1 (without the addition funnel). After the TMPDA was completely dissolved, 17.0000g of BTDA (0.05276 moles) was slowly added via a glass funnel to the stirring diamine solution and the funnel was rinsed with 25ml of NMP. After the BTDA was added, the reaction solution turned a dark red color and an exotherm of approximately 10°C was observed. The deep red solution turned to a golden yellow solution and the exotherm subsided after approximately 20 minutes. The reaction was allowed to continue for at least 8 hours under a nitrogen gas purge at room temperature to insure that high molecular weight poly(amic acid) was obtained. The viscosity of the solution rose steadily as the poly(amic acid) reaction proceeded. The clear golden colored high molecular weight poly(amic acid) obtained was immediately cyclodehydrated to form the polyimide.

3.3.2. High Molecular Weight Poly(amic acid) Copolymers

High molecular weight poly(amic acid) copolymers were synthesized by a similar solution condensation reaction by either varying the ratio of the moles of two different aromatic diamines or the ratio of the moles of two different aromatic dianhydrides. The following are representative

synthetic procedures for both types of copolymer synthesis.

3.3.2.1. Poly(amic acid) copolymers by varying the mole ratio of aromatic diamines

6.1168g of TMPDA (0.03724 moles) was dissolved in 40ml of dried NMP in a 250ml three necked round bottom flask equipped as shown in Figure 3.3.1 (without the addition funnel). Next, 4.9729g of TM Bis-P (0.01241 moles) was added to the stirring solution via glass funnel and rinsed with 40ml of NMP in order to ensure all the diamine was washed into the flask. After both the diamines were completely dissolved, 16.0000g of BTDA (0.04965) was added to the stirring solution and washed with 30ml more of NMP. The reaction solution immediately turned a dark red color after the addition of dianhydride, and an exotherm of approximately 10°C was observed. After 20 minutes of reaction time the solution turned from dark red to golden yellow color and the exotherm subsided. The reaction was allowed to proceed for 8 more hours at room temperature under a dry nitrogen gas purge. The clear golden colored poly(amic acid) copolymer obtained was immediately cyclodehydrated to form the polyimide.

3.3.2.2. Poly(amic acid) Copolymers by varying the mole ratio of aromatic dianhydrides

Copolymers made by varying the mole ratio of dianhydrides were made by a reverse monomer addition procedure. Rather

than first dissolving the diamine and then adding the dianhydride, the two dianhydrides were dissolved first and the diamine was added to the stirring solution. This was done to insure that more random copolymers were formed.

5.0000g of BTDA (0.01552 moles) was dissolved in 30ml of distilled NMP in a 250ml round bottom flask equipped as shown in Figure 3.3.1 (without the addition funnel). 6.8932g of 6FDA (0.01552 moles) was added to the stirring solution via a glass funnel and the funnel was rinsed with 30ml of NMP in order to wash all the dianhydride into the reaction flask. After the dianhydrides were completely dissolved, 5.0972g of TMPDA (0.03106 moles) was added to the stirring solution through the glass funnel and washed into the flask with 30ml more of NMP. The reaction solution turned a dark red color and an exotherm of 10°C was observed. After approximately 20 minutes the reaction solution turned a golden yellow color and the reaction temperature returned to room temperature. The poly(amic acid) solution was allowed to react for 8 more hours under a dry nitrogen purge to insure that high molecular weight was obtained. The viscosity of the solution increased as the reaction proceeded. The golden yellow poly(amic acid) solution was then imidized to form the high molecular weight polyimide.

3.3.3. High Temperature poly(amic acid) synthesis

Poly(amic acid) homo- and copolymers made with the Bis-

P diamine had to be synthesized by a modified high temperature poly(amic acid) solution condensation procedure due to the insolubility of the Bis-P diamine in NMP at room temperature. Therefore, the NMP solution had to be heated above 60°C in order for the diamine to completely dissolve and allow a homogeneous solution to be formed.

1.6038g of Bis-P (0.004656 moles) was dissolved in 25ml of NMP at 65°C in a 250ml three-necked round bottom flask equipped as shown in Figure 3.3.1 (without the addition funnel). The round bottom flask was heated to 65°C by an oil bath. After the Bis-P completely dissolved, 5.5951g of TMBis-P (0.01397 moles) was added to the stirring solution and rinsed with 25ml of NMP. Next, 6.0000g of BTDA was added to the stirring diamine solution and 25ml of NMP was used to rinse the residual BTDA into the reaction flask. A dark red solution was formed during the addition of BTDA. After approximately 5 minutes of reaction time, the BTDA completely dissolved and the reaction solution turned a golden yellow color. The heat was then removed from the reaction flask and since oligomers had already formed the solution remained clear and homogeneous when the temperature of the solution reached room temperature. The reaction was allowed to proceed for 8 more hours at room temperature under a dry nitrogen gas purge in order to insure that high molecular weight poly(amic acid) was obtained. The poly(amic acid) was then cyclodehydrated to form the polyimide.

3.3.4. Poly(amic acid siloxane) segmented copolymers

Due to the mismatch in solubilities of the aromatic monomers and aminopropyl terminated polydimethyl siloxane oligomers it was necessary to use a cosolvent system of NMP and THF in order to synthesize high molecular weight poly(amic acid siloxane) copolymers. The siloxane oligomers were soluble in THF but were not soluble in the dipolar aprotic solvents. On the other hand, the aromatic monomers and poly(amic acid siloxane) copolymers formed were not totally soluble in THF. Therefore, to obtain a homogeneous clear reaction solution both NMP and THF were employed at various volume percentages (140,141). The order of monomer addition was also found to be an important parameter in achieving homogeneous solutions and random segmented copolymers by Summers et al. (140,141). He found that by dissolving the dianhydride in a NMP/THF cosolvent system and adding dropwise a THF solution of the siloxane oligomer to the rapidly stirring dianhydride solution an anhydride capped siloxane oligomer could be obtained. Addition of a second aromatic diamine would react with the capped siloxane oligomer forming a more homogeneous solution. Even high weight percents of siloxane oligomers and high molecular weight siloxane oligomers could be incorporated into the polymer backbone using this "capping procedure" (140,141). Therefore, a similar procedure was used for all siloxane modified photoreactive polyimide copolymers. A representative

procedure will be discussed here.

8.0000g of BTDA (0.02483 moles) was dissolved in 40ml of NMP and 60ml of THF in a 500ml round bottom flask equipped as shown in Figure 3.3.1. 3.0788g of aminopropyl polydimethyl siloxane oligomer (0.001249 moles) with a number average molecular weight 2,465g/mole was dissolved in 20ml of THF and placed in an addition funnel. The siloxane oligomer was added dropwise to the rapidly stirring BTDA solution. After all the siloxane oligomer was added, 25ml of THF was placed in the addition funnel and added dropwise to the solution in order to rinse out any residual siloxane oligomer into the reaction flask.

The solution was allowed to react further for 10 minutes before addition of the second aromatic diamine. 9.4455g of TMBis-P (0.02358 moles) was added to the stirring solution via a glass funnel and 30ml of NMP was added to rinse the TMBis-P into the reaction flask. After the addition of TMBis-P, the solution turned a dark orange color and an exotherm of 5°C was observed. The reaction solution turned from dark orange to a golden yellow solution in approximately 10 minutes. The solution was slightly cloudy due to incomplete solvation of the siloxane oligomer. Therefore, 25ml of THF was added to the flask and a clear solution was obtained. The reaction was allowed to proceed for 18 hours at room temperature in a nitrogen gas purge. The golden colored

poly(amic acid siloxane) solution was then cyclodehydrated to form the polyimide siloxane copolymer.

3.3.5. Imidization of poly(amic acid) prepolymers

3.3.5.1 Bulk thermal imidization

A common procedure for cyclodehydrating a poly(amic acid) to the polyimide form is via thermal bulk imidization. This procedure is limited to polyimide films or coatings and typically renders an insoluble product.

The preformed poly(amic acid) solution was poured onto a clean dry glass plate and a "doctor blade" was used to draw down a uniformly thick film ranging in thickness from 5-25 mils. The glass plate was then placed in a level vacuum oven or forced air convection oven at 80°C for one hour to remove most of the solvent. The temperature was increased to 100°C for one hour, then raised to 200°C for another hour, and finally raised to 300°C for one hour. After the cure cycle, the oven was turned off and the film was allowed to cool slowly to room temperature. The cured film was removed from the glass plate using a razor blade to pry up a small section of the film. Typically, the film would release itself from the glass plate within a few minutes. Films that would not come off the plate by themselves were placed in a water bath in order to float the films off the plate. Films that were in contact with water were placed back into the oven at 150°C

for two hours. An identical cure cycle was used for all poly(amic acids) imidized in bulk.

3.3.5.2. Solution Imidization

This method of imidization was commonly used for cyclodehydrating poly(amic acid) prepolymers and was found to be highly versatile for obtaining soluble fully cyclodehydrated polyimide homo- and copolymers (140-143). Some polyimides obtained were not soluble due to their chemical composition and rigid polymer backbone structure and would prematurely precipitate out of solution. However, a majority of the photoimageable polyimides described herein were found to be soluble and processable when imidized by this method.

A cosolvent solution of NMP and cyclohexyl pyrrolidinone (CHP) was used in the solution imidization procedure. The ratio of NMP to CHP was approximately 80/20 volume percent. The CHP acts as an "azeotroping solvent" and effectively removes the water of imidization from the reaction solution and drives the reaction to completion without hydrolyzing the poly(amic acid). Since the polymer was solvated by the dipolar aprotic solvents during imidization, a soluble high molecular weight polyimide was formed. The solution imidizations were generally run at 10 to 20 percent solids content. A representative detailed procedure will be outlined for a solution imidization of a poly(amic acid siloxane) with

15 weight percent siloxane (molecular weight of 2,465g/mole) content. The poly(amic acid siloxane), 20g total, was present in its reaction solution of 70ml of NMP and 130ml of THF.

A four necked 500ml round bottom flask equipped with a nitrogen gas inlet, thermometer, Dean-Stark trap, condenser, drying tube, and mechanical stirrer was set up as shown in Figure 3.3.5.2.1. 30ml of NMP and 25ml of CHP were added to the round bottom flask and heated to 165°C via a hot oil bath. The poly(amic acid siloxane) solution was slowly poured into the flask via a glass funnel while the heated NMP/CHP solvents were stirring. The THF boiled off rapidly and was carried over and collected by the Dean-Stark trap by a nitrogen gas purge. After approximately 15 minutes, all 130ml of THF was collected. The solution imidization was allowed to proceed for 18 hours at 165°C under a nitrogen gas purge. The water of imidization and small amounts of NMP were collected in the Dean-Stark trap during the imidization procedure. 35ml of NMP was added to the stirring solution, and the solution was allowed to cool to room temperature by removing the hot oil bath. The dark brown viscous poly(imide siloxane) solution was transferred to a 500ml separatory funnel and precipitated dropwise into a rapidly stirring solution of methanol and water, 75% of the solution was methanol. The solid poly(imide siloxane) was isolated by vacuum filtration, and placed in a vacuum oven at 100°C for 24 hours. A second precipitation was done by redissolving the polyimide in either NMP or methylene

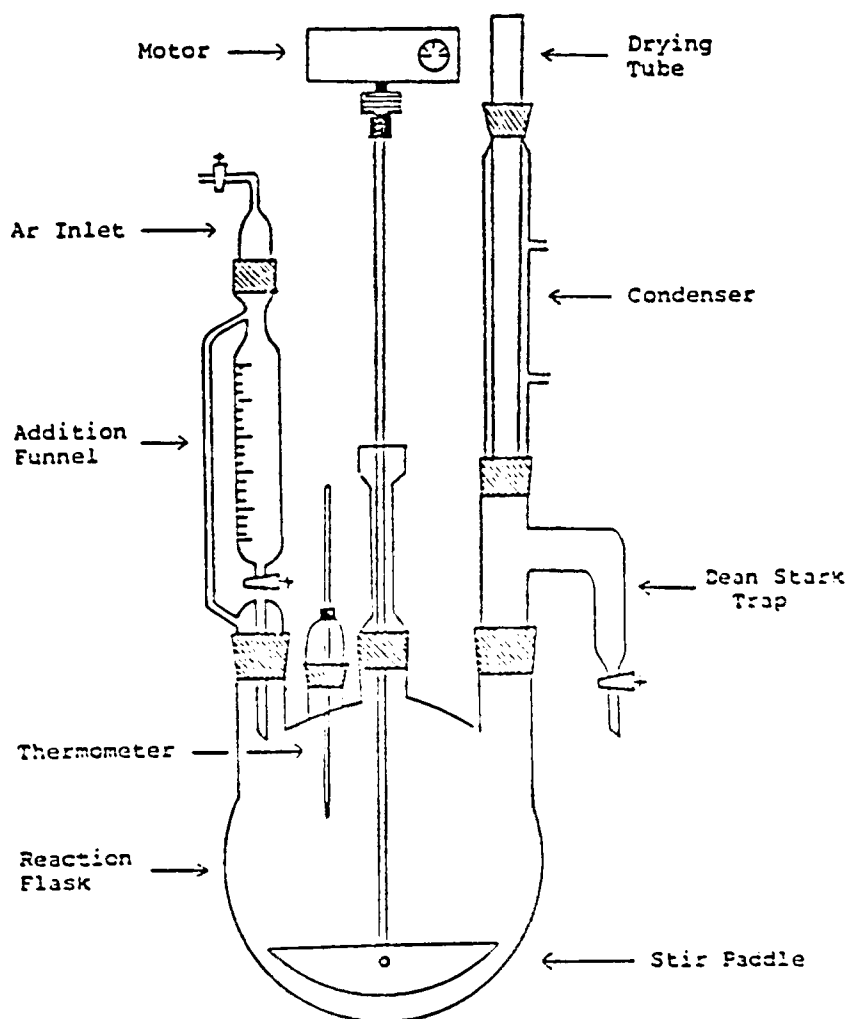


Figure 3.3.5.2.1. Apparatus used for solution imidization

chloride and reprecipitated and isolated as described above. The final dried poly(imide siloxane) was placed in a dark brown glass jar to ensure that UV light would not crosslink the polymer during storage.

3.4. Characterization of polymers and monomers

3.4.1. Titration of aminopropyl terminated siloxane oligomers

Potentiometric titrations of the amine functional siloxane oligomers were carried out using a Fisher Scientific Titrimeter II operated in the automatic endpoint seeking mode. A standard calomel electrode and reference electrode were used in the titrations and were stored in buffered solutions when not in use.

The aminopropyl polydimethylsiloxane oligomers were dissolved in isopropanol in a 100ml beaker and stirred until completely solvated. The electrodes were inserted into the solution and the titration was started by computer control. The aminopropyl endgroups were titrated with 0.1N alcoholic HCl. The computer controlled titrator both detected and recorded the endpoint by measuring the change in potential upon addition of the titrant. A reference titration was performed on just the blank isopropanol by titrating the exact volume used with the sample until the potential endpoint was reached. The reference was then subtracted from the endpoint

value of the sample and the number average molecular weight of the siloxane oligomer was calculated by the computer using the formula:

$$M_n = (\text{wt}) (N) / (C) (V)$$

where (wt) is the weight of aminopropyl terminated siloxane oligomer in the sample, (N) is the number of endgroups per molecule (in this case 2), (C) is the concentration of the titrant (0.1N HCl) and (V) is the corrected volume of the titrant used.

3.4.2. Intrinsic Viscosities

Intrinsic viscosities were determined for a various polyimide homo- and copolymers in order to determine relative molecular weights. Cannon-Ubbelohde dilution viscometers with various capillary sizes were used to collect data to determine intrinsic viscosities. Typically samples were dissolved in NMP and run at 25°C in a temperature controlled water bath. The intrinsic viscosity values were obtained by using four different polymer concentrations and the results were linearly extrapolated to the zero concentration.

3.4.3. Fourier Transform Infrared Spectroscopy (FTIR)

FTIR was used to both monitor the imidization process during solution imidization and to obtain IR spectra of the final polymers and monomers using a Nicolet MX-1 spectrophotometer. Polymer samples were analyzed by casting

thin films on salt plates and low molecular weight monomers were run as KBr pellets. The spectra were stored on magnetic disk for later reference. Progress of the solution imidization was monitored by the appearance of spectral imide bands at 1778 cm^{-1} and 725 cm^{-1} and the disappearance of the amide bond spectral band at 1546 cm^{-1} .

3.4.4. Proton Nuclear Magnetic Resonance ($^1\text{H-NMR}$)

Proton NMR was used to obtain chemical composition information of both polymers and monomers synthesized. Samples were run in deuterated solvents such as deuterated chloroform and DMSO at concentrations ranging from 5 to 15% and at ambient temperatures using either an Bruker 270 MHz WP270SY instrument or the Bruker 200 MHz WP200SY instrument.

3.4.5. Ultraviolet and Visible Spectrophotometry (UV-Vis)

UV-Vis spectra were obtained on thin polymer films spun cast on quartz wafers using an IBM 9430 UV-Visible spectrophotometer. The thin polyimide films were cast from approximately ten percent solid solutions of polyimide in NMP by using a spin coater at speeds in the range of 2,000 to 6,000 rpms. The quartz wafers were placed on a hot plate at 125°C for 15 minutes to drive off residual solvent. The UV spectra were generally recorded from 200nm to 400nm. Optical densities of the various polyimide films were then calculated by dividing the absorbance of the polyimide film at a certain

wavelength by the film thickness as determined by a profilometer.

3.4.6. Profilometer film thickness measurement

A Dektak II profilometer was used to measure the film thickness of solution spin-coated polyimide films. The diamond tipped stylus was placed in contact with the surface of the film and the bare quartz wafer and subjected to a shear stress. The displacement of the stylus from the film to the bare quartz surface was recorded by computer and the thickness of the film was determined. Film thickness could be measured with a precision of $\pm 10\text{nm}$.

3.4.7. Differential Scanning Calorimetry (DSC)

DSC was used to determine the glass transition temperatures of the polyimide homo- and copolymers with either a Perkin Elmer Model DSC-II or the DuPont Instruments 912 DSC. DSC scans were run under a nitrogen atmosphere at $10^{\circ}\text{C}/\text{min}$ with a sensitivity of $10\text{ mcal}/\text{sec}$. The samples were scanned at least two times to accurately determine T_g values. The values reported were obtained from the second heating cycle after heating once and rapid cooling. The transition temperatures were taken as the midpoint of the endotherm.

3.4.8. Dynamic Mechanical Thermal Analysis (DMTA)

Glass transition temperatures of certain polyimide films

were also determined using a Polymer Laboratories Dynamic Mechanical Thermal Analyzer (DMTA). Films with thicknesses ranging from 3 to 10 mils were used in the measurements. A heating rate of 5°C/min and a frequency of 1Hz were used during analysis. Both the storage modulus and tan delta curves were obtained for all samples run. The glass transition temperature was taken as the peak of the tan delta damping curve.

3.4.9. Thermogravimetric Analysis (TGA)

TGA was performed on either a Perkin Elmer TMS-2 instrument or a DuPont Instruments 951 Thermogravimetric Analyzer in order to determine relative thermal stabilities of the homo- and copolymer samples. Thin films of the polymers were placed in a platinum pan which was connected to an electronic microbalance. Scans were run at a heating rate of 10°C/min in either an air or nitrogen atmosphere and the weight loss was measured as a function of time or temperature. Dynamic temperature scans were examined in the range of 25°C to 800°C. Isothermal scans were also run at 350°C for four hours in air and nitrogen atmospheres.

3.4.10 X-Ray Photoelectron Spectroscopy (XPS)

XPS surface analysis was performed on a Perkin Elmer PHI 5300 ESCA spectrometer using a Mg electrode as the X-ray source operated at 15kV. Spectra were obtained at two

different take-off angles of 15 degrees and 90 degrees. The 15° take-off angle was used to determine the surface atomic concentration of the elements in the polymer films relative to farther into the bulk of the films as determined by the 90° take-off angle. Thin films of siloxane modified polyimide copolymers were analyzed by securing free standing films directly to the sample holder using double stick tape. The binding energy of each photopeak was referenced to C 1s at 285eV. For data evaluation the Perkin-Elmer 7500 computer (PHI software version 1.8) was used to obtain atomic concentration values. Only one sample was analyzed for each polyimide system studied. No noticeable degradation of the polymer was observed after XPS analysis.

3.4.11. Photosensitivity and Contrast

Photosensitives of the various polyimide homo- and copolymers were determined by analyzing photosensitive response plots for each individual polymer system. Photosensitive response plots are typically used in determining the photosensitive properties of photoresists and are a plot of the film thickness remaining after exposure to UV light and development as a function of the exposure dose given to the polymer film. A typical photosensitive response plot for a negative photoresist is shown in Figure 3.4.11.1. The useful information obtained from such a plot is the gel dose (D_g), D_i , and the contrast. The gel dose is defined as

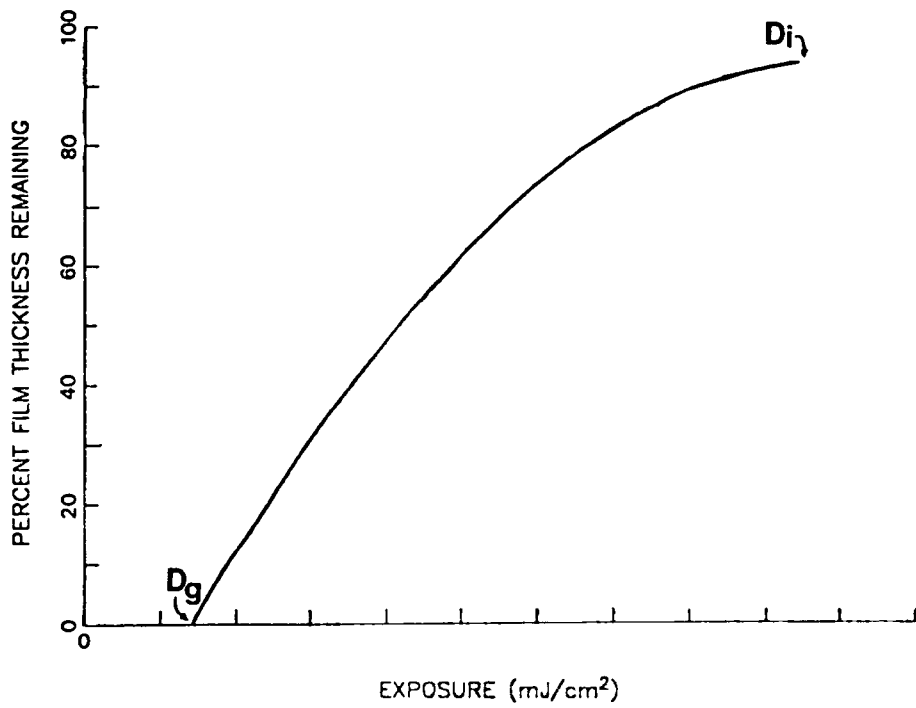


Figure 3.4.11.1. Photosensitive response plot for a negative photoresist

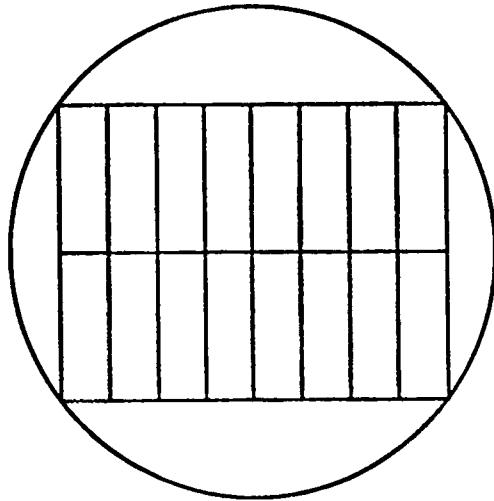
the dose at which the polymer begins the crosslink and become insoluble. The D_i is the dose required to make a film of a given thickness totally insoluble. The contrast (γ) is defined by the following relationship:

$$\gamma = [\log (D_i) / (D_g)]^{-1}$$

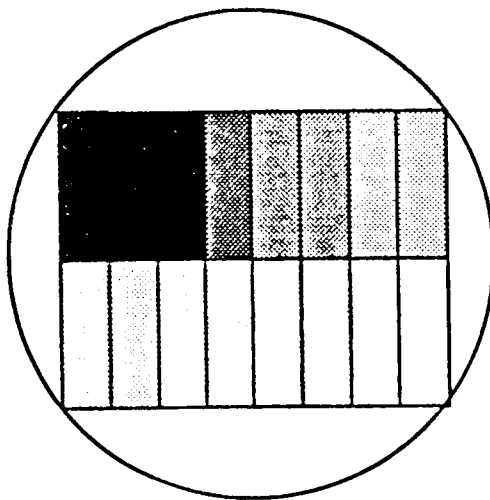
and is the exposure range over which the photoresist will respond. The resolution in patterning of a photoresist is related to the contrast, and it is desirable to have a high contrast value photoresist system in order to minimize resist response to low level radiation from diffraction effects.

Photosensitivities of photoreactive polyimides were determined by exposing thin films with a 1,000 watt high pressure Hg-Xe arc lamp using an Optical Associates Inc., Hybralign Series 400 mask alignment and exposure system. The polyimide homo- and copolymers were spin coated onto quartz from 10-15% solid NMP solutions. The wafers were then baked for 10 minutes on a hot plate at 125°C to drive off solvent. The thin polyimide films were exposed in air through the underside of the quartz wafer using narrow band gap filters of the desired wavelength (313nm or 365nm). The exposure intensity of the UV light through the narrow band gap filters was determined by use of a Research Radiometer model IL 1700 using of ILSED 400 Vacuum Photodiode with diffuser that measures the wavelength in the range of 200 to 600nm. The exposure doses could be measured to within $\pm .1 \text{ mJ/cm}^2$. After exposure the thin films were developed in a NMP solution and

washed with methanol. Instead of casting numerous films to make a photoresponse plot the quartz wafer was divided into 16 sections as shown in Figure 3.4.11.2. Each of the rectangles was given different exposure doses, so when they were developed in NMP and washed with methanol each rectangle had a different film thickness remaining as illustrated by Figure 3.4.11.2. The quartz wafers were dried at 125°C for at least 5 minutes on a hot plate after development. The film thicknesses were measured using a Dektak II profilometer with a precision of $\pm 10\text{nm}$ and a plot of the film thickness remaining after development was plotted as a function of the exposure dose given the individual films. The D_g and D_i were then determined from this plot. Each point or value on the photoresponse plot is determined by one measurement. The normalized film thickness was plotted as a function of the log of the exposure dose and the slope of the line was the determined contrast of the polyimide system.



a) Quartz Wafer Divided into 16 sections. Polyimide Spin Coated onto the opposite Side.



b) After Wafer was Exposed and Developed, Different Film Thicknesses Remain.

Figure 3.4.11.2. Quartz wafer used in sensitivity studies

4.0 Results and Discussion

4.1 Introduction

The research that is discussed in this chapter can be best presented by dividing the chapter into four major sections. The first section will be concerned with the synthesis of photoreactive polyimide homo- and copolymers. The second will discuss the effect of methyl substituent concentration on the photosensitive properties of these polymers. The third section will focus on the influence of aromatic ketone concentration on the photosensitive properties of the photoreactive polyimides. The final section will be concerned with the synthesis and characterization of photocrosslinkable poly(imide siloxane) copolymers.

4.2 Synthesis of photoreactive polyimide homo- and copolymers

The photosensitive polyimide homo- and copolymers were synthesized by the classical two-step polymerization procedure (50,51). The first step was the generation of soluble poly(amic acid) prepolymers by reacting aromatic diamines with aromatic dianhydrides in the dipolar aprotic solvent NMP. The second step was to imidize the poly(amic acid) prepolymers by either a conventional bulk thermal cure or by the solution imidization procedure to cyclodehydrate the poly(amic acid). Both produce polyimides via evolution of water (see scheme 2.5.1.2). The aromatic diamines and dianhydrides and amino-propyl terminated siloxane oligomers used during the course

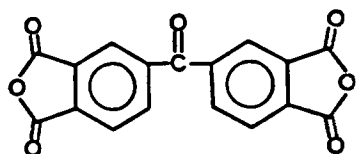
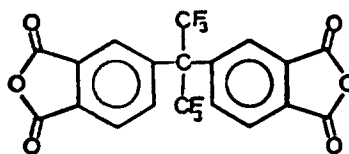
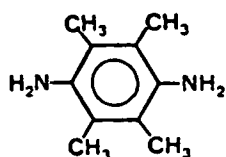
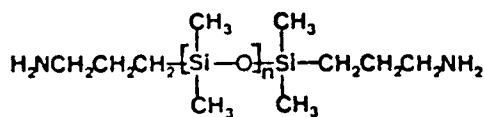
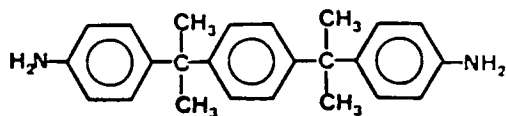
of this research are listed in Table 4.2.1.

In order to obtain high molecular weight poly(amic acid) prepolymers the reaction conditions had to be strictly controlled. Extremely pure monomers (greater than 99 percent purity) were used and the moisture was excluded from the reaction. Therefore, monomers and solvents were carefully purified and dried just prior to use. To ensure that anhydrous conditions were maintained during the entire reaction, solvents were handled with syringe techniques and the reaction apparatus used was flamed under a nitrogen gas purge immediately prior to use. Another important consideration was the order of monomer addition to the reaction flask. It has been previously reported that the highest molecular weight poly(amic acids) are obtained by the addition of the aromatic dianhydride to the stirring diamine solution (55). This method of monomer addition is thought to minimize the possibility of anhydride hydrolysis which would upset the 1:1 stoichiometry of the reaction. In order to obtain photoreactive polyimides with high sensitivity a 1:1 stoichiometry of the diamine to dianhydride was used to synthesize high molecular weight prepolymers.

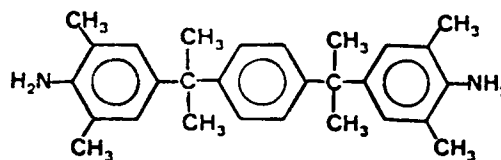
A slightly modified procedure had to be employed for synthesizing homo- and copolymers where the Bis-P diamine was used as outlined in Scheme 4.2.1. Since Bis-P is not soluble in NMP at room temperature the reaction solution had to be heated to above 60°C in order for it to completely dissolve.

Table 4.2.1

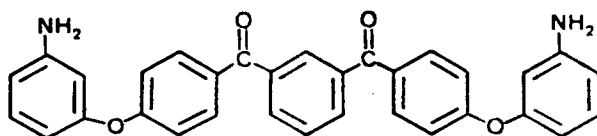
Monomers Employed in Homo- and Copolymerization Studies

Benzophenone Tetracarboxylic
Dianhydride (BTDA)6-Fluoro Dianhydride
(6FDA)Tetramethyl Phenylene Diamine
(TMPDA)Aminopropyl Polydimethyl
Siloxane (PSX) Mn = 2,500 g/mole

Bis Aniline P (Bis-P)



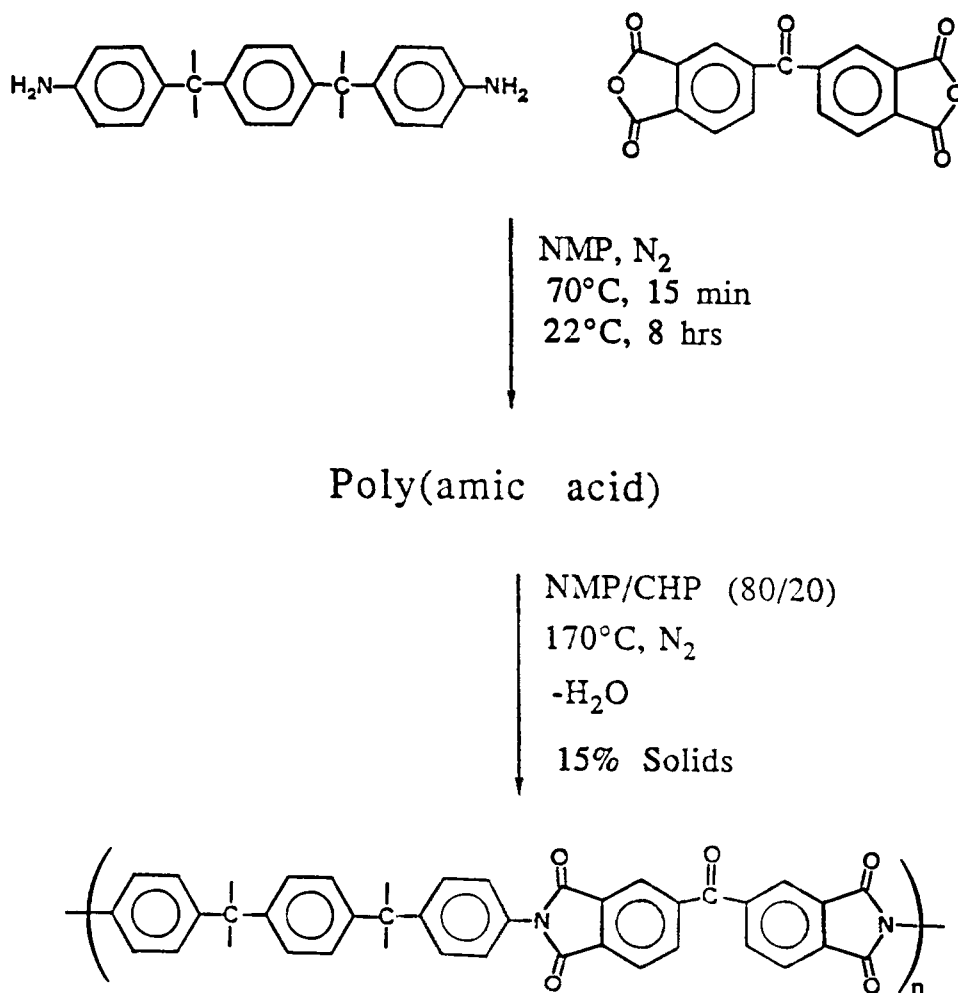
Tetramethyl Bis Aniline P (TM Bis-P)



1,3 Bis(3-Aminophenoxy-4'-Benzoyl) Benzene (DKDEDA)

Scheme 4.2.1

Synthetic Process Used for Polyimide Homo- and Copolymers where the Bis-P Diamine was Employed



The solid dianhydride was added to the stirring solution at this elevated temperature. After the dianhydride completely dissolved the heat was removed from the reaction flask and the reaction solution was allowed to cool to room temperature. Since oligomers had already been formed, the reaction solution remained homogeneous even when it reached room temperature. The poly(amic acid) was allowed to react for 8 more hours at room temperature in order to ensure that high molecular weight polymers were obtained.

The poly(amic acid) prepolymers were converted to the corresponding polyimides by either the conventional high temperature bulk imidization of solution cast poly(amic acid) films (53,54) or by the solution imidization technique which uses moderate temperatures and a cosolvent system of NMP and an "azeotroping" solvent such as CHP (140-143).

Bulk imidization was used to compare polyimides obtained from this method to polyimides obtained by the solution imidization procedure. In the former case, poly(amic acid) solutions were cast onto clean dry glass plates and spread into uniform thickness films by use of a "doctor blade." Heat was applied in a stepwise fashion as typically reported in other literature procedures describing this widely used method of imidization. Firstly, the glass plates with the solution cast films were placed in the oven at a low temperature (80°C) to remove most of the solvent. They were then heated to higher temperatures in a step-wise fashion to induce

imidization. The temperature was finally raised to 300°C in an attempt to provide adequate chain mobility which is necessary for quantitative imidization. After the imidization procedure, the films were allowed slowly cool to room temperature and were removed by the use of a razor blade to gently peel them off the plate.

The solubilities of the bulk imidized films were determined by placing a piece of a film in 10 ml of the appropriate solvent. All the films were insoluble in all the solvents tried! Even the dipolar aprotic solvents could not dissolve the films after heating to 100°C and stirring over night. This observation is quite common for polyimides that have been imidized by the bulk "cure" procedure (78). Typically insoluble films are obtained from this method. Therefore, this method could not be used to obtain solvent soluble fully imidized photoreactive polyimide homo- and copolymers.

Poly(amic acid) homo- and copolymers were also quantitatively imidized at moderate temperatures using a coamide solvent solution consisting of N-methylpyrrolidone and N-cyclohexylpyrrolidone. This method of imidization was found to yield solvent soluble polyimide homo- and copolymers in our laboratory by Summers et al. (140-143). Other scattered reports have shown that imidization could be achieved in solution without loss in molecular weight if the polyimide remained completely soluble during the entire process (78).

It is also important that the water evolved during imidization was effectively removed from the reaction solution before it could hydrolyze the poly(amic acid) (78). In the cosolvent system NMP and CHP, the NMP was used to completely solvate the polymer during imidization and the CHP was used to effectively remove the water of imidization from the system in order to both prevent hydrolytic degradation of the poly(amic acid) and to also drive the reaction to completion.

Like NMP, CHP is a cyclic dipolar aprotic amide solvent and is commercially available from GAF. The difference in structure between the NMP and CHP is that CHP has a cyclohexyl ring, rather than a methyl group as in NMP, attached to the amide nitrogen. CHP has a higher boiling point than NMP of 290°C at atmospheric pressure and is a liquid at room temperature. Summers found that since CHP is immiscible with water at elevated temperatures it made an excellent azeotroping solvent for solution imidization when coupled with NMP (140-143). However, when used alone to imidize poly(amic acids) CHP was often found to solvate inadequately partially imidized polar polyimides and premature precipitation of the polymer would occur during the imidization procedure (140-143). Johnson earlier demonstrated that the synthesis of high molecular weight polysulfones was also found to be successful using the NMP/CHP cosolvent azeotroping system instead of the conventional NMP/toluene cosolvent system (144).

The NMP/CHP cosolvent mixture was used to solution imidize all photosensitive poly(amic acid) systems with a NMP/CHP cosolvent ratio of 80 volume percent NMP to 20 volume percent CHP. The cosolvent system was heated to 165°C before the poly(amic acid) solution was added in order to remove the water of imidization more efficiently, since water removal does not take place until elevated temperatures are reached.

The progress of the reaction was monitored by use of FTIR. Small quantities of samples were removed during the course of the solution imidization and thin films were cast on salt plates and placed in the vacuum oven at 70°C for one hour. By placing the salt plates in the vacuum oven at 70°C the solvent was removed without causing significant amounts of further imidization to occur. The FTIR spectrum of a fully imidized polyimide homopolymer made by reacting BTDA with TMBis-P is shown in Figure 4.2.1. The absence of the strong absorption band at 1546 cm^{-1} and the presence of absorption bands at 1776 cm^{-1} and 725 cm^{-1} indicated the polymer is fully imidized. The poly(amic acid) would have a strong absorption band at 1546 cm^{-1} due to the amide band and would not have absorption peaks at 1776 cm^{-1} and 725 cm^{-1} which are imide bands. A list for the FTIR assignments for the absorption bands of the BTDA/TMBis-P polyimide homopolymer are given in Table 4.2.2. The imidization reaction was allowed to occur until complete disappearance of the strong amide band at 1546 cm^{-1} had occurred. At a 165°C reaction temperature,

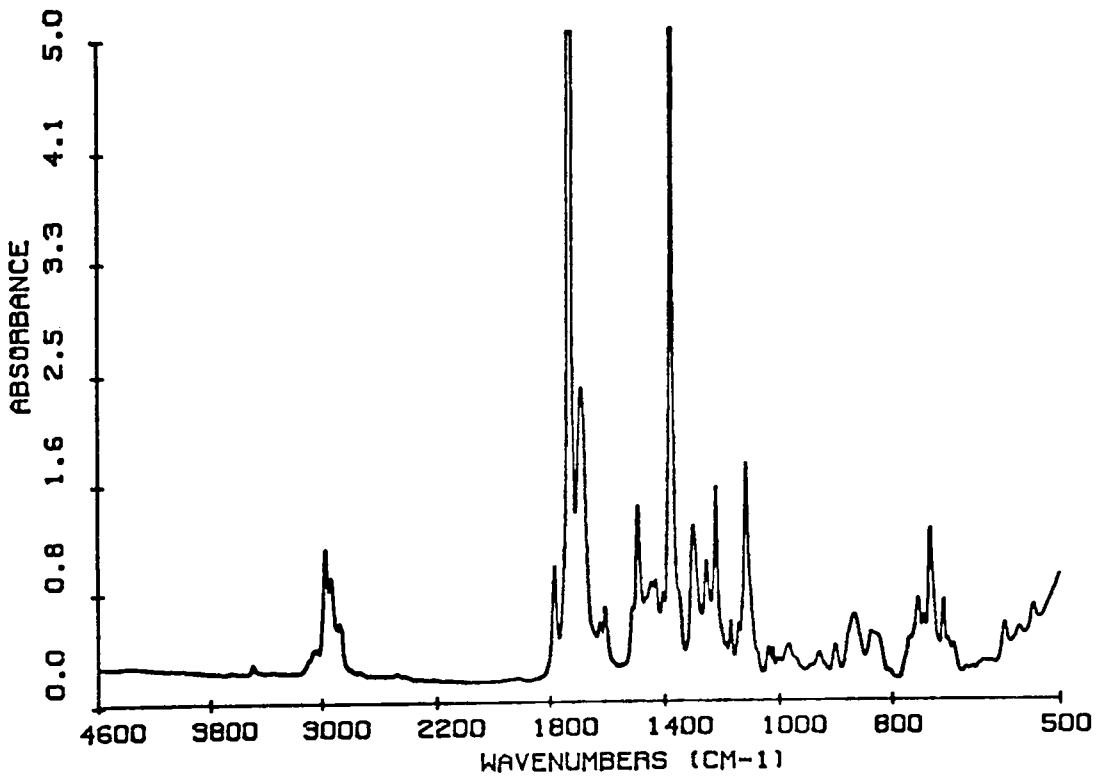


Figure 4.2.1. FT-IR Spectrum of a Fully Imidized Polyimide (BTDA/TMBis-P Based)

Table 4.2.2

FTIR Assignments for the BTDA/TMBis-P based Homopolymer

Frequency (cm ⁻¹)	Assignment
2968	C-H stretch (methyl substituents)
1778 1724	Imide carbonyl stretch vibrations
1684	C=O stretch (benzophenone moiety)
1370	imide band
728	imide band

imidization took approximately 15 hours to complete. All solution imidizations of poly(amic acids) were allowed to proceed for at least 18 hours to ensure complete imidization was reached. Solvent soluble fully imidized polyimide homo- and copolymers were obtained using this solution imidization technique.

The photocrosslinking reaction which occurs when these soluble polyimide homo- and copolymers are exposed to UV light is based on the photosensitive crosslinking reaction of the tetramethyl Bis-A polyarylene ether ketones proposed earlier by Mohanty et al. in our laboratory (14,15,16). The photocrosslinking reaction is outlined in Scheme 4.2.2. The photocrosslinking reaction is based on the UV absorbance of the benzophenone moiety forming the 1,2 diradical in its triplet excited state, and a subsequent intermolecular hydrogen abstraction reaction of the diradical with the methyl substituent to form a more stable benzylic type radical and a diphenylhydroxymethyl radical. The combining of radicals from two different chains forms a crosslink network rendering the polymer system insoluble.

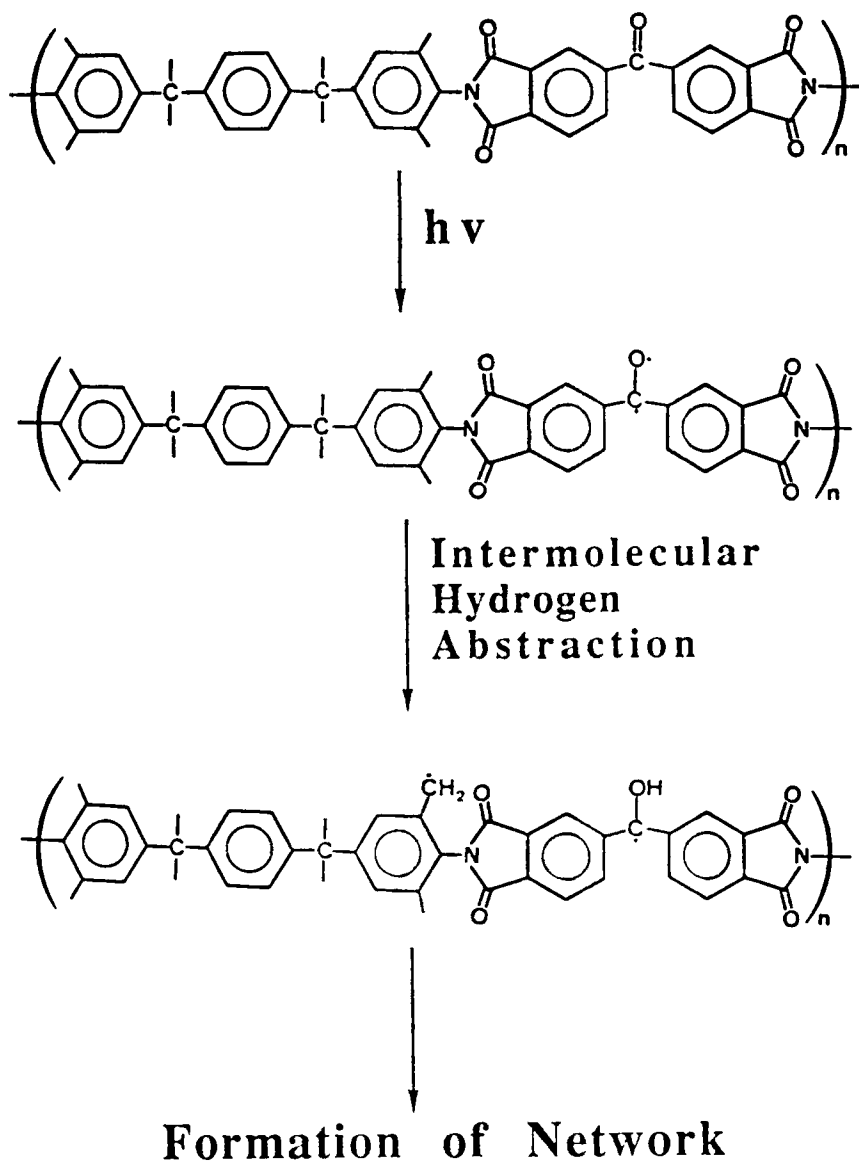
4.3 Characterization of the BTDA Dianhydride, and Bis-P and TMbis-P Diamine based homo- and copolymers

4.3.1 Intrinsic viscosity and glass transition temperatures

A series of high molecular weight homo- and copolymers was synthesized using the BTDA dianhydride and Bis-P and

Scheme 4.2.2

Photocrosslinking Reaction of the Photosensitive Polyimides



TMBis-P diamines. Relative molecular weights of the soluble homo- and copolymers were determined through the use of the intrinsic viscosity values. The intrinsic viscosities and glass transition temperatures of the homo- and copolymers are listed in Table 4.3.1.1. As judged by the high intrinsic viscosity values, high molecular weight homo- and copolymers were obtained throughout the entire series of polyimides studied. Further evidence for this conclusion is supported by the fact that all polyimide samples formed transparent and creasable films possessing good mechanical properties.

The glass transition temperature of the BTDA and Bis-P based homopolymer determined by differential scanning calorimetry was found to be 264°C. The analogous homopolymer with four methyl substituents along the polymer backbone, based on BTDA and TMBis-P, had an increased glass transition temperature of 288°C. The 24°C increase in glass transition temperature is probably due to the increased steric barrier to rotation that the methyl substituents incorporate to the polymer backbone. The copolymers synthesized by incorporating varying mole percent of the two different diamines have glass transition temperatures between the two values of the homopolymers. The higher the TMBis-P content the higher the glass transition temperature of the polyimide formed.

Table 4.3.1.1

Intrinsic Viscosities and Glass Transition Temperature of
BTDA, TMBis-P and Bis-P Based Homo- and Copolymers

Polyimide System	$[\eta]$ (dl/g)	Tg (°C) by DSC
BTDA/Bis-P	0.71	264
BTDA/Bis-P(75%) TM Bis-P(25%)	0.97*	261
BTDA/Bis-P(50%) TM Bis-P(50%)	0.59*	272
BTDA/Bis-P(25%) TM Bis-P(75%)	1.67	278
BTDA/TM Bis-P	0.90	288

*in THF at 25°C

Other intrinsic viscosities in NMP at 25°C

4.3.2 Polymer Solubility

One major objective of this research was to obtain soluble polyimides in order to allow processability of the photoimageable polyimides. Increased solubility in a variety of solvents will increase the ease of processing and the amount of solvents able to be used as developing agents in the photoimaging process. Historically polyimides have not been processable in the fully imidized state due to their insolubility, and therefore, had to be processed in the poly(amic acid) form. In fact, using the conventional bulk imidization procedure rendered the whole series of polyimides listed in Table 4.3.1.1 totally insoluble even at elevated temperatures in dipolar aprotic solvents. However, when solution imidized at moderate temperatures in a NMP and CHP cosolvent, totally soluble fully imidized homo- and copolymers were obtained. Solubilities of the series of polyimides based on BTDA dianhydride and Bis-P and TMBis-P diamines are shown in Table 4.3.2.1 in a variety of solvents. The solubilities were determined by dissolving the polyimide in the appropriate solvent at room temperature in order to obtain 10% solid solutions. In most cases the polyimides dissolved within 15 minutes yielding clear high viscosity solutions. The homopolymer based on BTDA and Bis-P was easily soluble in the dipolar aprotic solvents such as NMP and DMAc, and was also soluble in the low boiling solvent methylene chloride. However, the homopolymer was only marginally soluble in THF

Table 4.3.2.1

Solubilities of BTDA/TMBis-P/Bis-P Based Homo- and Copolymers

Polyimide System	NMP	DMAc	THF	CH ₂ Cl ₂	ØCl	Tol
BTDA/Bis-P	S	S	MS	S	MS	IS
BTDA/Bis-P(75%) TM Bis-P(25%)	S	S	S	S	S	IS
BTDA/Bis-P(50%) TM Bis-P(50%)	S	S	S	S	S	IS
BTDA/Bis-P (25%) TMBis-P (75%)	S	S	S	S	S	IS
BTDA/TM Bis-P	S	S	S	S	S	IS

NMP = N-Methyl Pyrrolidinone

THF = Tetrahydrofuran

Tol = Toluene

CH₂Cl₂ = Methylene Chloride

ØCl = Chlorobenzene

DMAc = Dimethyl Acetamide

S = Easily Soluble

MS = Marginally Soluble

IS = Insoluble

and chlorobenzene. By marginally soluble, it means that the solution had to be heated above room temperature in order to obtain a fully soluble polymer, and after the solution was cooled to room temperature it began to precipitate out of solution. After 25 mole percent of TMBis-P diamine was incorporated into the polymer backbone the copolymer was easily soluble in THF and chlorobenzene. Therefore, not only do the methyl substituents increase the glass transition temperature, but they also enhance the solubility properties of polyimides. The fact that they had enhanced solubility allowed the polymers to be processed in a variety of solvents. However, after the thin films were heated in an oven at 300°C for over 15 minutes, the polyimide films were rendered totally insoluble. This observation was also reported for the inherently photosensitive polyimides by workers at Ciba-Geigy (10). The insolubility of these polymers is probably due to a thermal crosslinking reaction that can take place when polyimides containing aliphatic substituents along the polymer backbone are heated to high temperatures (145).

4.3.3 Thermo-Oxidative Stability

Polyimides are well known for their excellent thermal stabilities even in an oxidative environment such as air. Therefore, it was expected that photoreactive polyimides would have high thermal stabilities. Polyimides used in electronic applications often see very high processing temperatures

during integrated circuit fabrication. The highest temperature seen by many computer chips is the final soldering temperature which can reach in excess of 350°C. Therefore, if the polyimide is going to remain an integral part of the integrated circuit as an interlayer dielectric or passivation layer it must be able to withstand this high temperature without degradation.

The thermal stabilities of the series of polyimide homo- and copolymers based on the BTDA dianhydride and Bis-P and TMBis-P diamines were determined by thermogravimetric analysis in an air environment. Thin films of the polyimides were analyzed at a heating rate of 10°C per minute. The comparison of the thermogravimetric analysis weight loss curves as a function of temperature is shown in Figure 4.3.3.1. As can be seen by the thermogravimetric curves the homopolymer based on BTDA and Bis-P has greater weight loss at lower temperatures compared to the copolymers containing the TMBis-P diamines. This apparent thermal oxidative stability enhancement of the polymers containing methyl substituents was probably due to a thermal crosslinking reaction that can take place at elevated temperatures when methyl substituents are incorporated into the polymer backbone (10,145). Since the polymers can crosslink the temperature required to cause weight loss was slightly enhanced. The temperatures of 5% weight loss of the polyimides shown in Figure 4.3.3.1 were all found to be over 500°C in air.

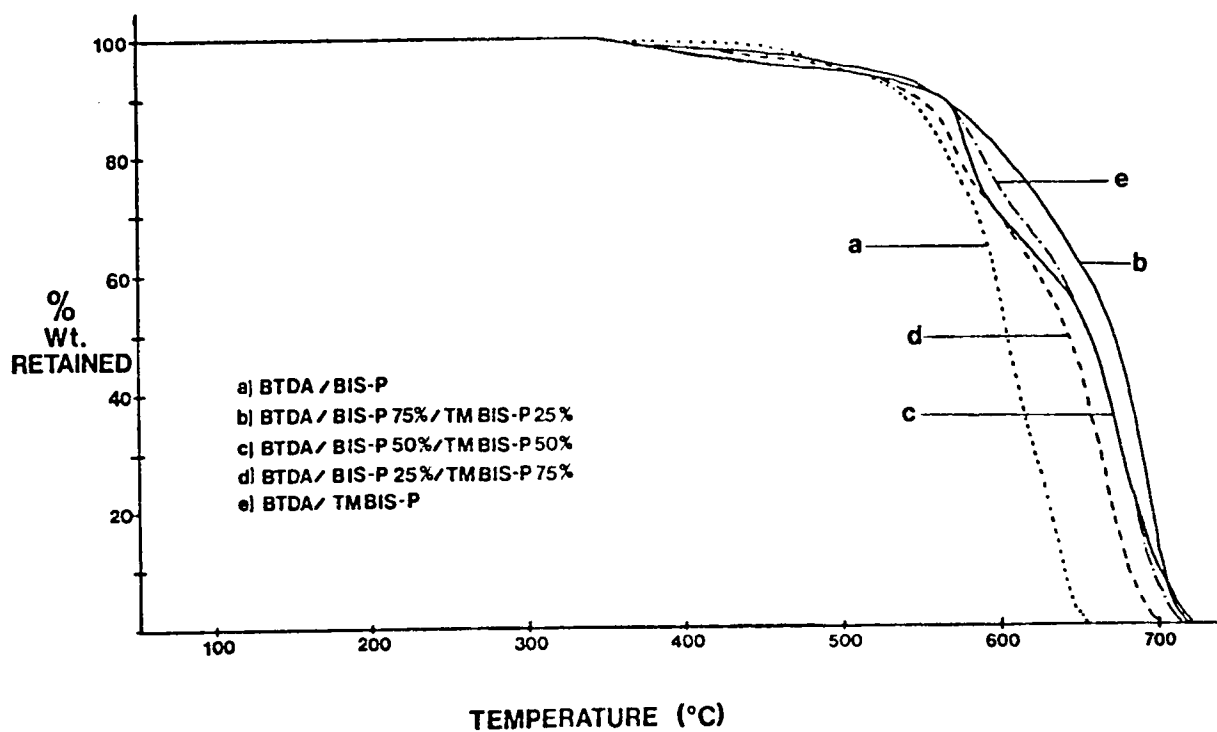


Figure 4.3.3.1. Thermogravimetric Analysis of BTDA/TM Bis-P/Bis-P Based Homo- and Copolymers (10°C/minute; air atmosphere)

4.3.4 Photosensitive Properties of BTDA, TMBis-P and Bis-P based polyimides

The major objective of this research was to produce soluble, high molecular weight, photosensitive polyimide homo- and copolymers and to study the effects of chemical and structural changes in the polymer backbone on the photosensitive properties of the resulting polyimides. During this study on the series of polyimides listed in Table 4.3.1.1, the effects of the wavelength of exposure, and the amount of tetramethyl substituted diamine incorporation on the photosensitive properties of the photoreactive polyimide systems were determined.

The photosensitivity of the homopolymer based on BTDA and TMBis-P was found to be greatly dependent on the wavelength of exposure. Figure 4.3.4.1 shows a UV absorption spectrum of a 1.0 micron thick BTDA-TMBis-P based polyimide film from 250nm to 400nm. The major absorption peak below 280nm was due to the π to π^* transitions of the aromatic rings along the polymer backbone, while the shoulder peak between 290nm and 320nm was found to be due to the n to π^* transition of the aromatic carbonyl group in its triplet state. The photosensitivity of the homopolymer was determined at two different wavelengths; 313nm and 365nm. These wavelengths were chosen for two reasons. The first reason was because 313nm wavelength is right around the shoulder absorbance peak of the aromatic carbonyl and 365nm was at a higher wavelength at which the polymer has a lower optical density. The second

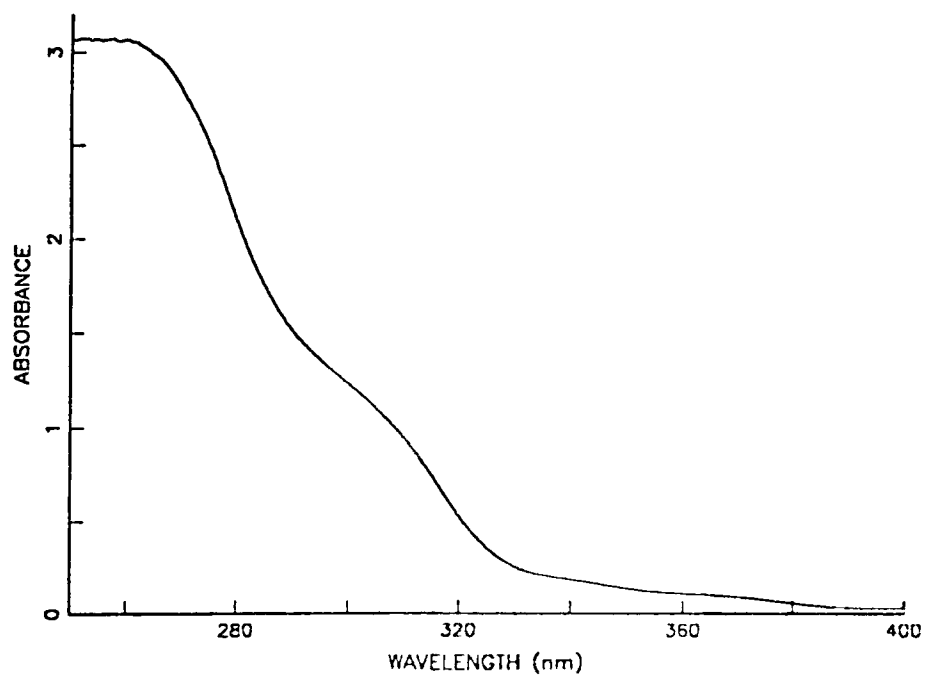


Figure 4.3.4.1. UV Absorption Spectrum of the BTDA/TMBis-P Polyimide Homopolymer (one micron thick film).

reason these wavelengths were chosen was because 313nm and 365nm are the two most intense emission peaks of the high pressure Hg-Xe arc lamp used as the UV exposure source (see Figure 2.2.2). As can be seen in Figure 4.3.4.2, the photosensitive response plot of the BTDA-TMBis-P homopolymer has a gel dose, D_g , of approximately 13 mJ/cm^2 and a D_i , the exposure dose required to make a film of given thickness totally insoluble, of approximately 225 mJ/cm^2 when exposed at the 313nm wavelength. The contrast of this polymer was determined by plotting the normalized film thickness as a function of the log of the exposure dose as shown in Figure 4.3.4.3. The slope of this straight line formed in this plot is the contrast of the homopolymer system at the 313nm exposure wavelength, and was found to be 0.89. However, when exposed at the 365nm wavelength the gel dose was found to be 37.9 mJ/cm^2 and the D_i was determined to be 183 mJ/cm^2 (see Figure 4.3.4.4). The contrast of the homopolymer at the 365nm wavelength was found to be 1.39 (see Figure 4.3.4.5). The lower D_g at the 313nm exposure wavelength indicates that the homopolymer BTDA-TMBis-P was more photosensitive at this wavelength than at the longer wavelength at 365nm. However, the D_i is lower at the 365nm wavelength than at the 313nm wavelength causing the contrast to be higher for the polyimide system at 365nm. The reason the lower D_g and the higher D_i were both found at the 313nm wavelength was due to the optical density of the polyimide at this wavelength. Even though the

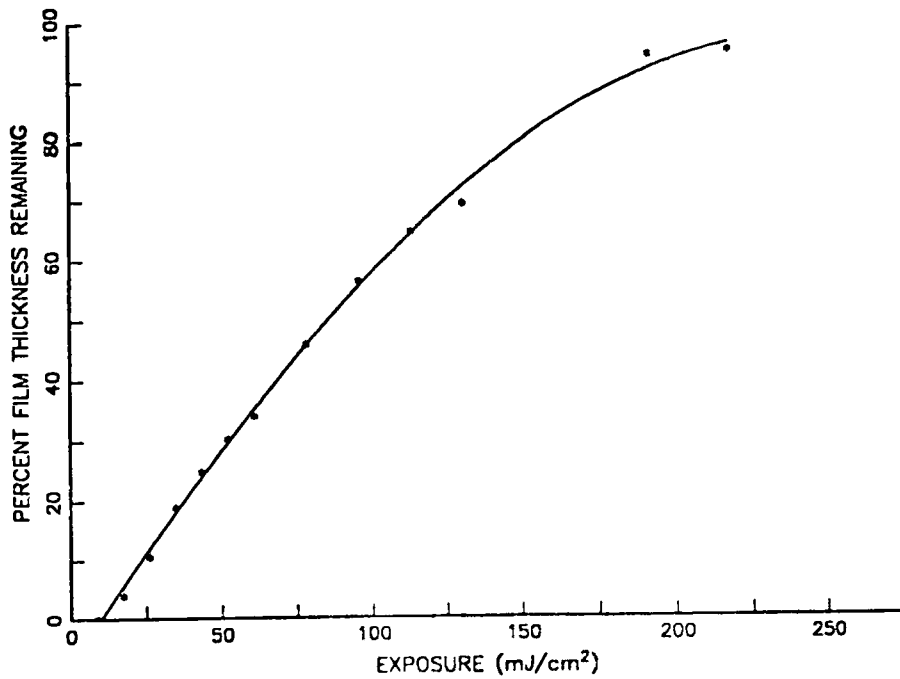


Figure 4.3.4.2. Photosensitive Response Plot for the BTDA/TMBis-P Homopolymer at the 313nm wavelength (Intrinsic viscosity of 0.90 dl/g NMP at 25°C; Film thickness: 1.35 microns).

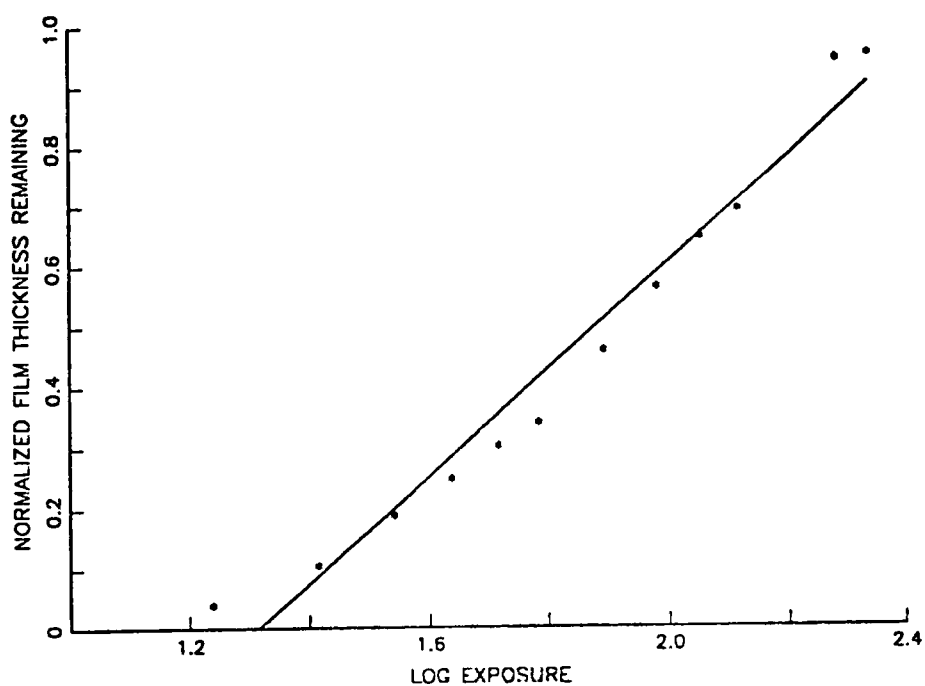


Figure 4.3.4.3. Contrast Plot for the BTDA/TMBis-P Homopolymer at the 313nm wavelength (Intrinsic viscosity of 0.90 dl/g in NMP at 25°C; film thickness: 1.35 microns).

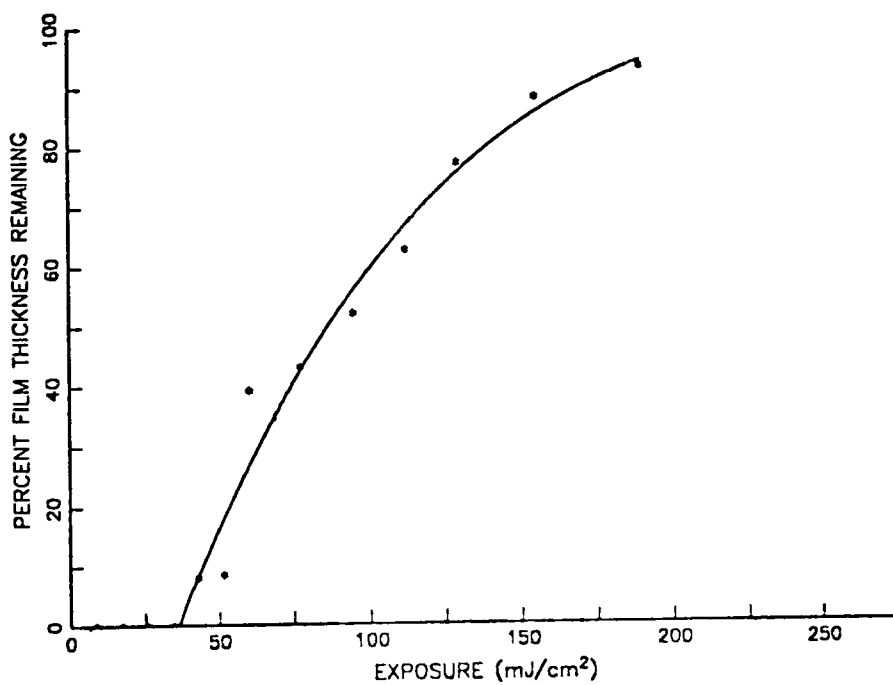


Figure 4.3.4.4. Photosensitive Response Plot for the BTDA/TMBis-P Homopolymer at the 365nm wavelength (Intrinsic viscosity of 0.90 dl/g in NMP at 25°C; film thickness: 1.30 microns).

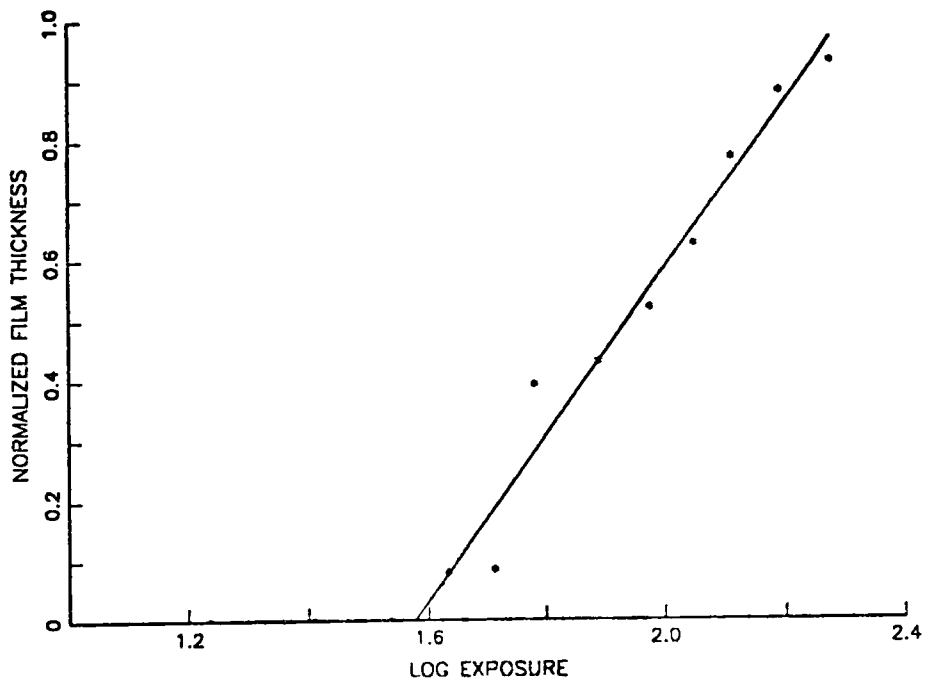


Figure 4.3.4.5. Contrast Plot for the BTDA/TMBis-P Homopolymer at the 365nm wavelength (Intrinsic viscosity of 0.90 dl/g in NMP at 25°C; film thickness: 1.30 microns).

polymer was found to be more sensitive at 313nm as indicated by the lower D_g , the optical density of the polymer is higher at this wavelength. Therefore, the UV light was highly absorbed by the polymer only allowing approximately 10% of the initial light through the film. Since the intensity of the UV light decreased as the light was absorbed by the polymer, the crosslinking reaction was depressed causing a higher D_i value at the 313nm wavelength. A more dramatic effect is shown for a lower molecular weight homopolymer (intrinsic viscosity 0.45 dl/g in NMP at 25°C) in Figure 4.3.4.6. D_g was lower at the 313nm wavelength. However, D_i was approximately the same for the homopolymer at both wavelengths. Therefore, the contrast value at 365nm was determined to be 2.1 while only 1.2 at the 313nm wavelength. The resolution of a resist has been found to be directly related to the contrast of the photoresist system (21,146,147). The higher the contrast value the higher the resolution of the imaged pattern. Since higher contrast values were determined at the 365nm wavelength, coupled with the fact that only film thickness less than 1.5 microns could be crosslinked at the 313nm wavelength due to the high optical density of the polyimide at this wavelength, the 365nm wavelength was used as the exposure wavelength for the rest of this study.

The photosensitives of the polyimide homo- and copolymers based on the BTDA dianhydride and Bis-P and TMBis-P diamines were found to be dependent on the amount of methyl

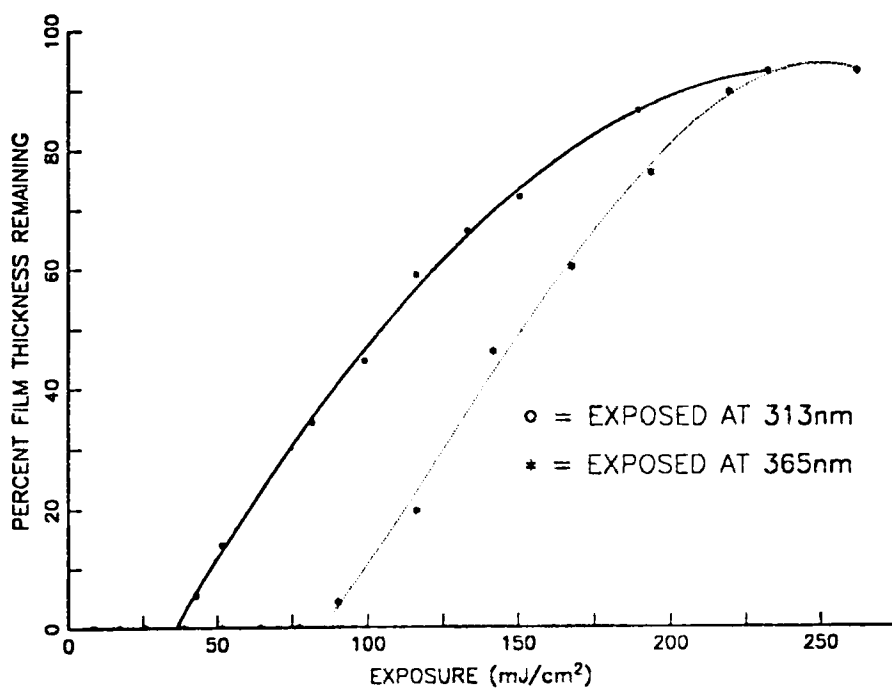


Figure 4.3.4.6. Comparison of the Photosensitive Response Plots for a low molecular weight BTDA/TMBis-P Homopolymer at the 313nm and 365nm wavelengths (Intrinsic Viscosity of 0.45 dl/g in NMP at 25°C)

substituents incorporated into the polyimide copolymer. The summarized photosensitive properties of the series of homo- and copolymers are listed in Table 4.3.4.1. At 75 to 100 mole percent TMBis-P diamine incorporation there was only a small difference in photosensitivities as determined by their low D_g and D_i values. However, in the copolymer with 50 mole percent of the Bis-P diamine incorporation the gel dose, D_g , at 365nm increased to $1,144 \text{ mJ/cm}^2$ for the copolymer compared to the 38 mJ/cm^2 of the homopolymer with 100 percent TMBis-P diamine incorporation. The exposure dose required to make a given film thickness totally insoluble, D_i , increased to 3658 mJ/cm^2 for the 50% Bis-P copolymer. This decreased photosensitivity effect was even more pronounced for the copolyimide containing only 25 mole percent of the tetramethyl substituted diamine TMBis-P as shown in Table 4.3.4.1. The copolymers with less TMBis-P content were less photosensitive than the homopolymer with 100 percent TMBis-P incorporation. In the copolymers with greater amounts of Bis-P diamine incorporation there were less methyl groups in close proximity to the triplet excited state of the carbonyls when the polymer was exposed to UV light, and therefore the intermolecular hydrogen abstraction and subsequent crosslinking reactions were inhibited

Table 4.3.4.1

Effect of Amount of Tetramethyl Diamine Incorporation on Photosensitivity and Contrast (Exposed at the 365nm wavelength)

<u>Polyimide System</u>	D_g (mJ/cm ²)	D_i (mJ/cm ²)	χ	<u>Film Thickness</u>	$[\eta]$ (dl/g)
BTDA/TM Bis-P	37.9	183	1.39	1.30 μ m	0.90
BTDA/75% TM Bis-P/ 25% Bis-P	16.1	164	0.94	2.30 μ m	1.67
BTDA/50% TM Bis-P/ 50% Bis-P	1144	3658	1.88	1.60 μ m	0.59
BTDA/25% TM Bis-P/ 75% Bis-P	2879	6719	2.58	0.81 μ m	0.97

D_g = Gel Dose - the dose at which the polymer begins to crosslink.

D_i - the dose required to totally crosslink the film at a given thickness.

χ = Contrast - the exposure range over which the material will respond.

4.4 Characterization of the BTDA Dianhydride and TMPDA and DKDEDA Diamine Based Polyimide Homo- and Copolymer

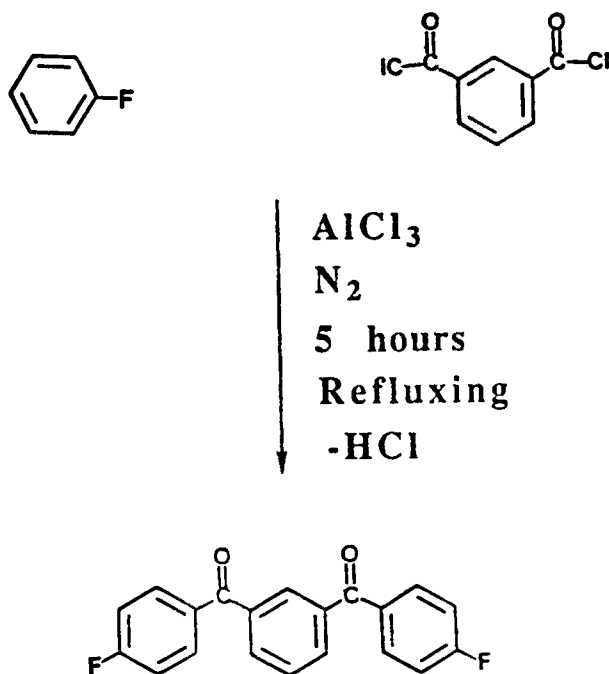
4.4.1 Synthesis of 1,3-Bis (3-Aminophenoxy-4'-Benzoyl) benzene (DKDEDA)

A series of high molecular weight homo- and copolymers were synthesized using the BTDA dianhydride and the TMPDA and DKDEDA diamines in order to determine the effect of increased aromatic keto concentration on the photosensitive properties of the polyimides. In order to synthesize this series of polyimides the diketo diether diamine (DKDEDA) had to be synthesized first.

The 1,3-Bis(3-Aminophenoxy-4'-Benzoyl)benzene was synthesized in two steps. The first step was to synthesize 1,3-Bis-4-fluorobenzoyl)benzene by a Friedel-Crafts acylation of fluorobenzene with isophthaloyl chloride using anhydrous aluminum chloride as the Lewis acid (see Scheme 4.4.1.1). The FTIR of a KBr pellet of this compound is shown in Figure 4.4.1.1. The major IR bands for the 1,3-Bis-4-Fluorobenzoyl) benzene are 1656 cm^{-1} due to the C=O stretch and $1240\text{-}1156\text{ cm}^{-1}$ due to the C-F stretch band. A small sample of the difluoride was sent to Atlantic Microlab, Inc. to be analyzed for the carbon and hydrogen weight percentages. The theoretical values were calculated to be 74.53% carbon and 3.75% hydrogen. The determined weight percentages were found to be 74.63% carbon and 3.75% hydrogen. These values are in close agreement with the calculated theoretical values. The

Scheme 4.4.1.1

Synthetic Process employed for 1,3-Bis(4-fluorobenzoyl)benzene



1,3-Bis(4-Fluorobenzoyl) Benzene

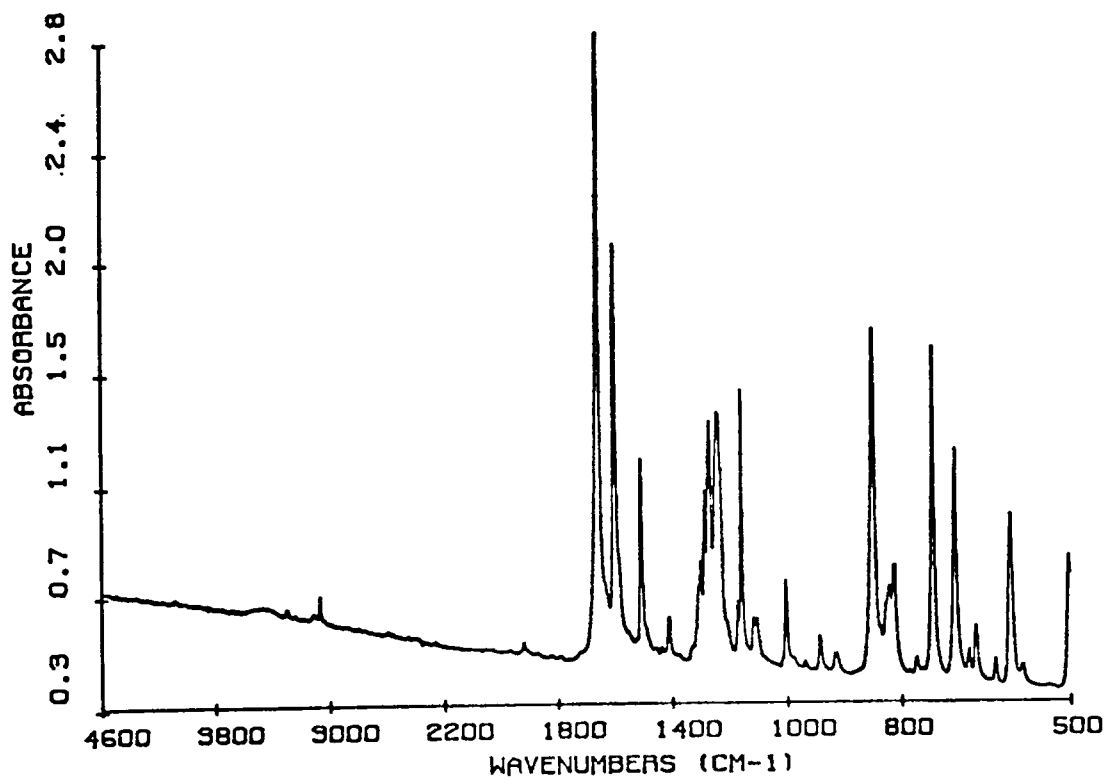


Figure 4.4.1.1. FTIR Spectrum of 1,3 Bis(4-Fluorobenzoyl) benzene

melting range of the difluoride crystals was found to be 179-180°C which is close to the literature values of 177.5-178.5°C (137).

Proton NMR was used to confirm the chemical structure of the difluoride obtained from the Friedel-Crafts acylation reaction. Figure 4.4.1.2 shows the proton NMR spectrum from the 6.5ppm to 8.5ppm region and the assigned NMR peaks. The proton NMR data supports that the fluorobenzene was only attacked para to the fluorine atoms forming ketone linkages para to the fluorine atoms in the final product.

After the 1,3-Bis(4-fluorobenzoyl) benzene was synthesized and purified it was used in the synthesis of the diamine 1,3-Bis(3-Aminophenoxy-4'-Benzoyl) benzene. 1,3-Bis(3-Aminophenoxy-4'-Benzoyl)benzene was synthesized by a nucleophilic aromatic displacement reaction of 1,3-Bis(4-fluorobenzoyl)benzene by 3-aminophenol using anhydrous potassium carbonate as the base catalyst. This reaction was run in DMAc with toluene as the azeotroping solvent at 130°C for 19 hours and 5 hours at 145°C as shown in Scheme 4.4.1.2. The crude product was recrystallized from toluene to yield a pale yellow solid. The FTIR of a KBr pellet of the diamine is shown in Figure 4.4.1.3. The major IR bands are listed in Table 4.4.4.1.

A small sample of the diamine was sent to Atlantic Microlab, Inc. to be analyzed for the elemental analysis of the carbon, hydrogen and nitrogen weight percentages. The

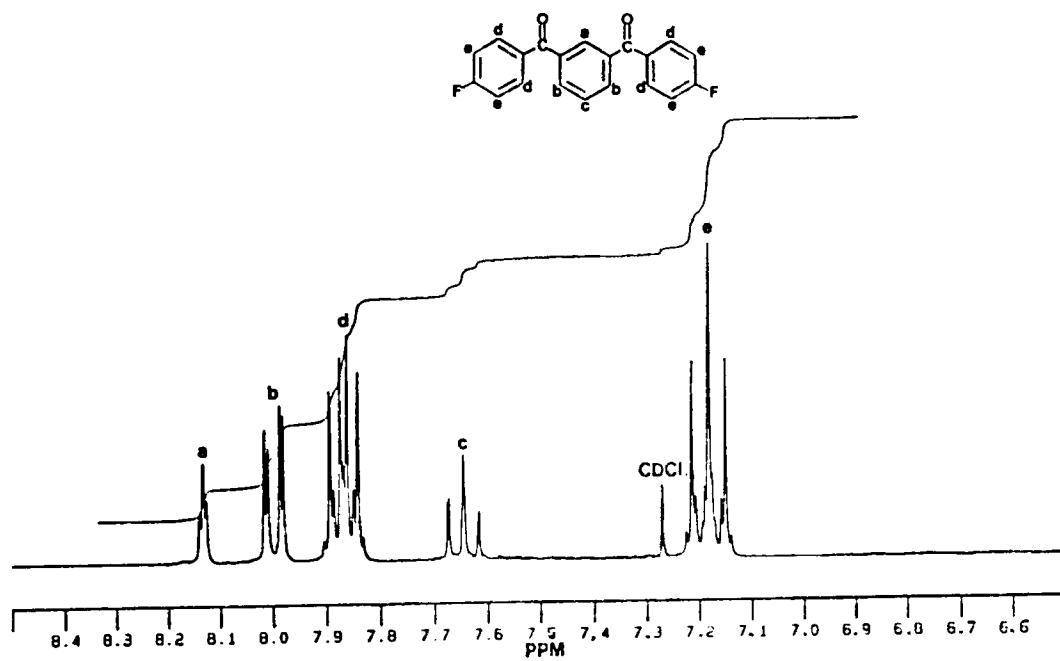
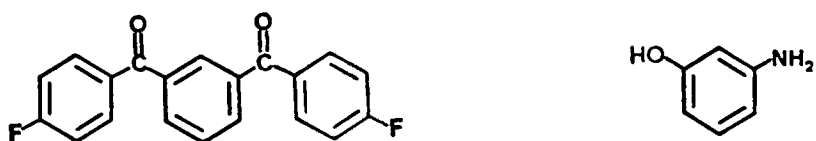


Figure 4.4.1.2. Proton NMR Spectrum of 1,3 Bis(4 Fluorobenzoyl) benzene

Scheme 4.4.1.2

Synthetic Process Employed for 1,3-Bis(3-aminophenoxy-4'-Benzoyl) Benzene



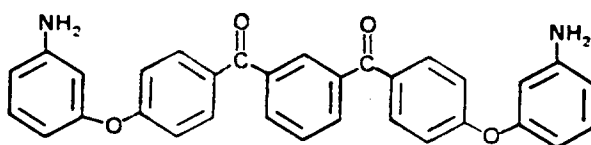
DMAC/Toluene (60/40)

K₂CO₃

N₂

130°C for 20 hours

145°C for 5 hours



1,3 Bis(3-Aminophenoxy-4'-Benzoyl) Benzene

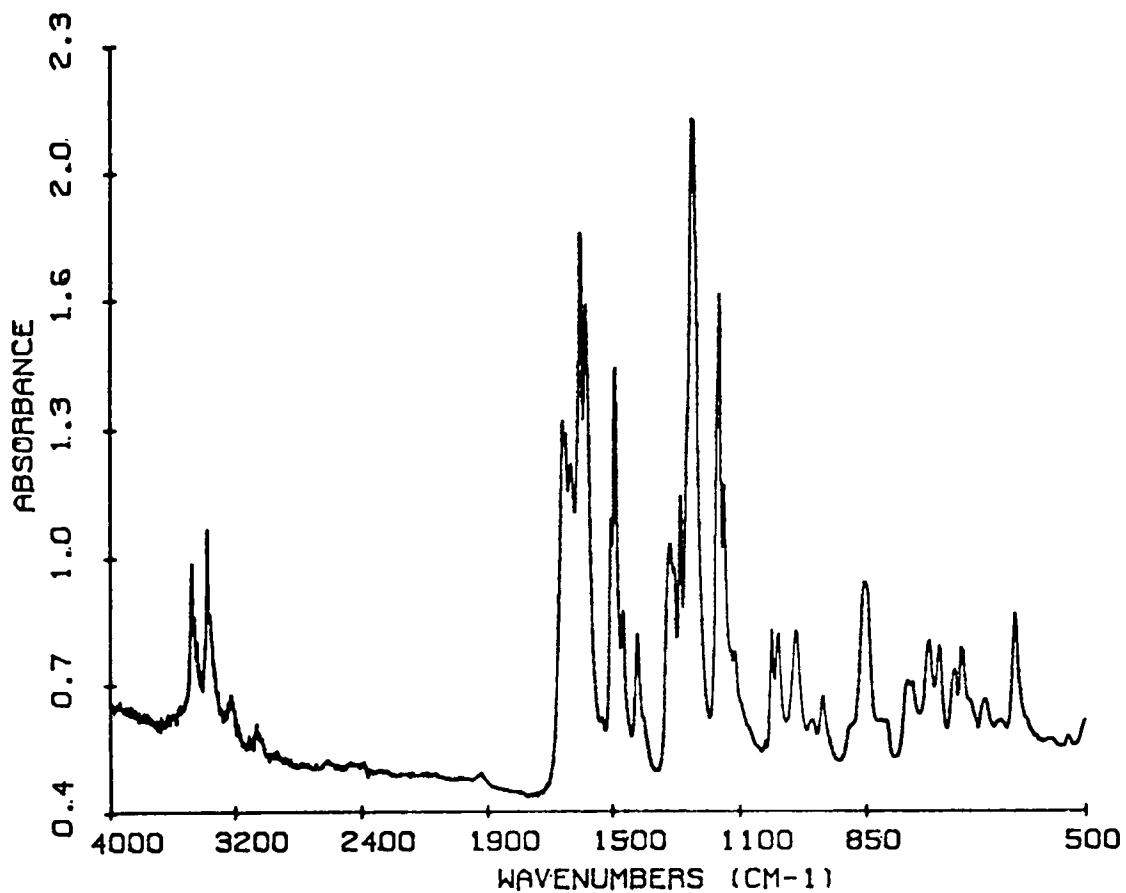


Figure 4.4.1.3. FTIR Spectrum of 1,3 Bis(3-aminophenoxy-4'-Benzoyl) Benzene

Table 4.4.1.1

FTIR Assignments for 1,3-Bis(3-Aminophenoxy-4'-Benzoyl)
Benzene

Frequency (cm ⁻¹)	Assignment
3466	Asymmetric N-H stretch
3371	Symmetric N-H stretch
1655-1570	C=O stretch
1486	N-H bending
1286	C-N stretch
1243	Asymmetric C-O-C stretch
1159	Symmetric C-O-C stretch

theoretical values were calculated to be 76.79% carbon, 4.83% hydrogen and 5.60% nitrogen. The determined weight percentages were found to be 76.66% carbon, 4.85% hydrogen and 5.52% nitrogen by elemental analysis. These determined values are in close agreement with the calculated theoretical values. The melting range of the DKDEDA solid was found to be 140 to 142°C which is close to the reported literature values of 142-144°C (137).

Proton NMR was used to confirm the chemical structure of the diamine obtained from the nucleophilic aromatic displacement reaction. Figure 4.4.1.4 shows the proton NMR of the 1,3-Bis(3-Aminophenoxy-4'-Benzoyl)benzene from 0 to 10 ppm region. The singlet peak at 3.8 ppm is due to the 4 protons on the amine functionalities and multiple peaks in the 6.4 to 8.2 region are due to the 20 aromatic protons on the diamine. Figure 4.4.1.5 shows an expansion of the proton NMR spectral region of the aromatic protons between 6.0 ppm and 8.5 ppm and the assigned peaks. The proton NMR data supports the fact that the 1,3-Bis(3-aminophenoxy-4'-Benzoyl)benzene was successfully synthesized.

4.4.2 Intrinsic viscosities and glass transition temperature

A series of high molecular weight homo- and copolymers was successfully synthesized using the BTDA dianhydride and TMPDA and DKDEDA diamines. The relative molecular weights of

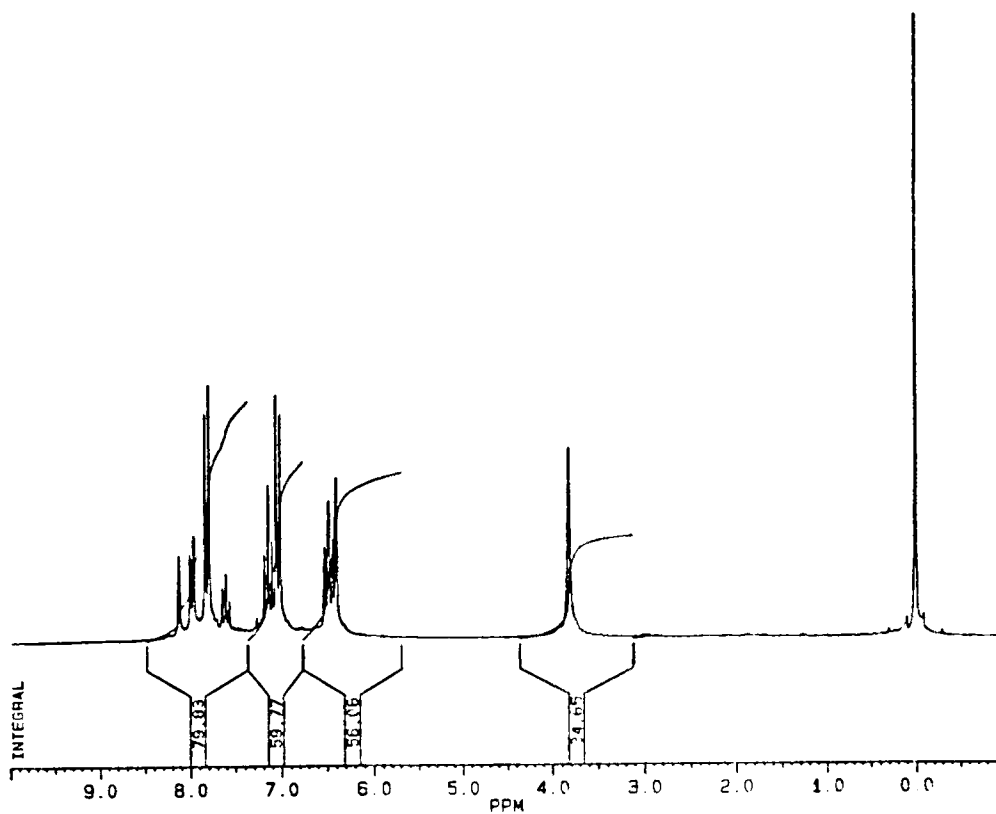


Figure 4.4.1.4. Proton NMR Spectrum of 1,3 Bis(3-aminophenoxy-4'-Benzoyl) benzene (0 to 10 ppm)

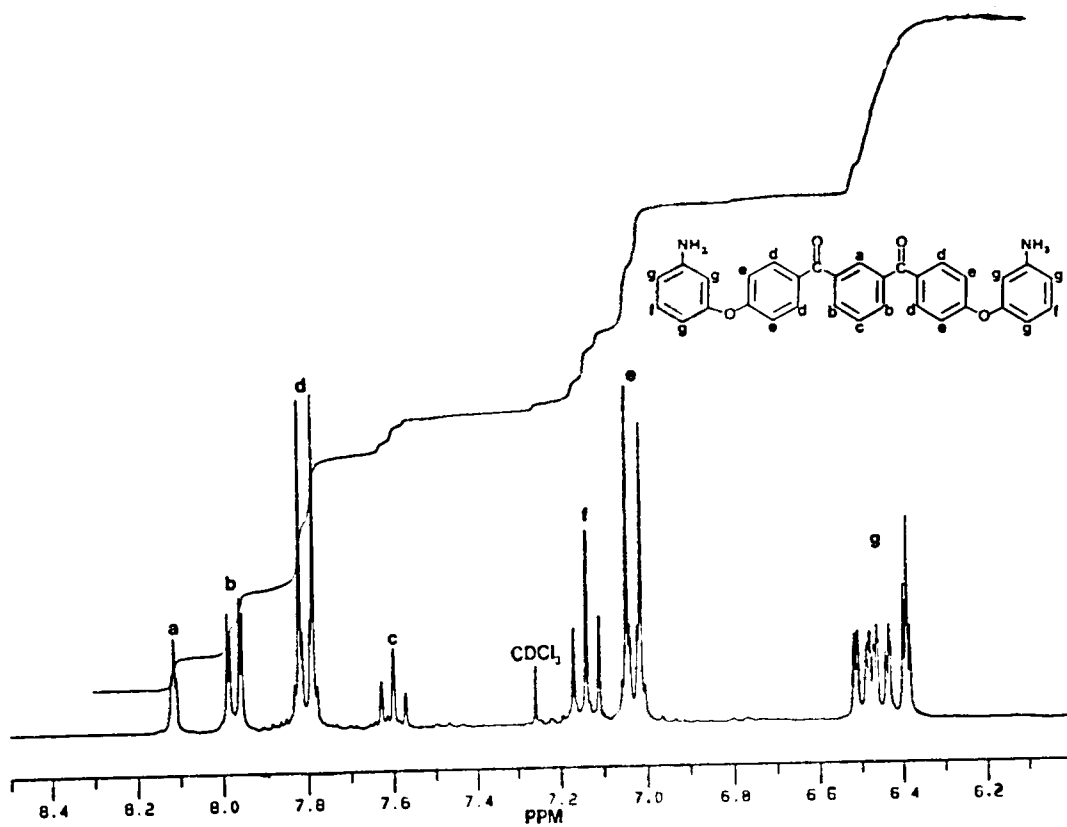


Figure 4.4.1.5. Proton NMR Spectrum of 1,3 Bis-(3-aminophenoxy-4'-Benzoyl) benzene (6.0 ppm to 8.5 ppm)

this series of polyimide homo- and copolymers were determined by intrinsic viscosity values in NMP at 25°C. The intrinsic viscosities and glass transition temperatures of this series of polymers are listed in Table 4.4.2.1. The high intrinsic viscosity values indicate that high molecular weight polyimides were obtained. This conclusion was supported by the fact that all the polyimide samples listed in Table 4.4.2.1 formed transparent and creasable films with good mechanical properties.

The glass transition temperature of the BTDA and TMPDA based homopolymer was found to be 439°C by dynamic mechanical thermal analysis. The glass transition temperature was determined by the tan delta damping peak as indicated in Figure 4.4.2.1. Since the tan delta damping peak was rather broad, starting at approximately 320°C and not peaking until 439°C, a thermal crosslinking reaction could be taking place as the polyimide homopolymer is being heated. The glass transition temperature of this homopolymer could not be determined by DSC because no endotherm was observed in the DSC scan.

The copolymers with varying amounts of DKDEDA incorporated into the polyimide backbone had lower glass transition temperatures than the BTDA-TMPDA based homopolymer. After 40 mole percent of the DKDEDA was incorporated into the polyimide backbone the glass transition temperature decreased to 279°C. The other copolymers had glass transition

Table 4.4.2.1

Intrinsic Viscosities and Glass Transition Temperatures of BTDA, TMPDA, and DKDEDA based homo- and copolymers.

Polyimide System	$[\eta]$ (dl/g)	T_g ($^{\circ}\text{C}$)
BTDA/TMPDA	0.50	439
BTDA/DKDEDA (10%) TMPDA (90%)	1.43	---
BTDA/DKDEDA (20%) TMPDA (80%)	0.82	346
BTDA/DKDEA (30%) TMPDA (70%)	0.66	295
BTDA/DKDEDA (40%) TMPDA (60%)	0.53	279

Note: Intrinsic viscosities measured in NMP at 25 $^{\circ}\text{C}$

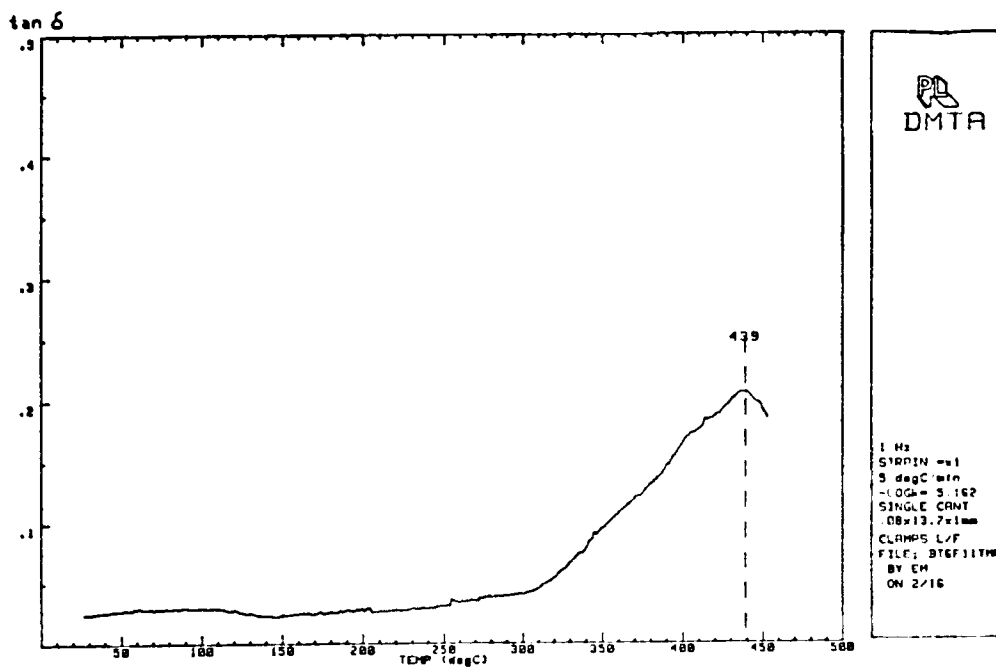


Figure 4.4.2.1. Dynamic Mechanical Thermal Analysis, Tan delta damping peak for the BTDA/TPDA based Homopolymer (5°C/minute; 1 Hz frequency)

temperatures between 279°C and 439°C depending on the mole percent DKDEDA incorporated into the polymer backbone.

4.4.3 Polymer Solubility

The polymer solubilities were determined in a wide variety of solvents by dissolving the polyimides in the appropriate solvent at room temperature in order to obtain 10% solid solutions. Solubilities of the series of polyimides based on BTDA dianhydride and DKDEDA and TMPDA diamines are listed in Table 4.4.3.1. The whole series of polyimide homo- and copolymers readily dissolved in the dipolar aprotic solvents such as DMAc and NMP and the low boiling solvent methylene chloride to form clear viscous polyimide solutions. The solubilities of the copolymers with increased DKDEDA content did not change at least in the series of solvents tested in Table 4.4.3.1. After fully imidized polyimide films were cast onto glass plates and heated to 300°C in an oven, the polyimides were rendered insoluble in all solvents tested. Again as with the other series of polyimides, these polyimides probably had undergone a thermal crosslinking reaction at the elevated temperatures (10,145).

4.4.4 Thermo-Oxidative Stability

The thermo-oxidative stabilities of the series of polyimide copolymers based on BTDA dianhydride and DKDEDA and TMPDA were determined by thermogravimetric analysis in an air

Table 4.4.3.1

Solubility of BTDA/TMPDA/DKDEDA Based Homo- and Copolymers

Polyimide System	Solvents					
	NMP	DMAc	THF	CH ₂ Cl ₂	ØCl	Tol
BTDA/TMPDA	S	S	IS	S	IS	IS
BTDA/DKDEDA (10%)/ TMPDA (90%)	S	S	IS	S	IS	IS
BTDA/DKDEDA (20%)/ TMPDA (80%)	S	S	IS	S	IS	IS
BTDA/DKDEDA (30%)/ TMPDA (70%)	S	S	IS	S	IS	IS
BTDA/DKDEDA (40%)/ TMPDA (60%)	S	S	IS	S	IS	IS

NMP = N-Methyl Pyrrolidinone

Tol = Toluene

ØCl = Chlorobenzene

THF = Tetrahydrofuran

CH₂Cl₂ = Methylene Chloride

DMAc = Dimethyl Acetamide

S = Easily Soluble MS = Marginally Soluble IS = Insoluble

environment at a heating rate of 10°C per minute. The polyimides were analyzed as thin films. Figure 4.4.4.1 shows a comparison of a copolymer with 10% DKDEDA incorporation and a copolymer with 40% DKDEDA incorporation. As can be seen by the thermogravimetric analysis weight loss curves, the thermal stability of the copolymers is almost exactly the same. The thermo-oxidative stability of the copolymers does not change when more DKDEDA is incorporated into the polymer backbone at least with the series of polyimides studied. All polyimides in this series had a 5% weight loss at greater than 500°C in an air environment.

4.4.5 Photosensitive Properties of BTDA, DKDEDA and TMPDA based polyimides

The series of polyimide homo- and copolymers with varying amounts of DKDEDA was synthesized in order to determine the effect of increased aromatic keto group concentration on the photosensitive properties of the polyimides obtained. As one might expect, the optical densities of copolymers increased with increasing DKDEDA incorporation at both the 313nm and 365nm wavelengths as shown in Table 4.4.5.1. The increase in optical density was due to the increase in the amount of aromatic ketone groups available to absorb the UV light.

Since the optical densities of the homo- and copolymers at the 313nm wavelength were extremely high, the 365nm wavelength was chosen to study the photosensitive properties of this series of polyimides.

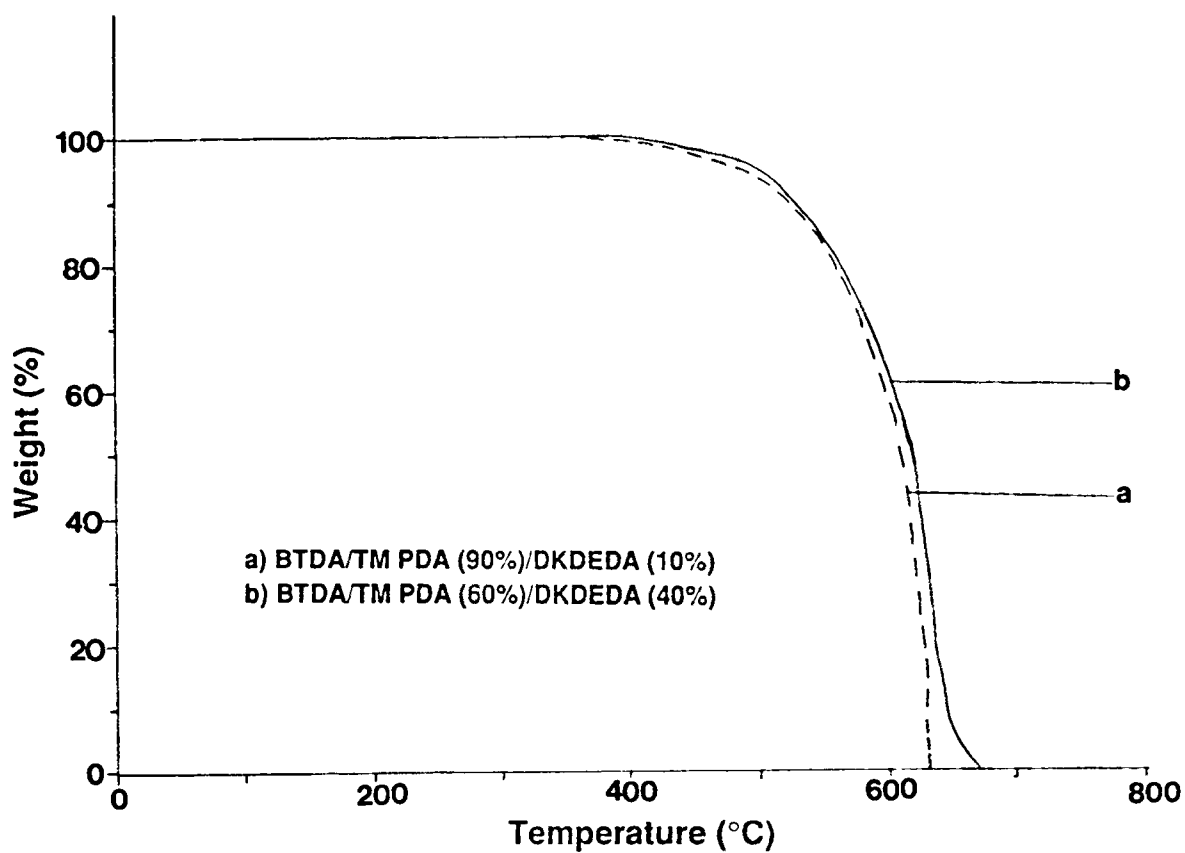


Figure 4.4.4.1. Thermogravimetric analysis of BTDA/TMPDA/DKDEDA Based Homo- and Copolymers (Air atmosphere; 10°C/minute).

Table 4.4.5.1

Optical Densities of BTDA/TMPDA/DKDEDA Based Homo- and Copolymers

Polyimide System	Wavelength	
	313nm	365nm
BTDA/TMPDA	1.580/ μ m	0.138/ μ m
BTDA/DKDEDA (10%)/ TMPDA (90%)	1.530/ μ m	0.139/ μ m
BTDA/DKDEDA (20%)/ TMPDA (80%)	1.615/ μ m	0.162/ μ m
BTDA/DKDEDA (30%)/ TMPDA (70%)	1.717/ μ m	0.179/ μ m
BTDA/DKDEDA (40%)/ TMPDA (60%)	1.751/ μ m	0.188/ μ m

Optical Density = the UV absorbance per one micron thick film.

The photosensitive properties of these polyimides were determined by analyzing photosensitive response plots and using them to determine the gel dose, D_g , and the exposure dose required to render a film of given thickness totally insoluble, D_i . The contrast of this series of polyimides were determined by plotting the normalized film thickness remaining as a function of the log of the exposure dose. The slope of the straight lines formed by these plots were the determined contrasts, γ , of the given polyimide systems. Table 4.4.5.2 summarizes the results obtained from the various photosensitive response and contrast plots for the series of polyimides based on the BTDA dianhydride and the TMPDA and DKDEDA diamines.

The homopolymer based on BTDA and TMPDA had a gel dose of 36.1 mJ/cm^2 , a D_i of 188 mJ/cm^2 and a contrast of 1.33 when exposed at the 365nm wavelength. The copolymers with 10 and 20 mole percent DKDEDA incorporation did not show much change from the homopolymer. The lower D_g and D_i of the 10 mole percent DKDEDA copolyimide was due to the very high relative molecular weight of this polymer as indicated by the high intrinsic viscosity value of 1.43 dl/g determined in NMP at 25°C . However, after 30 mole percent of the DKDEDA was incorporated into the polymer backbone a sharp increase in both the D_g and D_i was determined, indicating that the photosensitivity of the copolyimide had decreased. A further increase in the D_g and D_i was seen for the 40 mole percent

Table 4.4.5.2

Photosensitive Properties of BTDA/TMPDA/DKDEDA Based homo- and copolymers
(Exposed at 365nm)

<u>Polyimide System</u>	<u>D_g (mJ/cm²)</u>	<u>D_i (mJ/cm²)</u>	<u>χ</u>	<u>Film Thickness</u>	<u>$[\eta]$ (dl/g)</u>
BTDA/TMPDA	36.1	188	1.33	1.2 μ m	0.50
BTDA/DKDEDA (10%)/ TMPDA (90%)	14.8	80	1.28	1.1 μ m	1.43
BTDA/DKDEDA (20%)/ TMPDA (80%)	41.1	134	1.83	1.2 μ m	0.82
BTDA/DKDEDA (30%)/ TMPDA (70%)	194	617	1.87	1.2 μ m	0.66
BTDA/DKDEDA (40%)/ TMPDA (60%)	729	1,388	3.36	1.2 μ m	0.53

D_g = Gel Dose - the dose at which the polymer begins to crosslink.

D_i - the dose required to totally crosslink the film at a given thickness.

χ = Contrast - the exposure range over which the material will respond.

DKDEDA copolymer with a D_g of 729 mJ/cm^2 and a D_i of $1,388 \text{ mJ/cm}^2$. The decrease in photosensitivity was found to be due to the decrease in the amount of methyl substituents incorporated into the copolymers backbone. The more DKDEDA incorporated into the polymer backbone the less TMPDA that could be incorporated, since both were incorporated as mole percentages of the total diamine content. Therefore, as the amount of DKDEDA was increased the amount of methyl substituents incorporated was decreased. As found in the previous study, the less methyl substituents along the polymer backbone the greater the exposure dose required for the D_g and D_i . This is due to the fact that a methyl substituent must be in close proximity to the 1,2 diradical of the benzophenone moiety in order for a hydrogen abstraction reaction to take place. If the hydrogen abstraction reaction is inhibited the crosslinking reaction is also inhibited. Therefore, even though the amount of UV absorbing aromatic carbonyl groups was increased the photosensitivity of the copolymers was decreased due to the lack of methyl substituents available to undergo an intermolecular hydrogen abstraction reaction and subsequent combining of the radicals to form a crosslinked network.

4.5 Characterization of the BTDA and 6FDA Dianhydride and TMPDA Diamine Based Polyimide Homo- and Copolymers

4.5.1 Intrinsic viscosities and glass transition temperatures

A series of high molecular weight homo- and copolymers was synthesized using both BTDA and 6FDA dianhydrides and the TMPDA diamine in order to determine the effect of decreased aromatic keto concentration on the photosensitive properties of the polyimides obtained. Relative molecular weights of this series of homo- and copolymers were determined by the intrinsic viscosities values in NMP at 25°C. Table 4.5.1.1 lists the intrinsic viscosities and glass transition temperatures of the polyimide series. The high intrinsic viscosity values indicate that high molecular weight polyimides were obtained. All of the polyimide samples listed in Table 4.5.1.1 formed transparent and creasable films with good mechanical properties, giving further support that high molecular weight copolymers were formed.

This particular series of copolymers was synthesized by a reverse addition method of adding the diamine to a stirring solution of the dianhydride. Generally, the highest molecular weight polyimides have been synthesized by the addition of the solid dianhydride to a stirring diamine solution (55). This procedure is typically used to avoid possible anhydride hydrolysis which could occur by the reaction of anhydride with residual water in the solvent, which in turn could cause an upset in the 1:1 stoichiometry of the diamine to dianhydride required for high molecular weight polymer. However, even though this series was synthesized by the reverse addition method in order to obtain more uniform copolymers, high

Table 4.5.1.1

Intrinsic viscosities and glass transition temperatures of BTDA, 6FDA and TMPDA based homo- and copolymers

Polyimide System	$[\eta]$ (dl/g)	Tg (°C) by DMTA
BTDA/TMPDA	0.50	439
BTDA (90%)/6FDA (10%)/ TMPDA	1.49	---
BTDA (75%)/6FDA (25%)/ TMPDA	1.38	439
BTDA (65%)/6FDA (35%)/ TMPDA	1.01	---
BTDA (50%)/6FDA (50%)/ TMPDA	0.97	439
BTDA (35%)/6FDA (65%)/ TMPDA	0.95	---
BTDA (25%)/6FDA (75%)/ TMPDA	0.85	---
6FDA/TMPDA	0.74	---

Note: intrinsic viscosity measured in NMP at 25°C

molecular weight polyimides were still obtained. This conclusion is supported by the fact that high intrinsic viscosity values were obtained. Apparently the system was sufficiently dry to avoid hydrolysis problems.

The glass transition temperatures of this series of polyimides were not able to be determined by differential scanning calorimetry (DSC) and therefore dynamic mechanical thermal analysis (DMTA) was employed. The glass transition temperature of the homopolymer based on BTDA and TMPDA was found to be 439°C by the tan delta damping peak at a heating rate of 5°C per minute and a frequency of 1 Hz. Note that this value is somewhat enhanced by crosslinking at high temperatures. Crosslinking probably occurs at high temperatures via benzoyl methyl oxidation coupling. After 50 mole percent 6FDA dianhydride was incorporated into the polyimide backbone the same glass transition temperature of 439°C was observed. This indicated that the polyimide's glass transition temperature was not greatly affected by changing the dianhydride from BTDA to 6FDA. Similar observations were made by Arnold et al. when synthesizing homopolymers using the diamines 3,3'-Diaminodiphenyl sulfone (3,3'DDS) and Bisanaline P (Bis-P) with the dianhydrides BTDA and 6FDA (148,149). The homopolymer made from BTDA and 3,3'DDS had a glass transition temperature of 265°C while the homopolymer based on 6FDA and 3,3'DDS was found to have a glass transition temperature of 270°C (148,149). Similarly, the homopolymer based on BTDA and

Bis-P had a glass transition temperature of 264°C, while the homopolymer based on 6FDA and Bis-P had a glass transition temperature of 267°C (148,149). Only changes of 5°C or less were observed in the glass transition temperatures when changing the dianhydride from BTDA to 6FDA in the homopolymers.

Other glass transition temperatures of the copolymers not listed in Table 4.5.1.1 were unable to be measured due to premature cracking in the thin polymer films when being analyzed by DMTA. However, the glass transition temperatures are expected to be similar to the homo- and copolymers that were able to be measured. Therefore, the copolymers should all have damping peaks close to 439°C for this series of polyimides.

4.5.2 Polymer Solubility

The polyimide solubilities were determined in the same variety of solvents as for the other series of polyimide homo- and copolymers already discussed. The solubilities were determined by dissolving the polyimides in the appropriate solvent at room temperature in order to obtain 10% solid solutions. The solubilities of the series of polyimide homo- and copolymers based on the BTDA and 6FDA dianhydrides and the TMPDA diamine are shown in Table 4.5.2.1. Like the other series of polymers already discussed, these polyimides were soluble in the dipolar aprotic solvents such as DMAc and NMP.

Table 4.5.2.1

Solubilities of BTDA/6FDA/TMPDA based Homo- and Copolymers

Polyimide System	Solvents					
	NMP	DMAc	THF	CH ₂ Cl ₂	ØCl	Tol
BTDA/TMPDA	S	S	IS	S	IS	IS
BTDA (90%)/6FDA (10%)/TMPDA	S	S	IS	S	IS	IS
BTDA (75%)/6FDA (25%)/TMPDA	S	S	IS	S	IS	IS
BTDA (65%)/6FDA (35%)/TMPDA	S	S	S	S	IS	IS
BTDA (50%)/6FDA (50%)/TMPDA	S	S	S	S	IS	IS
BTDA (35%)/6FDA (65%)/TMPDA	S	S	S	S	IS	IS
BTDA (25%)/6FDA (75%)/TMPDA	S	S	S	S	IS	IS
6FDA/TMPDA	S	S	S	S	IS	IS

NMP = N-Methyl Pyrrolidinone

THF = Tetrahydrofuran

Tol = Toluene

CH₂Cl₂ = Methylene Chloride

ØCl = Chlorobenzene

DMAc = Dimethyl Acetamide

S = Easily Soluble MS = Marginally Soluble IS = Insoluble

The homopolymer based on BTDA and TMPDA was also soluble in the low boiling solvent methylene chloride but not in tetrahydrofuran. However, after incorporating 35 mole percent of the 6FDA into the polymer, the copolyimide formed was easily soluble in tetrahydrofuran. Therefore, by incorporating the 6FDA into the polymer backbone the solubility of the homo- and copolymers was increased. This observation was also reported for other polyimide systems using the 6FDA instead of the BTDA dianhydride (148,149).

4.5.3 Thermo-Oxidative Stability

Thin films of the polyimides based on the BTDA and 6FDA dianhydrides and TMPDA diamine were analyzed by thermogravimetric analysis in an air environment in order to determine their thermo-oxidative stability. Figure 4.5.3.1 shows a comparison of the thermal scans for the homo- and copolymers at a heating rate of 10°C per minute. The homopolymer based on BTDA and TMPDA had less weight loss at the higher temperatures than the homo- and copolymers with 6FDA incorporation, and therefore, appears to have more thermo-oxidative stability. The copolymer with 10% 6FDA incorporation has an increased weight loss at high temperatures compared to the BTDA homopolymer. However, after 50 mole percent of the 6FDA incorporation into the polyimide backbone there seemed to be a leveling off effect. The homo- and copolymers with 50 to 100 mole percent of the 6FDA

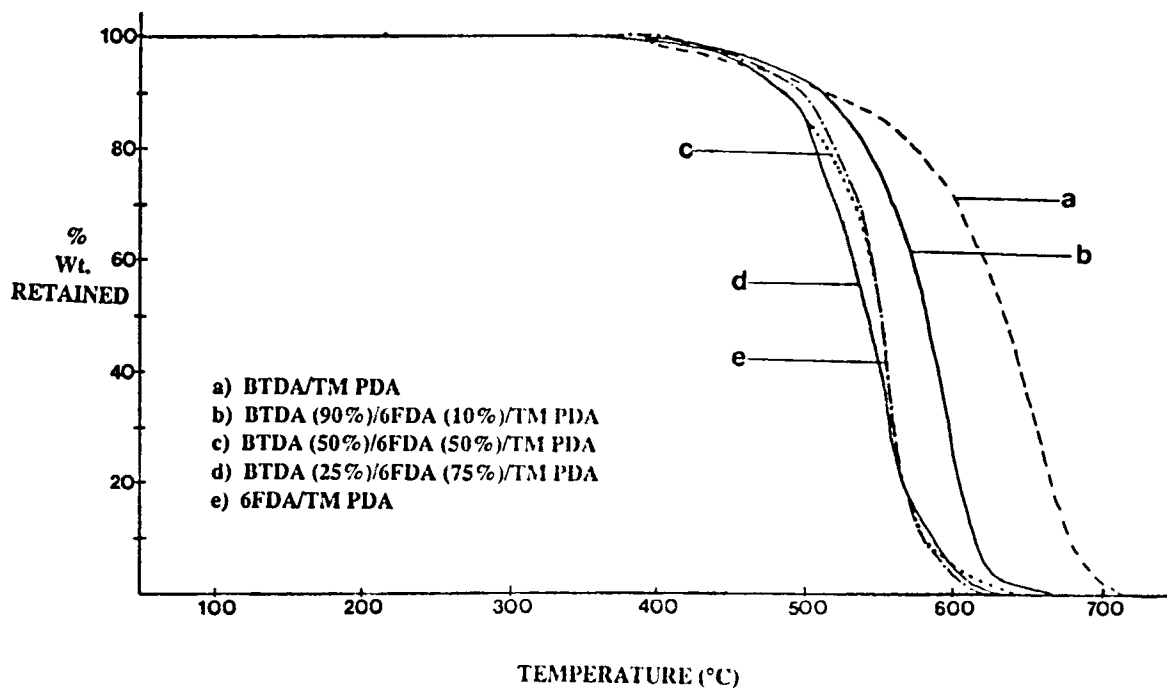


Figure 4.5.3.1. Thermogravimetric Analysis of BTDA/6FDA/TMPDA based Homo- and Copolymers (air atmosphere: 10°C/minute).

incorporation into the polyimide backbone essentially had the same amount of weight loss at a given temperature as judged by the thermal scans shown in Figure 4.5.3.1. This apparent decrease in thermal stability compared to the homopolymer may be due to a decrease in the amount of thermal crosslinking that can take place when the 6FDA is incorporated at high mole percentages. With a decrease in thermal crosslinking the weight loss will be greater at a lower temperature compared to a polyimide that can thermally crosslink to a high extent.

4.5.4 Photosensitive Properties of BTDA, 6FDA, and TMPDA based polyimide homo- and copolymers

A series of polyimide homo- and copolymers with varying amounts of BTDA and 6FDA dianhydride was synthesized in order to determine the effect of decreased aromatic ketone concentration on the photosensitive properties of the polyimides obtained. Figure 4.5.4.1 shows the effect of 6FDA incorporation on the optical densities of the homo- and copolymers at 365nm. Since the 6FDA does not have the benzophenone moiety to absorb the UV light the optical densities of the copolymers decreased with increasing 6FDA content. The homopolymer based on BTDA and TMPDA has an optical density of approximately .14 absorbance per micron thick film at the 365nm wavelength. However, the homopolymer based on 6FDA and TMPDA has a much lower optical density of 0.03 absorbance units per micron thick film. Therefore, the more 6FDA incorporated into the polyimide backbone the more

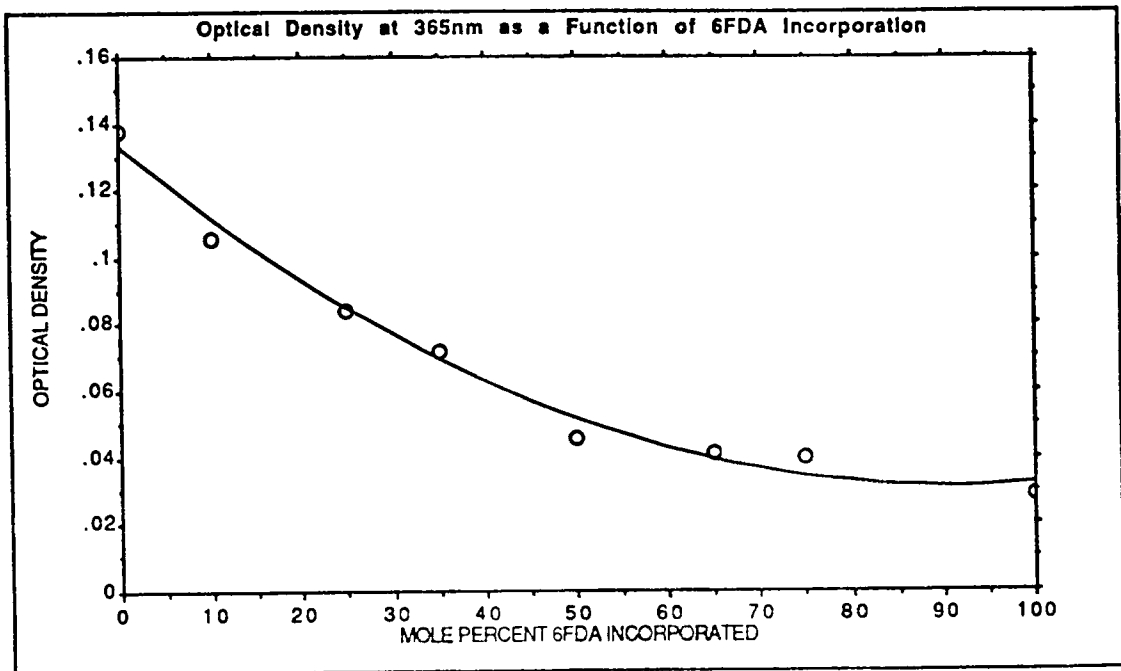


Figure 4.5.4.1. Optical Densities as a Function of the mole percent 6FDA incorporation at the 365nm wavelength.

transparent the polymer film was to UV light at 365nm.

A similar decrease in optical density was found at the 313nm wavelength. Figure 4.5.4.2 shows a plot of the optical density at 313nm as a function of the mole percent 6FDA incorporated into the polymer. The homopolymer based on BTDA and TMPDA had an optical density of approximately 1.58 absorbance units per micron thick film. This optical density is too high to effectively crosslink one micron thick films because the UV light would be totally absorbed at 313nm. However, the homopolymer based on 6FDA and TMPDA had a decreased optical density at the 313nm wavelength of 0.3 absorbance units per micron thick film. Therefore, the copolymers with high 6FDA content could be exposed at 313nm due to the significant decrease in UV light absorption.

The photosensitive properties of these polyimides were determined by plotting photosensitive response plots for each individual polyimide system and using them to determine the gel dose, D_g , and the exposure dose required to make a film of given thickness totally insoluble, D_i . The contrasts of each polyimide system was determined by plotting the normalized film thickness remaining as a function of the log of the exposure dose. The slopes of the straight lines formed by this type of plot were the determined contrasts, γ , of the given polyimide systems.

Table 4.5.4.1 shows a summary of the photosensitive properties for the series of polyimides based on the BTDA and

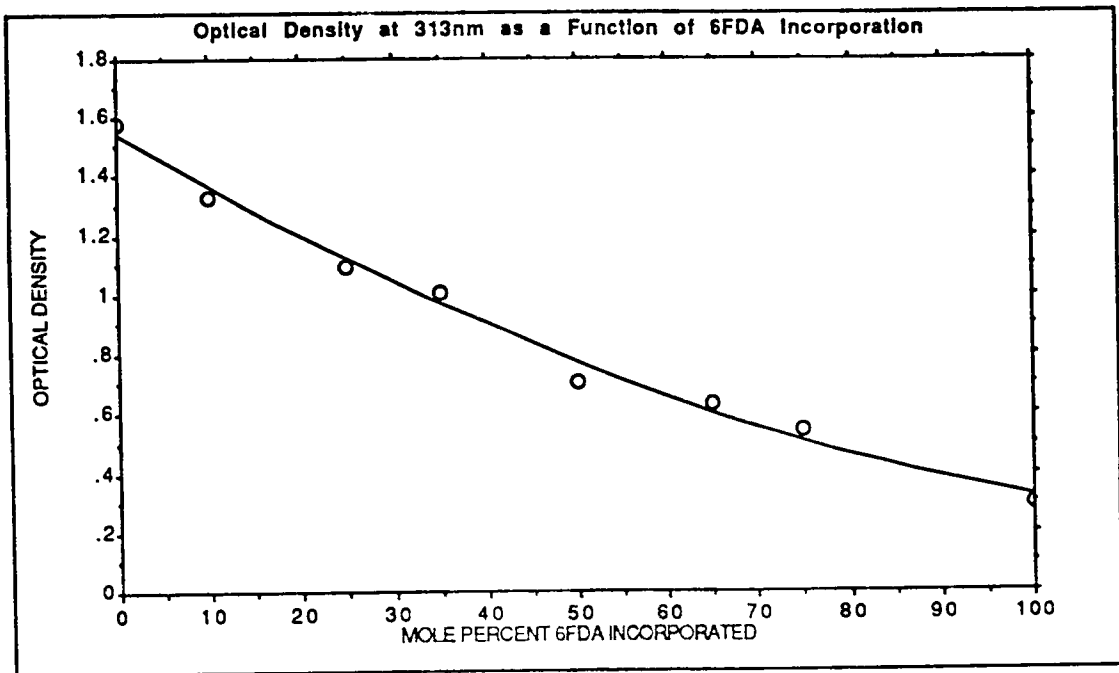


Figure 4.5.4.2. Optical Densities as a function of the mole percent 6FDA incorporation at the 313nm wavelength.

Table 4.5.4.1

Photosensitive Properties of BTDA/6FDA/TMPDA based Homo- and Copolymers
(Exposed at 365nm)

<u>Polyimide System</u>	$D_g(\text{mJ}/\text{cm}^2)$	$D_i(\text{mJ}/\text{cm}^2)$	χ	<u>Film Thickness</u>	$[\eta](\text{dl}/\text{g})$
BTDA/TMPDA	36.1	188	1.33	1.2 μm	0.50
BTDA (90%)/6FDA (10%)/ TMPDA	6.7	41.0	1.19	1.5 μm	1.49
BTDA (75%)/6FDA (25%)/ TMPDA	5.4	36.9	1.13	1.2 μm	1.38
BTDA (65%)/6FDA (35%)/ TMPDA	23.7	93.5	1.58	2.4 μm	1.01
BTDA (50%)/6FDA (50%)/ TMPDA	37.7	123	1.83	1.1 μm	0.97
BTDA (35%)/6FDA (65%)/ TMPDA	39.5	114	2.04	1.8 μm	0.95
BTDA (25%)/6FDA (75%)/ TMPDA	55.2	165	1.98	1.3 μm	0.85

D_g = Gel Dose - the dose at which the polymer begins to crosslink.

D_i - the dose required to totally crosslink the film at a given thickness.

χ = Contrast - the exposure range over which the material will respond.

6FDA dianhydrides and the TMPDA diamine at the exposure wavelength of 365nm. The homopolymer based on the BTDA and TMPDA had a gel dose, D_g , of 36.1 mJ/cm^2 , a D_i of 188 mJ/cm^2 and a contrast, γ , of 1.33. However, after 50 mole percent 6FDA was incorporated into the copolymer a D_g of 37.7 mJ/cm^2 and a lower D_i value of 123 mJ/cm^2 was found giving rise to a higher contrast value of 1.83 compared to the BTDA and TMPDA based homopolymer. Even at a higher 6FDA concentrations of mole percent 6FDA the D_g was found to be 55.2 mJ/cm^2 and the D_i was found to be 165 mJ/cm^2 giving an even higher value for the contrast of 1.98. This indicates that even at low aromatic ketone concentrations the copolymers were still photosensitive, and only a small amount of the benzophenone moieties had to be incorporated into the polyimide backbone to obtain a photocrosslinkable polyimide. However, the 6FDA and TMPDA based homopolymer, without any benzophenone moieties incorporated into the polyimide, was found not to be photosensitive even at high exposure doses. Therefore, the benzophenone moiety is important in the crosslinking but only small mole percentages have to be incorporated into the polymer.

In general an increase in the contrast value is very desirable in a photoresist system, since the contrast is directly related to the resolution capabilities of a photoresist. The higher contrast values determined for the polyimide systems with high 6FDA content was due to their

lower optical densities. Because they had lower optical densities, more UV light can pass through a given film thickness causing the photocrosslinking reaction to be more efficient. Therefore, thicker films can be crosslinked at lower exposure doses.

Even more significant, the polyimides with greater than 50 mole percent 6FDA incorporation had a low enough optical density to allow them to be exposed at 313nm. Generally, greater resolutions in photoresist patterns can be obtained for a photoresist that can be exposed at lower wavelengths (146). For this reason the amount of research being reported in the "deep UV" region of the UV light spectrum is rapidly increasing. Table 4.5.4.2 shows the photosensitivity parameters for the copolyimides containing 50 mole percent or greater 6FDA incorporation exposed at the 313nm wavelength.

The D_g and D_i values for these polyimides are greatly reduced compared to the D_g and D_i values determined at the higher 365nm wavelength for the same polyimide systems. Instead of a gel dose of 37.7 mJ/cm^2 and a D_i of 123 mJ/cm^2 determined when the 50 mole percent of 6FDA copolyimide was exposed at 365nm, a gel dose of 2.2 mJ/cm^2 and a D_i of 17.6 mJ/cm^2 was found. The lower exposure doses required for the copolymers at the lower wavelength can be attributed to the fact that the benzophone moieties absorb more UV energy and form the 1,2-diradical more efficiently at 313nm than at 365nm.

Table 4.5.4.2

Photosensitive Properties of BTDA/6FDA/TMPDA based Homo- and Copolymers
(Exposed at 313nm)

<u>Polyimide System</u>	D_g (mJ/cm ²)	D_i (mJ/cm ²)	χ	<u>Film Thickness</u>	$[\eta]$ (dl/g)
BTDA (50%)/6FDA (50%)/ TMPDA	2.2	17.6	1.0	.75 μ m	0.97
BTDA (35%)/6FDA (65%)/ TMPDA	4.4	22.3	1.34	1.1 μ m	0.95
BTDA (25%)/6FDA (75%)/ TMPDA	3.8	33.7	1.0	1.0 μ m	0.85

D_g = Gel Dose - the dose at which the polymer begins to crosslink.

D_i - the dose required to totally crosslink the film at a given thickness.

χ = Contrast - the exposure range over which the material will respond.

4.6 Synthesis of poly(imide siloxane) segmented copolymers

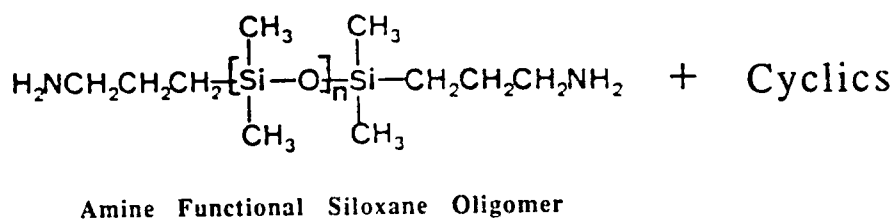
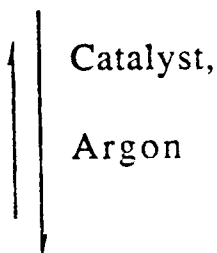
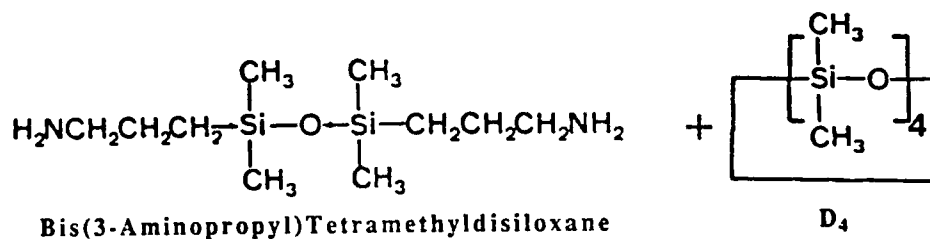
4.6.1 Synthesis of aminopropyl polydimethylsiloxane Oligomers

The synthesis of aminopropyl terminated polydimethylsiloxane oligomers was accomplished by an anionic ring opening equilibration reaction of the cyclic dimethylsiloxane tetramer, commonly known as D_4 , in the presence of the dimer bis(aminopropyl) tetramethyldisiloxane with a quaternary ammonium siloxanolate catalyst. The equilibration reaction is outlined in Scheme 4.6.1.1. The base catalyst attacks the electropositive silicon atom between the silicon and oxygen atoms in order to generate siloxanolate ions and to initiate the ring opening polymerization. The reaction continues by a making and breaking of Si-O bonds. The aminopropyl disiloxane monomer acts as an effective "end capper" or chain transfer agent since the Si-O-Si bond in the cyclic monomer, growing chain, and the dimer are quite similar in reactivities while the silicon-alkyl bond is more covalent in nature and therefore stable during the polymerization.

The equilibration reactions were run for 48 hours under neat bulk conditions at 80°C in a dry nitrogen gas purge to insure anhydrous conditions. However, previous studies have shown that shorter times are required to reach equilibrium (139). After the 48 hours, the reaction temperature was raised to 150°C for approximately 3 hours to decompose the catalyst into the volatile byproducts trimethylamine and methanol (139). The low boiling cyclics left after

Scheme 4.6.1.1

Synthesis of Aminopropyl Terminated polydimethylsiloxane
Oligomers



equilibration were removed by vacuum stripping. Approximately 8.0 weight percent of the reaction product was found to be cyclic via chromatographic analysis, with D_4 being the predominant species (139).

The molecular weight of the siloxane oligomers were controlled by the ratio of D_4 to aminopropyl terminated siloxane dimer. The number average molecular weight of the siloxane oligomer was determined by potentiometric titration of the amine end groups with alcoholic HCl. The actual value of a siloxane oligomer with a theoretical number average molecular weight of 2,500 g/mole was found to be 2,465 g/mole. The glass transition temperature of the 2,500 g/mole siloxane oligomer was found to be -123°C by DSC.

The infrared spectrum of the 2,500 g/mole siloxane oligomer is shown in Figure 4.6.1.1 and the assignments of the important absorbance bands are listed in Table 4.6.1.1 for the characteristic siloxane motions.

The proton NMR of the siloxane oligomer had one characteristic resonance peak at 0.3 ppm due to methyl groups on the siloxane. However, the molecular weight of the oligomers could not be determined by the proton NMR because the molecular weight was too high to accurately observe the resolved aminopropyl end groups.

4.6.2 Synthesis of Poly(imide siloxane) copolymers

Poly(imide siloxane) segmented copolymers were

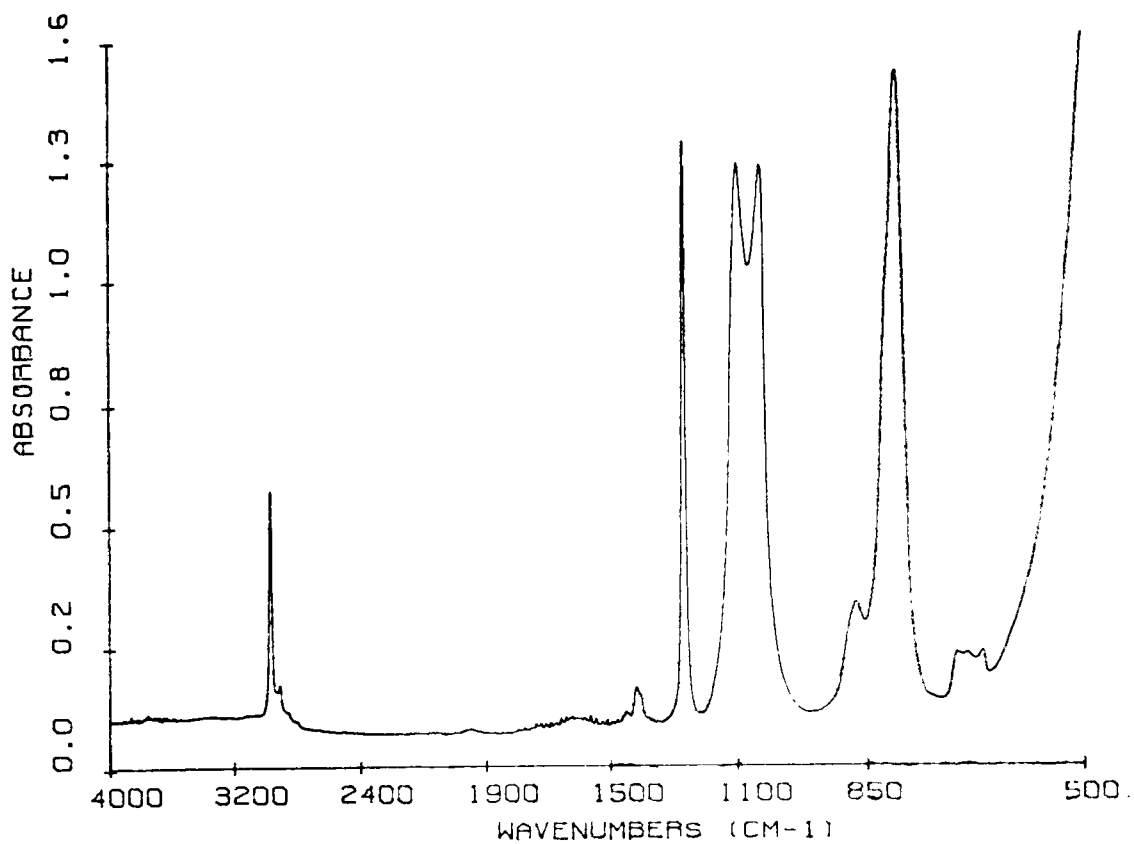


Figure 4.6.1.1. FTIR spectrum of an Aminopropyl Terminated Polydimethyl Siloxane Oligomer ($M_n = 2,500$ g/mole).

Table 4.6.1.1

FTIR Assignments for an Aminopropyl Terminated polydimethyl siloxane Oligomer

Frequency (cm ⁻¹)	Assignment
2463	C-H methyl stretch
1410	Si(CH ₃) ₂ O asymmetric deformation
1260	Si(CH ₃) ₂ O asymmetric deformation
1130-1000	Si-O-Si stretch vibration
800	Si(CH ₃) ₂ O stretch, methyl rock
715	Si(CH ₃) ₂ O stretch,
510	Si-O-Si bending vibration

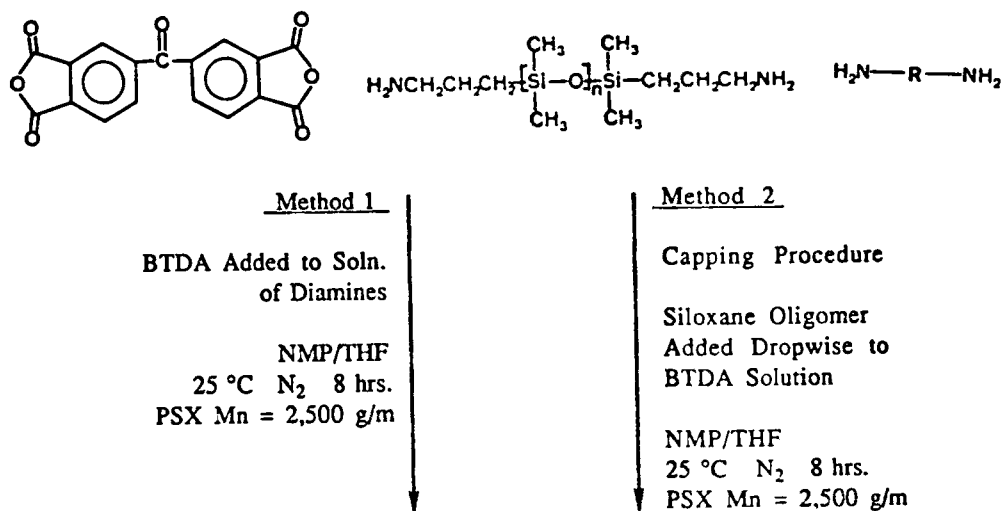
synthesized by the conventional two step approach of first synthesizing the poly(amic acid siloxane) followed by a cyclodehydration step to form the polyimide. The poly(amic acid siloxane) was synthesized using a cosolvent system of NMP and THF due to the solubility differences between the siloxane oligomer, the aromatic monomers, and the poly(amic acid) formed. The major factor in this synthesis was maintaining a homogeneous reaction solution by controlling the ratio of NMP to THF.

The general synthetic procedure for obtaining high molecular weight poly(imide siloxanes) is outlined in Scheme 4.6.2.1. The poly(amic acid) intermediates could be synthesized by one of two methods. The first method was modeled after the conventional procedure in which poly(amic acids) are synthesized, by adding the solid dianhydride to a solution of the diamines in the NMP/THF cosolvent system. This procedure required careful solvent additions during the reaction in order to keep the reaction solution homogeneous, and was only found to be useful for low molecular weight siloxane oligomers of 2,000 g/mole or less (141). High molecular weight poly(amic acids) were not obtained when this method was employed for high molecular weight siloxane oligomers due to the solubility constraints of the constituents.

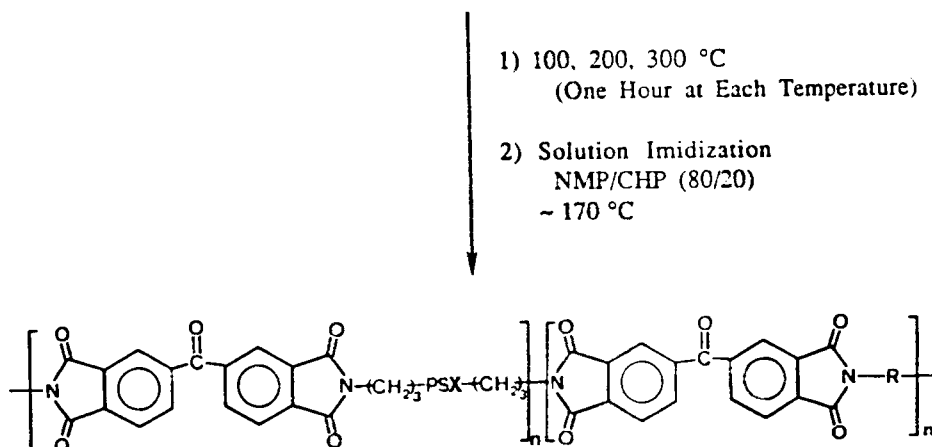
However, a second method was found to be useful for high molecular weight siloxane oligomers even at high siloxane

Scheme 4.6.2.1

Synthesis of Poly(Imide Siloxane) Copolymers.



Poly(amic Acid Siloxane)



All Films Are Transparent and Creasable

content (141). In this synthetic procedure a reverse monomer addition process is used. The siloxane dissolved in THF is slowly added dropwise to the stirring dianhydride solution to avoid premature chain extension of the polydimethylsiloxane, and to insure that the siloxane oligomers are capped at both ends with anhydride end groups. By capping the siloxane oligomers first, an enhanced solubility is obtained of the capped siloxane in the dipolar aprotic solvent NMP. Therefore, a more homogeneous reaction solution is obtained. After all the siloxane oligomer is capped by the dianhydride, the stoichiometric amount of the second aromatic diamine is added to the reaction to cause chain extension and to form the high molecular weight poly(amic acid). Since this method formed the most homogeneous reaction conditions, this method was used to form all the poly(amic acid siloxanes) discussed herein.

The poly(amic acid siloxanes) were cyclodehydrated by both the conventional bulk thermal imidization and the solution imidization procedure using the NMP and CHP cosolvent system, as previously discussed. The bulk imidization method, casting thin films on glass plates and heating to high temperatures, caused the polyimides formed to be totally insoluble in all solvents tested. However, all poly(imide siloxanes) formed by the solution imidization procedure in the NMP/CHP cosolvent system at moderate temperatures were easily soluble in the dipolar aprotic solvents.

An FTIR spectrum of a poly(imide siloxane) based on BTDA and TMPDA containing 20 weight percent polydimethylsiloxane content is shown in Figure 4.6.2.1. A list of the FTIR assignments for this polyimide copolymer is shown in Table 4.6.2.1. Both the polyimide IR bands and the IR bands associated with polydimethylsiloxane remain present in the copolymer spectrum. The intensity of the IR bands depends on the amount of siloxane content in the copolymers.

Proton NMR was used to determine if the polydimethyl siloxane was successfully incorporated into the polyimide copolymers. Figure 4.6.2.2. shows a proton NMR spectrum of a solution imidized poly(imide siloxane) segmented copolymer with 20 weight percent polydimethyl siloxane incorporation dissolved in CDCl_3 without TMS. This spectrum shows a strong resonance peak at 0.07 ppm due to the siloxane methyl groups, a peak at 2.1 ppm due to the methyl substituents on the diamine, and a series of aromatic proton resonances at approximately 8.2 ppm due to the aromatic protons in the polyimide. The absence of other peaks above 10 ppm indicated that no residual carboxylic acid groups were present and there was quantitative conversion of the amic acid to the polyimide.

The actual amount of siloxane incorporated into the copolymers was also determined by using the integrated NMR spectra. The amount of siloxane incorporated into the copolymer was determined by ratioing the peak integration intensities of the siloxane methyl groups to the other protons

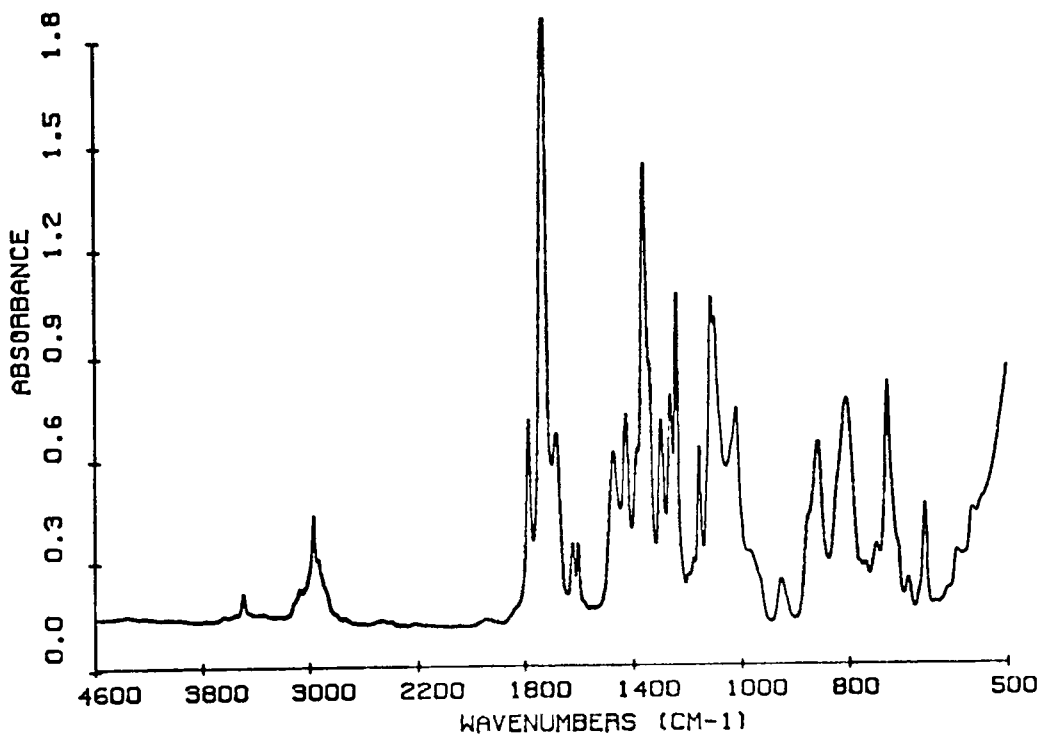


Figure 4.6.2.1. FTIR spectrum of a BTDA/TMPDA based poly(imide siloxane) copolymer (PSX Mn = 2, 465 g/mole).

Table 4.6.2.1

FTIR assignments for BTDA/TMPDA based poly(imide siloxane) copolymers

Frequency (cm ⁻¹)	Assignment
3100	Aromatic protons (imide segments)
2960	Aliphatic protons (siloxane segments)
1780 1725	Imide carbonyl stretch vibrations
1680	C=O stretch (benzophenone moiety)
1420	Aromatic C-C stretching
1260	Si-C Stretch vibration
1096 1028	Si-O Stretch vibration
725	Imide band

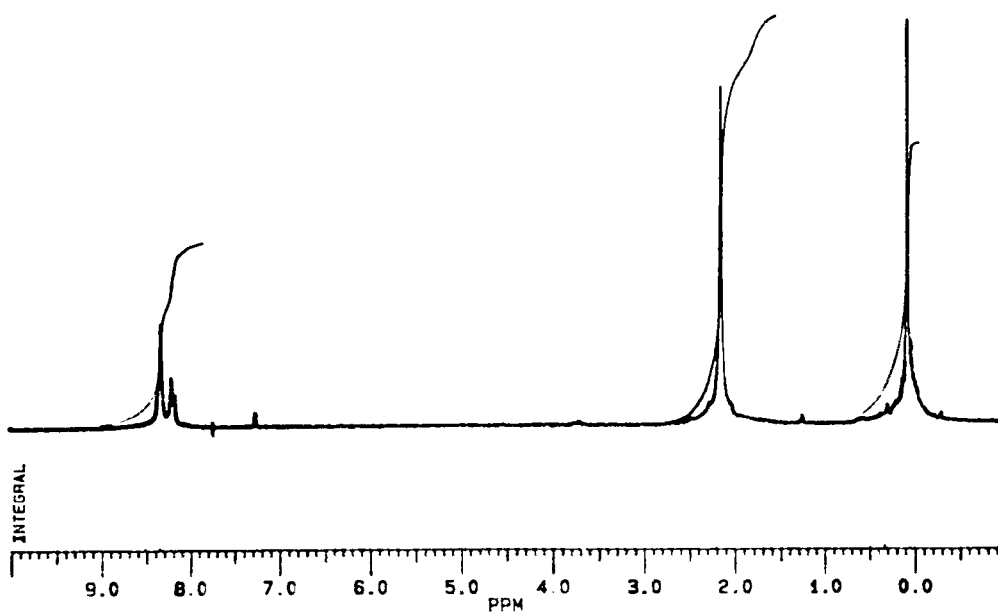


Figure 4.6.2.2. Proton NMR spectrum of a BTDA/TMPDA based poly(imide siloxane) copolymer with 20 weight percent siloxane incorporation. (PSX: $M_n = 2,465$ g/mole).

found in the copolymer. The integration values for the peaks due to the siloxane methyls and other polyimide protons were rationed using the relation:

$$\frac{[I(A) \times M(A)]/N(A)}{[I(A) \times M(A)]/N(A) + [I(B) \times M(B)]/N(B)} \times 100 = \%A$$

where I(n) is the integrated intensity of the peak due to component n, M(n) is the repeat unit molecular weight of the component n, and N(n) is the number of protons giving rise to peak n. Table 4.6.2.2 shows the determined weight percent of the siloxane incorporated into the polyimide copolymer compared to the theoretical weight percent siloxane that should have been incorporated for a series of poly(imide siloxane) copolymers. The polyimide copolymer with a theoretical weight percent siloxane incorporation of 20 was found to have 18.8 weight percent siloxane determined by the proton NMR method described above. This was in close agreement with the theoretical value indicating that siloxane was successfully incorporated into the copolymer backbone.

4.7 Characterization of poly(imide siloxane) copolymers

4.7.1 Intrinsic viscosities and glass transition temperatures

A series of high molecular weight poly(imide siloxane) copolymers was synthesized using the BTDA dianhydride and the TMPDA diamine along with aminopropyl terminated polydimethyl siloxane oligomers. The relative molecular weight of the copolymers was determined via the intrinsic viscosity values

Table 4.6.2.2

Amount of polydimethyl siloxane incorporated into polyimide copolymers determined by Proton NMR

Polyimide system	theoretical wt %	wt % PSX found
BTDA/TMPDA/10% PSX	10%	9.3%
BTDA/TMPDA/15% PXS	15%	14.5%
BTDA/TMPDA/20% PXS	20%	18.8%

in NMP at 25°C. The intrinsic viscosities and glass transition temperatures of the homopolymer and siloxane modified copolymers are listed in Table 4.7.1.1. The high values of the intrinsic viscosities indicate that high molecular weight copolymers were formed. Thin, creasable transparent films were obtained for each polyimide sample, farther evidence that high molecular weight copolymers were formed.

The glass transition temperatures of this series of polyimides were determined by dynamic mechanical thermal analysis (DMTA) instead of differential scanning calorimetry (DSC) because no endothermic peaks were observed in the DSC scans. The homopolymer based on BTDA and TMPDA had a glass transition temperature of 439°C determined by the tan delta damping peak. The copolymer with 20 weight percent polydimethyl siloxane had an upper glass transition temperature of 414°C. The two tan delta damping peaks of the homopolymer and 20 weight percent siloxane modified copolymer are compared in Figure 4.7.1.1. The upper glass transition temperatures of the siloxane modified polyimides were only slightly depressed relative to the homopolymer control, indirectly indicating that a microphase separation between the "soft" siloxane segment and "hard" polyimide segment was achieved. However, the upper glass transition temperatures were dependent upon the amount of siloxane oligomers incorporated indicating a partial phase mixing had occurred.

Table 4.7.1.1

Intrinsic Viscosities and Glass Transition Temperatures for the BTDA and TMPDA based poly(imide siloxane) Copolymers

Polyimide System	$[\eta]$ (dl/g)	Tg(°C) by DMTA
BTDA/TMPDA	0.50	439
BTDA/TMPDA/PSX (10%)	0.40	436
BTDA/TMPDA/PSX (15%)	0.53	420
BTDA/TMPDA/PSX (20%)	0.60	414

Note: intrinsic viscosities measured in NMP at 25°C

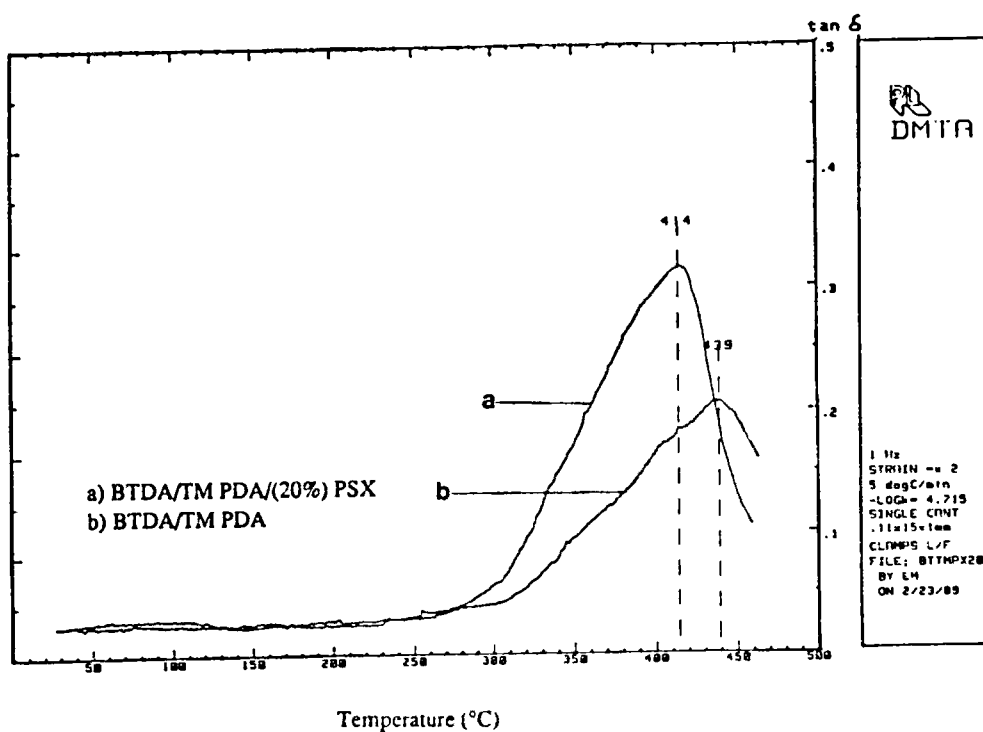


Figure 4.7.1.1. Tan delta damping curves for the homopolymer and 20 weight percent polydimethyl siloxane modified copolymer (5°C/minute; 1 Hz frequency).

4.7.2 Polymer Solubility

The solubility of the siloxane modified poly(imide siloxane) copolymers was determined by dissolving the polyimide copolymer in the appropriate solvent at room temperature to yield a 10 weight percent solution. The solubility of the series of polyimides is shown in Table 4.7.2.1. All the solution imidized polyimides were soluble in the dipolar aprotic solvent and the low boiling solvent methylene chloride. There was no observable difference in the solubilities of the copolymers compared to the homopolymer. However, it was previously reported that incorporating siloxane at different weight percentages could enhance the solubility of the copolymer in a variety of solvents depending on the weight percent siloxane incorporated (140-143). After thin films of the siloxane modified polyimides were heated to 300°C for approximately 15 minutes, the once soluble polyimides were rendered insoluble due to a thermal crosslinking reaction that occurred at the elevated temperatures.

4.7.3 Thermo-Oxidative Stability

Thermogravimetric analysis (TGA) was used to measure the thermo-oxidative stability of thin poly(imide siloxane) films in an air environment at a heating rate of 10°C per minute. Since both polyimides and polyorganosiloxanes are known for their excellent thermal stabilities, it was expected that the

Table 4.7.2.1

Solubilities of Poly(imide siloxane) Copolymers based on BTDA and TMPDA

Polyimide System	Solvents					
	NMP	DMAc	THF	CH ₂ Cl ₂	ØCl	Tol
BTDA/TMPDA	S	S	IS	S	IS	IS
BTDA/TMPDA/10% PSX	S	S	IS	S	IS	IS
BTDA/TMPDA/15% PSX	S	S	IS	S	IS	IS
BTDA/TMPDA/20% PSX	S	S	IS	S	IS	IS

NMP = N-Methyl Pyrrolidinone

THF = Tetrahydrofuran

Tol = Toluene

CH₂Cl₂ = Methylene Chloride

ØCl = Chlorobenzene

DMAc = Dimethyl Acetamide

S = Easily Soluble MS = Marginally Soluble IS = Insoluble

copolymers formed by the combination of the two would form soluble poly(imide siloxane) copolymers with excellent thermal stabilities. Thermogravimetric analysis weight loss curves for the various poly(imide siloxane) copolymers are compared in Figure 4.7.3.1. The samples maintained good thermal stabilities even at the 20 weight percent siloxane content. The char yields left at the high temperatures were found to be proportional to siloxane content, due to the silicate-type of product obtained as a degradation product of the siloxane in the air environment.

4.7.4 XPS Surface Analysis

Many siloxane block modified segmented copolymers have been studied in the past due to their novel surface properties. Some of the copolymers studied include poly(styrene siloxane) (150), poly(ester siloxane) (151), poly(urethane siloxane) (152), poly(carbonate siloxane) (153,154), poly(sulfone siloxanes) (151), and poly(imide siloxane) (140-143). X-ray photoelectron spectroscopy studies determined that the surface compositions of these copolymers were dominated by siloxane, even at low amounts of siloxane incorporation. The low free energy of the siloxane provides a thermodynamic driving force for migration of the siloxane to the air interface. Since the surfaces were predominately siloxane, the surface properties of these copolymers closely matched those of the siloxane, while the bulk properties

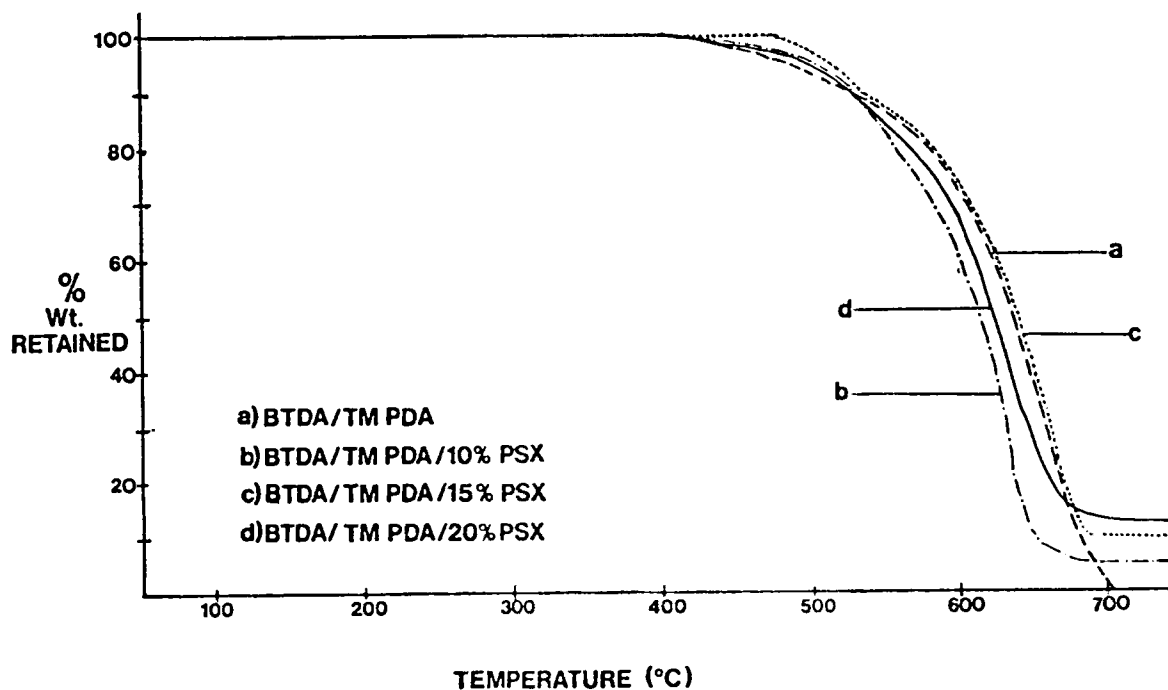


Figure 4.7.3.1. Thermogravimetric Analysis of BTDA/TMPDA based Poly(imide siloxane) copolymers (Air atmosphere; 10⁰C minute).

largely remained those of the "hard" polyimide segment of the copolymer.

Poly(imide siloxane) copolymers have been extensively studied (140-143,148,149). At low amounts of siloxane incorporation it was found that the copolymers possessed the mechanical strength and thermal stability of the homopolymer, but the surface properties were modified by the siloxane domination. The hydrophobic siloxane surface was found to decrease the amount of moisture uptake of the copolymer when immersed in distilled water at room temperature (141). Electrical properties such as the dielectric constant are greatly dependent on the amount of moisture absorbed by the polymer. Therefore, by incorporating small amounts of siloxane into the polyimide backbone, the amount of moisture absorbed by the polymer can be decreased, desirably affecting the dielectric constant of the copolymer. Another benefit of having a siloxane rich surface was found to be oxygen plasma etch resistance (141). Siloxane has been reported to be remarkably stable to atomic oxygen degradation (155,156,157). Poly(imide siloxane) copolymers have also demonstrated increase oxygen resistance in an oxygen plasma environment (141). XPS studies showed that the surface siloxane can react with oxygen to form an inorganic silicate ceramic like layer when exposed to oxygen plasmas, thus protecting the underlying substrates from further oxidative degradation (141). Oxygen plasma etch resistance of photoresists is important in the

microelectronic industry. Plasma etching techniques are often employed to transfer the patterned form by the photoresist to an underlying layer. Therefore, if the photoresist has increased oxygen plasma resistance the ease of the pattern transfer process can be increased due to the thinner films required to act as an oxygen etch barrier.

For these reasons it was of interest to incorporate small amounts of siloxane oligomers (up to 20 weight percent) into the photocrosslinkable polyimides. X-ray photoelectron spectroscopy was used to quantify the surface composition of the siloxane modified polyimides. Two different depths of the copolymers surface were sampled by varying the take-off angle. A 15 degree grazing take-off angle analyzed atomic percents of the elements present in the uppermost surface (approximately 10 to 20 angstroms) rather than molecules from the bulk. On the other hand, compositional information more characteristic of the bulk of the copolymer was measured by a 90 degree take-off angle (approximately 50 to 100 angstroms). Figure 4.7.4.1 shows a typical XPS wide scan spectrum of a siloxane modified copolymer with 20 weight percent siloxane content measured at a 90° take-off angle.

The results of the XPS studies conducted on the homo- and copolymers at the different take-off angles are listed in Table 4.7.4.1. The binding energy of each element is listed in Table 4.7.4.2. The data indicates that the siloxane component of the copolymer dominates the surface by the

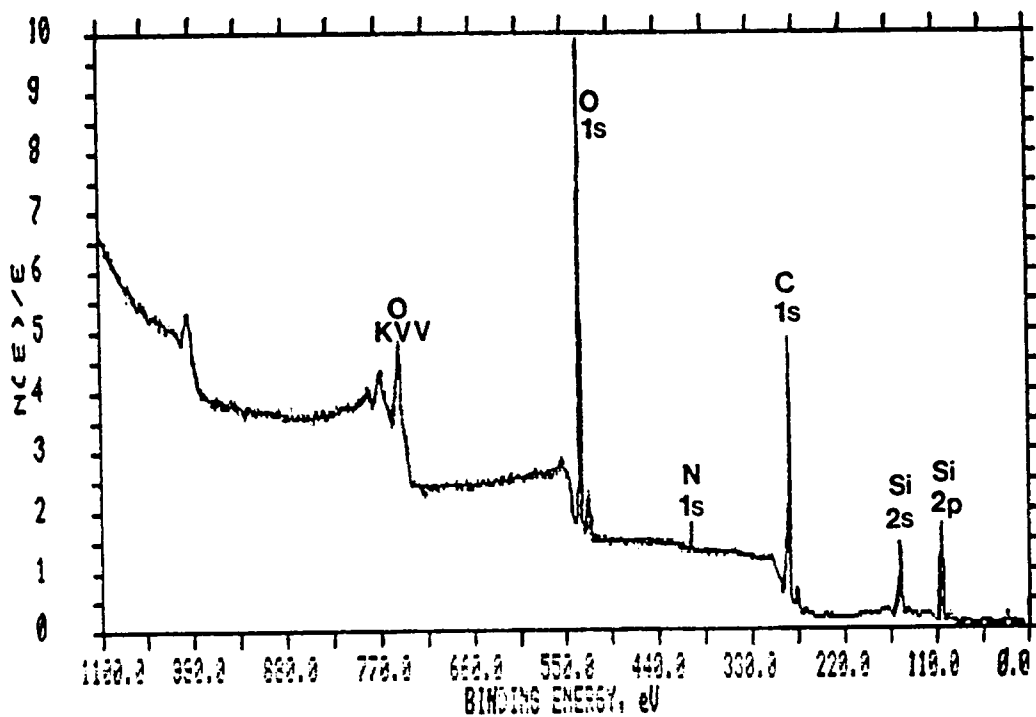


Figure 4.7.4.1. XPS Wide Scan Spectrum of a Siloxane Modified Polyimide; Siloxane Content = 20 wt %; Siloxane Mn = 2,465 g/mole (90° take-off angle).

Table 4.7.4.1

XPS Surface Analysis of Siloxane Modified Polyimide Thin Films
(BTDA/TMPDA based)

Polyimide System	take-off angle	Atomic percentages			
		C	O	N	Si
BTDA/TMPDA	90	76	17	7	--
BTDA/TMPDA/10% PSX	90	76	17	2	5
BTDA/TMPDA/10% PSX	15	76	16	1	7
BTDA/TMPDA/20% PSX	90	48	33	2	17
BTDA/TMPDA/20% PSX	15	44	32	1	23

Table 4.7.4.2

Binding Energies of Poly(imide Siloxane) Copolymers: XPS
Results (BTDA/TMPDA based)

Polyimide System	Take-off Angle	Binding Energies (eV)			
		C 1s	O 1s	N 1s	Si 2P
BTDA/TMPDA	90	285.0	532.5	400.4	--
BTDA/TMPDA/10% PSX	90	285.0	532.6	400.6	102.2
BTDA/TMPDA/10% PSX	15	285.0	532.5	400.2	102.2
BTDA/TMPDA/20% PSX	90	285.0	532.7	400.6	102.5
BTDA/TMPDA/20% PSX	15	285.0	532.7	400.5	102.6

increased atomic percentage of silicon at the surface relative to the bulk. The ten weight percent siloxane material showed a reduced amount of siloxane content at the surface relative to the 20 percent siloxane material. However, in the other polyimide systems previously studied it was found that surface composition was independent of the amount of siloxane incorporated. Even polyimides with low amounts of siloxane incorporation (5 to 10 weight percent) possessed surfaces that were as much as 85 percent siloxane (141).

During the course of the photosensitivity studies, conducted at IBM, on the siloxane containing polyimides, it was found that the polyimide copolymers containing siloxane did not require an adhesion promoter to form uniformly thick films, but the polyimide homo- and copolymers without any siloxane incorporation required an adhesion promoter in order to form good adhesion between the polyimide and the substrate. Polyimide adhesion to silicon dioxide and bare silicon surfaces is generally known to be rather poor (158). Therefore, a surface pretreatment using γ -amino-propyl-triethoxysilane as an adhesion promoter is typically employed before the polyimide is applied (159-162). Typically, the organosilane coupling agents are applied by spin coating a 0.1 weight percent solution of the organosilane in water onto the surface of the silicon or silicon dioxide just prior to spin coating the polyimide or poly(amic acid). The water hydrolyzes the ethoxy groups on the organosilane to form

silanol groups. The silanol groups on the coupling agents can then condense with the silanol groups on the silicon or silicon dioxide substrate to form an aminopropyl arm that can interact with the polyimide or poly(amic acid) to generate better adhesion between the two substrates (159,161).

Silicone-polyimide copolymers have been developed for integrated circuit applications and are claimed to require no adhesion promotor to surfaces such as silicon, silicon dioxide and silicon nitride since the silicon moiety serves to bind the polymer to the substrate (163-166). Commercially available siloxane polyimides are now available from companies such as General Electric, Hitachi, and M&T chemicals. These polymers are based on only the siloxane dimer instead of oligomers and therefore may suffer from problems such as a decreased glass transition temperatures and thermal stabilities.

Since the photosensitive poly(imide siloxanes) required no coupling agent to form good adhesion between the polyimide copolymer and the substrate, it was of interest to evaluate the surface properties of the siloxane modified copolymers at the silicon dioxide polymer interface. Thin films of the copolymers were analyzed by XPS on the glass side of the films after they were gently peeled from the glass surface using a razor blade. Two different depths of the copolymers were sampled by varying the electron take-off angle. The results of the studies conducted on the homo- and copolymers at the

different take-off angles are listed in Table 4.7.4.3. The binding energy for each element of the polyimides is listed in Table 4.7.4.4. The data indicates that the siloxane component of the copolymer is also dominant at the glass surface compared to the bulk of the film indicated by the increased atomic percentage of silicon at the surface. Therefore, the increased adhesion might be due to dipolar or acid base interactions of the siloxane with the silicon or silicon dioxide surface due to the similarities in their chemical nature.

4.7.5 Photosensitive Properties

A series of poly(imide siloxane) copolymers was synthesized in order to incorporate many of the beneficial properties of the siloxane polymer to the polyimide such as reduced moisture absorption and oxygen plasma etch resistance. Only copolymers consisting of up to 20 weight percent siloxane were synthesized in order to optimize the thermal, mechanical and photosensitive properties of the polyimides.

Since polydimethyl siloxane does not absorb UV light at the 313nm and 365nm wavelength the optical densities of the siloxane modified copolymers decreased with increasing siloxane content. Table 4.7.5.1 shows the optical densities of the copolymers at 313nm and 365nm for increasing siloxane content. The homopolymer based on BTDA and TMPDA has an optical density of $1.58/\mu\text{m}$ at 313nm and $0.14/\mu\text{m}$ at 365nm.

Table 4.7.4.3

XPS Surface Analysis of Siloxane Modified Polyimide Thin Films
on the glass side (BTDA/TMPDA based)

Polyimide System	Take-off Angle	Atomic percentages			
		C	O	N	Si
BTDA/TMPDA	90	76	17	7	--
BTDA/TMPDA/10% PSX	90	78	15	3	4
BTDA/TMPDA/10% PSX	15	76	15	2	7
BTDA/TMPDA/20% PSX	90	67	21	4	7
BTDA/TMPDA/20% PSX	15	60	24	2	14

Table 4.7.4.4

Binding Energies of Poly(imide Siloxane) Copolymers: XPS
results on glass side (BTDA/TMPDA based)

Polyimide System	Take-off Angle	Binding Energies (eV)			
		C 1s	O 1s	N 1s	Si 2P
BTDA/TMPDA	90	285.0	532.6	400.5	--
BTDA/TMPDA/10% PSX	90	285.0	532.6	400.3	102.1
BTDA/TMPDA/10% PSX	15	285.0	532.4	400.3	102.2
BTDA/TMPDA/20% PSX	90	285.0	532.3	400.4	101.9
BTDA/TMPDA/20% PSX	15	285.0	532.6	400.6	102.4

Table 4.7.5.1

Optical Denisities of BTDA/TMPDA based Poly(imide siloxane) copolymers

Polyimide System	Wavelength	
	313nm	365nm
BTDA/TMPDA	1.580/ μ m	0.138/ μ m
BTDA/TMPDA/10% PSX	1.400/ μ m	0.121/ μ m
BTDA/TMPDA/15% PSX	1.340/ μ m	0.112/ μ m
BTDA/TMPDA/20% PSX	1.060/ μ m	0.106/ μ m

Optical Density = the UV absorbance per one micron thick film.

The copolymer with 20 weight percent polydimethyl siloxane incorporation has an optical density of 1.06/ m at 313nm and 0.106/ m at 365nm.

The photosensitive properties of the poly(imide siloxane) copolymers are summarized in Table 4.7.5.2. The homopolymer based on BTDA and TMPDA had a gel dose, D_g , of 36.1 mJ/cm^2 and a D_i of 188 mJ/cm^2 . The copolymer with 20 weight percent polydimethyl siloxane had a comparable D_g of 30.2 mJ/cm^2 and a reduced D_i of 111 mJ/cm^2 . Since the D_i of the polymer was reduced for the siloxane containing material the contrast increased to 1.68 compared to 1.33 for the homopolymer. The high D_g and D_i values for the copolymer containing 10 weight percent siloxane were due to the low molecular weight of the material indicated by the low intrinsic viscosity value of 0.4 dl/g in NMP at 25°C.

Due to the higher contrast value and lower density of the 20 weight percent polydimethyl siloxane copolymer, thicker films were able to be crosslinked at lower exposure doses compared to the homopolymer. The working energy, or the energy required to make a given polymer thickness totally insoluble, D_i , was plotted as a function of film thickness for the 20 weight percent siloxane copolyimide in Figure 4.7.5.1. A film thickness of 7.0 microns was crosslinked at an exposure dose of 410 mJ/cm^2 at 365nm.

Table 4.7.5.2

Photosensitive Properties of BTDA/TMPDA based poly(imide siloxane) Copolymers

<u>Polyimide System</u>	\underline{D}_g (m/cm ²)	\underline{D}_i (m/cm ²)	$\underline{\chi}$	<u>Film Thickness</u>	$\underline{[\eta]}$ (dl/g)
BTDA/TMPDA	36.1	188	1.33	1.22 μ m	0.50
BTDA/TMPDA/10% PSX	173	612	1.73	1.18 μ m	0.40
BTDA/TMPDA/15% PSX	58.0	176	1.99	1.65 μ m	0.53
BTDA/TMPDA/20% PSX	30.2	111	1.68	1.57 μ m	0.60

\underline{D}_g = Gel Dose - the dose at which the polymer begins to crosslink.

\underline{D}_i - the dose required to totally crosslink the film at a given thickness.

$\underline{\chi}$ = Contrast - the exposure range over which the material will respond.

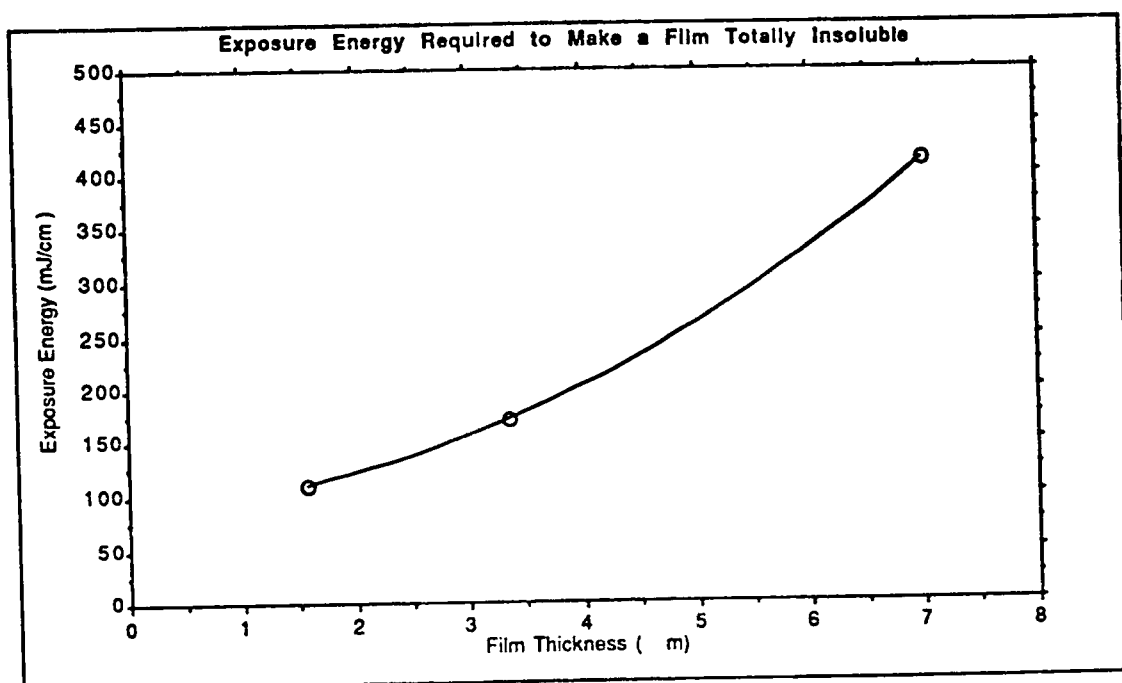


Figure 4.7.5.1. Working energy required to crosslink various film thickness of a 20 weight percent siloxane modified polyimide copolymer (BTDA/TMPDA based).

4.8 FT-IR study of the extent of photocrosslinking

The extent of the photocrosslinking reaction was monitored by FT-IR using the C=O stretching band at 1678 cm^{-1} due to the benzophenone moiety in the polyimide backbone. A one micron thick film of the homopolymer based on BTDA and TMPDA was spin coated from NMP onto a KBr salt plate and heated on a hot plate at 125°C for 15 minutes to drive off the solvent. Figure 4.8.1 shows the FTIR spectrum of the homopolymer based on BTDA and TMPDA before it was exposed to UV light. Table 4.8.1 shows the assignments of important IR bands for this homopolymer.

During the crosslinking reaction this band should decrease since the benzophenone 1,2-diradical formed during UV irradiation undergoes a hydrogen abstraction reaction to form a hydroxyl group instead of the ketone, therefore a broad band at $3600\text{--}3300\text{ cm}^{-1}$ should appear due to an increase in hydroxyl group formation. However, after a 220 mJ/cm^2 exposure dose of UV light at the 365nm wavelength there was no noticeable change in the IR spectrum of the polyimide, but the film was rendered totally insoluble. This indicates that the extent of photocrosslinking is too low to be detected by FT-IR but large enough to render the polymer insoluble. After a 440 mJ/cm^2 exposure dose of UV light is given to the polyimide sample (double the exposure dose required to make a one micron thick film totally insoluble), a slight decrease in the intensity of the peak at 1678 cm^{-1} was found, but no

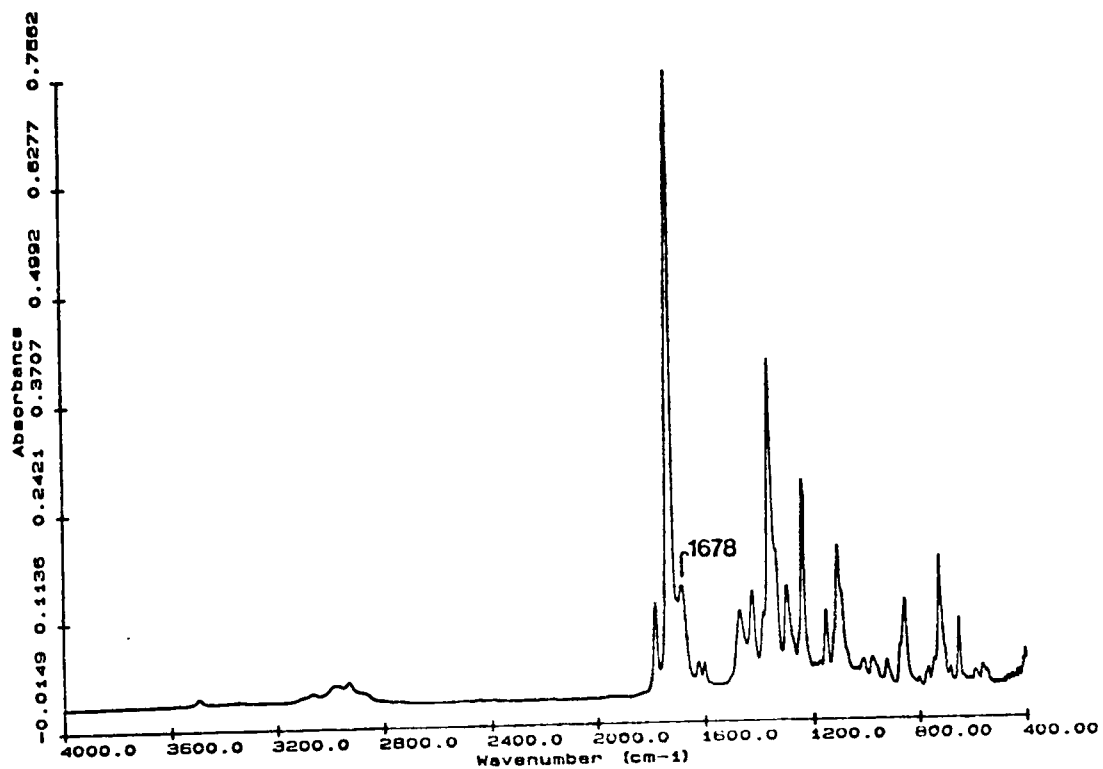


Figure 4.8.1. FTIR spectrum of a one micron thick film of a BTDA/TMPDA based homopolymer.

Table 4.8.1

FTIR Assignments for a BTDA/TMPDA based polyimide homopolymer

Frequency (cm ⁻¹)	Assignments
2970	C-H stretch (methyl substituents)
1778 1725	Imide carbonyl stretch vibrations
1678	C=O stretch (benzophenone moiety)
1370	imide band
726	imide band

noticeable peak due to the hydroxyl groups was formed (see Figure 4.8.2).

After an exposure dose of $2,640 \text{ mJ/cm}^2$ was given to the polyimide film (ten times the exposure dose required to make a one micron thick film totally insoluble), a further decrease in the 1678 cm^{-1} IR band can be seen and perhaps a slight indication of a broad band from 3600 cm^{-1} to 3300 cm^{-1} can be seen (see Figure 4.8.3). However, it is not until an exposure dose of $12,540 \text{ mJ/cm}^2$ (almost 60 times the exposure dose required to make the film totally insoluble) that the 1678 cm^{-1} IR band at 3600 cm^{-1} to 3300 cm^{-1} is formed (see Figure 4.8.4).

This series of IR spectra indicate that the extent of photocrosslinking required to make a photocrosslinkable polyimide insoluble is too low to be revealed by FT-IR. It is not until large excesses in exposure dose are given to the film that the extent of reaction is large enough to be seen by changes in the FT-IR spectra.

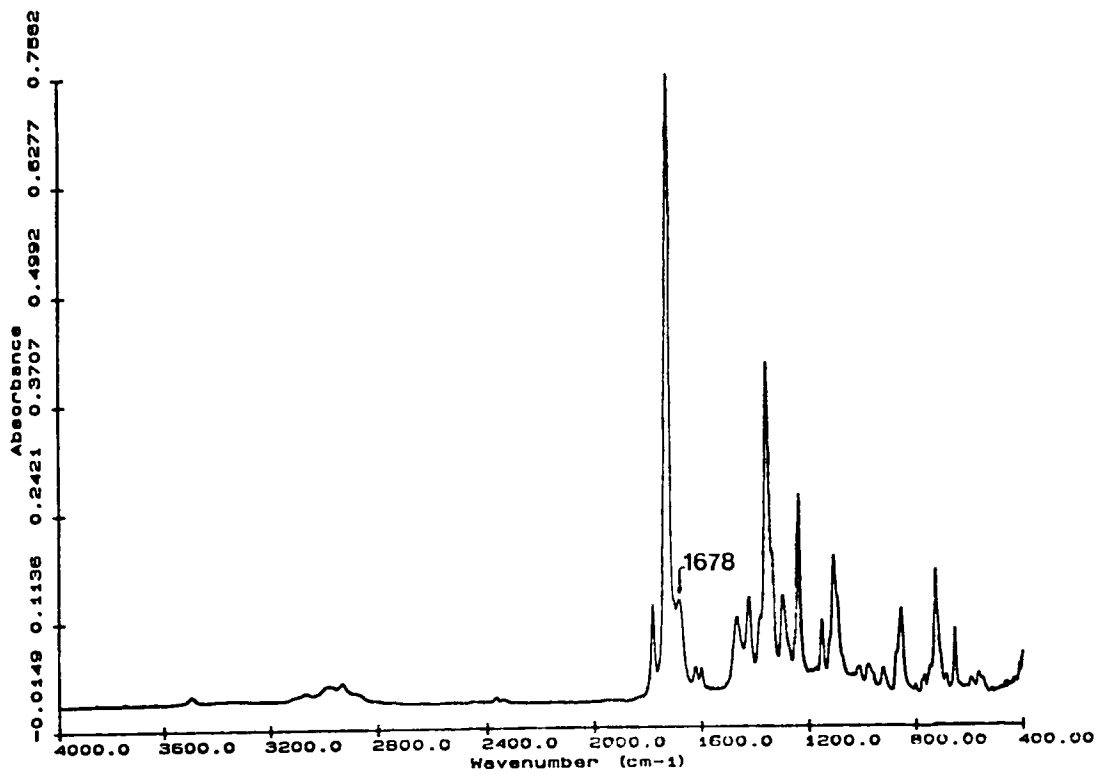


Figure 4.8.2. FTIR Spectrum of a one micron thick film of BTDA/TMPDA based homopolymer after a 440 mJ/cm² exposure dose at the 365 wavelength.

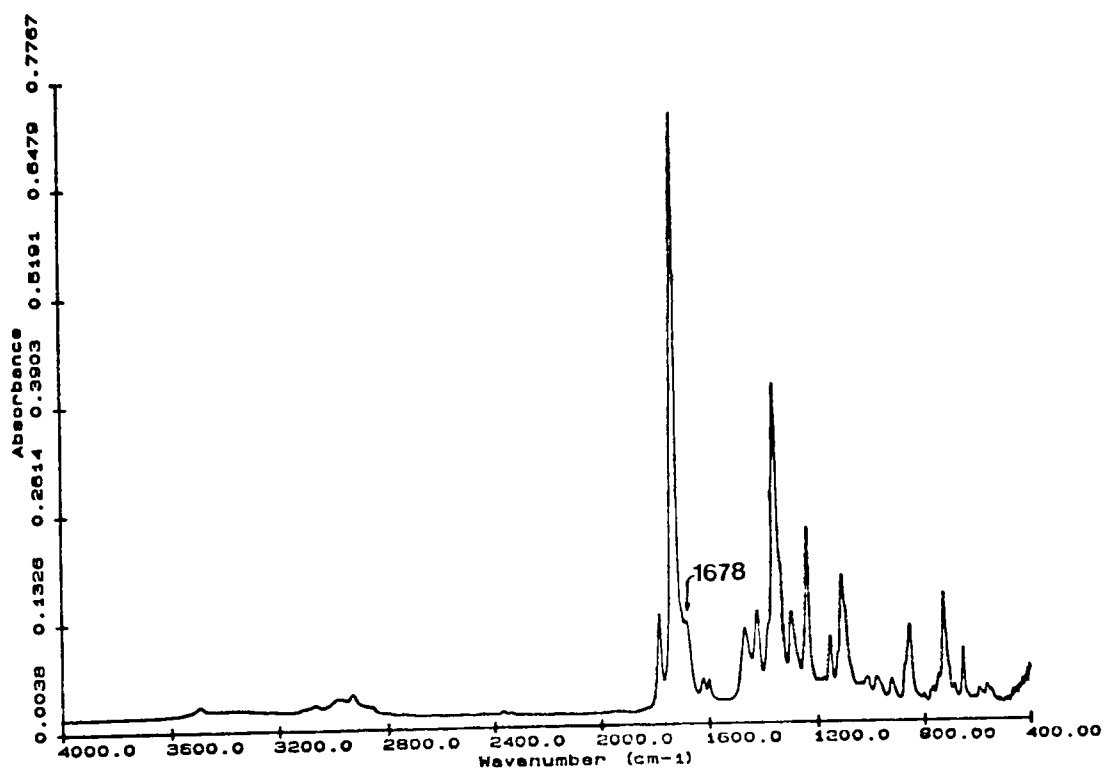


Figure 4.8.3. FTIR Spectrum of a one micron thick film of a BTDA/TMPDA based homopolymer after a 2,640 mJ/cm^2 exposure dose at the 365nm wavelength.

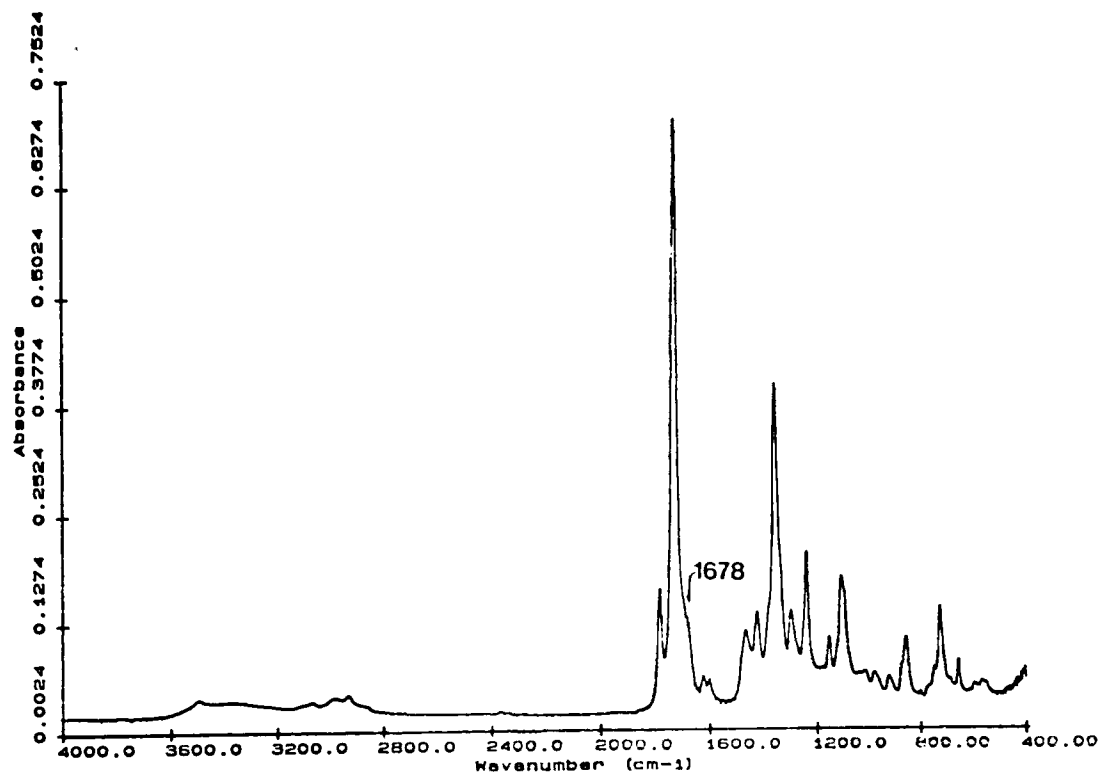


Figure 4.8.4. FTIR Spectrum of a one micron thick film of a BTDA/TMPDA based homopolymer after a 12,540 mJ/cm² exposure dose at the 365nm wavelength.

V. Conclusions

The major objectives of the research described in this dissertation were to synthesize high glass transition temperature, high molecular weight, photocrosslinkable polyimide and poly(imide siloxane) homo- and copolymers, and to study the effects of chemical structure on the photosensitive polymers obtained. Homo- and copolymers were prepared through the reaction of various aromatic dianhydrides with aromatic diamines in dipolar aprotic solvents to yield high molecular weight poly(amic acid) prepolymers. Siloxane modified copolymers were synthesized by reacting aromatic anhydrides with aminopropyl terminated polydimethylsiloxane oligomers and aromatic diamines in a cosolvent system consisting of a dipolar aprotic solvent and an ether solvent to achieve a homogeneous solution and a high molecular weight poly(amic acid siloxane) prepolymer. The best procedure employed to achieve a homogeneous solution and high molecular weight prepolymer was to "cap" the siloxane oligomer with excess dianhydride prior to the addition of the aromatic diamine.

Polyimides were subsequently prepared from the poly(amic acid) prepolymers through a thermal cyclodehydration procedure. Soluble fully imidized polymers were obtained using a solution imidization process employing a cosolvent system of 80 volume percent NMP and 20 volume percent CHP in the temperature range of 160-170°C. The NMP was used to

solvate the polymer while the CHP was responsible for removal of the water of imidization from the reaction to prevent hydrolysis of the poly(amic acid) and to drive the reaction to completion. A second type of imidization was used in order to compare cyclodehydration products. The well known technique of heating solution cast films to high temperatures was followed. Temperatures of 300°C were used to insure that quantitative ring closure was achieved. All polyimides formed by this method were rendered totally insoluble in all solvents tried.

Various techniques were employed to characterize the polyimides in order to determine the effects of changing the chemical structure on the properties of the polyimides. Polymer solubilities increased when the methyl substituted diamines were incorporated into the polymer backbone. Thermal properties such as glass transition temperature and thermo-oxidative stability also increased with increased methyl substituted diamine incorporation into the homo- and copolymers.

The adhesion of the siloxane modified copolymers to silicon or silicon dioxide substrates was greatly enhanced compared to the polyimide homo- and copolymers without siloxane incorporation. The poly(imide siloxane) copolymers did not require an adhesion promotor pretreatment prior to spin coating the polyimide onto the silicon or silicon dioxide wafers while the polyimide homo- and copolymers without

siloxane always required a surface pretreatment to enhance adhesion.

The photosensitive properties of the polyimide systems were found to be greatly dependent on wavelength of exposure and chemical structure of the polyimides. The photocrosslinking reaction was found to be more efficient at 313nm than at 365nm. However, the optical density is higher for the polyimides at 313nm and therefore, thick films could not be crosslinked at the 313nm. The more methyl substituents incorporated into the polymer backbone the more photosensitive the polyimide formed.

Incorporation of polydimethyl siloxane oligomers into the polyimide backbone was found to decrease the optical density at both 313nm and 365nm. However, the photosensitivity of the copolymers was not decreased. Therefore, a higher contrast value was obtained and thicker films were able to be crosslinked at lower exposure doses for the siloxane modified polyimides.

The photosensitive properties were also found to be dependent on the amount of aromatic ketone groups incorporated into the polymers backbone. Increased aromatic ketone concentration increased the optical density of the materials, however, it did not increase the photosensitivities. The photosensitivity decreased with increasing ketone concentration because the amount of methyl substituents was decreased when increased diketone diamine was incorporated.

When decreasing the amount of aromatic ketone incorporation by using a second dianhydride, the optical density of the copolymers decreased significantly without decreasing the photosensitive properties of the polyimide copolymers. This caused a higher contrast value for the polyimides with decreased ketone concentration and allowed much thicker films to be photocrosslinked. After the ketone concentration was decreased by 50 percent, the optical density decreased enough at 313nm to allow exposure at this wavelength. The photosensitivities of the polymers increased by almost a factor of ten for the copolymer with decreased ketone concentration when exposed at 313nm.

6.0 References

1. K. Mukai, A. Saiki, K. Yamanaka, S. Harada and S. Shoji, *IEEE J. Solid-State Circuits* 13, 462 (1978).
2. W.R. Iversen, *Electronics*, Sept. 11, 41 (1980).
3. R. Iscoff, *Semiconductor International*, Oct. 110 (1984).
4. R.E. Kerwin and M.R. Goldrich, *Polym. Eng. Sci.* 11, 425 (1971).
5. R. Rubner, H. Ahne, E. Kuhn, and G. Kolodziej, *Photographic Science and Engineering* 23, 303 (1979).
6. H. Ahne, H. Kruger, E. Pammer and R. Rubner, in "Polyimides: Synthesis Characterization, and Applications," Vol. 2, K.L. Mittal ed., Plenum Press, (1984) p. 905.
7. H.J. Merrem, R. Klug, and H. Hartner, in "Polyimides: Synthesis Characterization, and Applications," Vol. 2, K.L. Mittal ed., Plenum Press, (1984) p. 919.
8. F. Kataoka, F. Shoj, I. Takemoto, I. Obara, M. Kojima, H. Yokono, and T. Isogai in "Polyimides: Synthesis, Characterization, and Applications," Vol. 2, K.L. Mittal ed., Plenum Press, (1984) p. 933.
9. W.H. Shen, A.J. Yo, and B.M. Gong in "Polyimides: Synthesis, Characterization, and Applications," Vol. 2, K.L. Mittal ed., Plenum Press, (1984) p. 947.
10. J. Pfeifer and O. Rohde in "Recent Advances in Polyimide Science and Technology," W.D. Weber and M.R. Gupta ed., Society of Plastics Engineers, Inc., (1987) p. 336.
11. D.J. Harper and J.F. McKellar, *Chem. & Ind.*, London 848 (1972).
12. D.J. Harper and J.F. McKellar, *J. Appl. Polym. Sci.*, 17 3503 (1973).
13. G. Oster, G.K. Oster, and H. Moroson, *J. Polym. Sci.*, 34, 671 (1959).
14. D.K. Mohanty, Y. Sachdeva, J.L. Hedrick, J.F. Wolfe, and J.E. McGrath, *Polym. Prepr.*, 25(2) 19 (1984).

15. D.K. Mohanty, Y. Sachdeva, J.L. Hedrick, J.F. Wolfe, and J.E. McGrath in "Advances in Polymer Synthesis," B.M. Culbertson and J.E. McGrath, Editors, Plenum Press, (1985).
16. D.K. Mohanty, Ph.D. Thesis, VPI & SU, 1983.
17. A.A. Lin, V.R. Sastri, G. Tesoro, R. Eachus, and A. Reiser, *Macromolecules*, 21, 1665 (1988).
18. J.C. Scaiano, J.C. Netto-Ferreira, A.F. Becknell, and R.D. Small, in "Photopolymers: Principles, Processes and Materials" (Proc. of Technical Conference, Society of Plastics Engineers, Inc.), (1988) p. 313.
19. J.C. Scaiano, A.F. Becknell, and R.D. Small, *Journal of Photochemistry and Photobiology A: Chemistry*, 44, 99 (1988).
20. W.S. DeForest, in "Photoresist-Materials and Processes," McGraw-Hill, New York, 1975.
21. C. Grant Willson, in "Introduction to Microlithography," L.F. Thompson, C.G. Willson, and M.J. Bowden, Editors, American Chemical Society, Washington, D.C., 1983.
22. G. Samuelson, in "Polymer Materials for Electronic Applications," E.D. Feit and C.W. Wilkins, Jr., Editor, American Chemical Society, Washington, D.C., 1982 p. 93.
23. A.C. Adams in "VLSI Tehcnology," S.M. Sze, Editor, McGraw Hill, New York, 1983.
24. W. Kern, *Semiconductor International*, 8, 228 (1985).
25. W. Kern and R.S. Rosler, *J. Vac. Sci. Tehnol.*, 14, 1082, (1977).
26. A.M. Wilson, *Thin Solid Films*, 83, 145 (1981).
27. J. Economy, *Contemp. Top. Polym. Sci.*, 5, 35 (1984).
28. Bogert and Renshaw, *Journal of American Chemical Society*, 30, 1140 (1908).
29. A.M. Fraser in "High Temperature Resistant Polymers," John Wiley and Sons, Inc., New York, 1968.
30. J.F. Heacock and C.E. Barr, *SPE Trans.*, 105 (1965).
31. K. Sato, S. Harada, A. Saiki, T. Kimura, T. Okubo, K. Mukai, *IEEE Trans.*, PHP-9, 176 (1973).

32. K. Mukai, A. Saiki, K. Yamanaka, S. Hirada, S. Shoji, *IEEE J. Solid State Circuits*, 13, 462 (1978).
33. S. Miller, *Circuits Manufacturing*, 39 (April, 1977).
34. G. Samuelson, *Preprints Org. Coat. Plastics Chem.*, 43, 446 (1980).
35. L.B. Rothman, *J. Electro. Chem. Soc., Solid State Sci. Technol.*, 127, 2219 (1980).
36. G.A. Brown in "Polymer Materials for Electronic Applications," E.D. Feit and C. Wilkins Jr., eds., ACS Symposium Series 184, American Chemical Society, Washington, D.C., 1982, p. 151.
37. G. Goldsmith, P. Geldemans, F. Bedetti, G.A. Walker, *J. Vac. Sci. Tech. A*1, 407 (1983).
38. F.L. Givens and W.J. Daughton, *J. Electrochem. Soc.: Solid State Sci. Technol.*, 126, 269 (1979).
39. D. Makino, M. Suzuki, N. Kinjo, *Proc. 9th Biennial Univ./Gov./Ind. Microelectronic Symp.*, Miss. State Univ., X-48 (May, 1981).
40. A. Saiki, K. Mukai, and S. Harada in "Polymer Materials for Electronic Applications," E.D. Feit and C. Wilkins Jr., eds., ACS Symposium Series 184, American Chemical Society, Washington, D.C., 1982, p. 123.
41. C.C. Chao and W.V. Wang in "Polyimide: Synthesis, Characterization, and Applications," Vol. 2, K.L. Mittal ed., Plenum Press, (1984) p. 783.
42. D.R. Day, D. Ridley, J. Mario, and S.D. Senturia in "Polyimide, Synthesis, Characterization, and Applications," Vol. 2, K.L. Mittal ed., Plenum Press, (1984) p. 767.
43. S.J. Rhodes in "Polyimide, Synthesis, Characterization, and Applications," Vol. 2, K.L. Mittal ed., Plenum Press, (1984) p. 795.
44. G. Samuelson and S. Lytle in "Polyimide: Synthesis, Characterization, and Applications," Vol. 2, K.L. Mittal ed., Plenum Press, (1984) p. 751.
45. A.M. Wilson in "Polyimide: Synthesis, Characterization, and Applications," Vol. 2, K.L. Mittal ed., Plenum Press, (1984) p. 715.

46. M.A. Zuegel in "Methods and Materials in Microelectronic Technology," J. Bargon ed., Plenum Press, New York (1984) p. 269.
47. Y.K. Lee and J.D. Craig, in "Polymer Materials for Electronic Applications," American Chemical Society Symposium Series V. 184, American Chemical Society, Washington, D.C. (1982) p. 107.
48. A.M. Wilson, D. Laks, and S.M. Davis in "Polymer Materials for Electronic Applications," American Chemical Society Symposium Series V. 184, American Chemical Society, Washington, D.C. (1982) p. 140.
49. S.D. Senturia, R.A. Miller, D.D. Denton, F.W. Smith, III, and H.J. Neuhaus in "Recent Advances in Polyimide Science and Technology," W.D. Weber and M.R. Gupta eds., Society of Plastics Engineers, Inc., (1987) p. 351.
50. W.M. Edwards and I.M. Robinson, U.S. Pat. 2,710,853 (to DuPont) (1955).
51. W.M. Edwards and I.M. Robinson, U.S. Pat. 3,179,634 (to DuPont) (1965).
52. C.E. Scroog, J. Polym. Sci.: Macromol. Rev., 11, 161 (1976).
53. J.I. Jones, F.W. Ochynski, and F.A. Rackley, Chem. Ind., 1686 (1962).
54. C.E. Scroog, A.L. Endry, S.V. Abramo, C.E. Berr, W.M. Edwards, and K.L. Oliver, J. Polym. Sci., A-3, 1373 (1965).
55. C.S. Marvel, J. Macromol. Sci.: Rev., 13, 219 (1975).
56. G.M. Bower and L.W. Frost, J. Polym. Sci., A-1, 3135 (1963).
57. L.W. Frost and G.M. Bower, U.S. Pat. 3,179,635 (1965).
58. L.W. Frost and I. Kesse, J. Appl. Polym. Sci., 8, 1039 (1969).
59. E. Sacher and J.R. Susko, J. Appl. Polym. Sci., 26, 679 (1981).
60. E. Sacher and J.R. Susko, J. Appl. Polym. Sci., 23, 2355 (1979).

61. A.M. Wilson in "Polyimides: Synthesis, Characterization and Applications," K.L. Mittal, ed., Vol. II, Plenum Press, 1984, p. 715.
62. J.A. Kreuz, A.L. Erdrey, F.P. Gay, C.E. Sroog, J. Polym. Sci., A-1, 2607 (1966).
63. C.E. Sroog, J. Polym. Sci., C, 16, 1191 (1967).
64. R.A. Dine-Hart and W.W. Wright, Die Makromolekulare Chemie, 143, 189 (1971).
65. P.D. Frayer in "Polyimide: Synthesis, Characterization and Applications," K.L. Mittal, ed., Vol. I, Plenum Press, 1984, p. 273.
66. A.N. Krasovski, N.P. Antonov, and M.M. Koton, Polym. Sci. U.S.S.R., 21, 1038 (1980).
67. H. Ishida, S.T. Wellinghoff, E. Bear, and J.L. Koenig, Macromolecules, 13, 826 (1980).
68. S.I. Numata, K. Fujisaki, and N. Kinjo in "Polyimides: Synthesis, Characterization and Applications," Vol. I, K.L. Mittal, ed., Plenum Press, 1984, p. 259.
69. L.A. Laisus, M.I. Bessonov, and F.S. Florinskii, Polym. Sci. U.S.S.R., 13, 2257 (1971).
70. R. Ginsburg and J.R. Susko in "Polyimides: Synthesis Characterization and Applications," Vol. I, K.L. Mittal, ed., Plenum Press, 1984, p. 237.
71. A.K. St. Clair and T.L. St. Clair, Polym. Prepr., 27(2), 406 (1986).
72. A.I. Baise, J. Polym. Sci., 32, 4043 (1986).
73. P.R. Young and A.C. Chang, SAMPE J., 22, 70 (1986).
74. S.V. Lavrov, I.Y. Kardash, and A.N. Pravednikov, Polym. Sci. U.S.S.R., 19, 2374 (1977).
75. R.A. Dine-Hart and W.W. Wright, J. Appl. Polym. Sci., 11, 690 (1967).
76. A.J. Gregoritsch, Proc. IEEE Reliability Physics Sym., 14, 228 (1976).
77. S.V. Vinogradova, Y.S. Vygodskii, and V.V. Korshak, Polym. Sci. U.S.S.R., 12, 2254 (1970).

78. T. Takekoshi, J.E. Kochanowski, J.S. Manello, and M.J. Webber, *J. Polym. Sci.: Polym. Symp.*, 74, 93 (1986).
79. R.A. Meyers, *J. Polymer Science*, A-1, 2757 (1969).
80. P. Carleton, W. Farrissey, Jr. and J.S. Rose, *J. Appl. Polym. Sci.*, 16, 2983 (1972).
81. L. Alberino, W. Farrissey, Jr. and J.S. Rose, *U.S. Pat* 3,708,458 (to Upjohn Co.) (1973).
82. G.W. Miller, *U.S. Pat.* 3,662,525, (to Mobay Chemical Co.) (1971).
83. W. Farrissey and P. Andrews, *U.S. Pat.* 3,787,367, (to Upjohn Co.) (1974).
84. N. Ghatge and D. Dandge, *Angew. Makromolekular Chem.*, 56, 163, (1976).
85. W. Alvino and L. Edelman, *J. Appl. Polym. Sci.*, 22, 1983 (1978).
86. B.K. Onder, *U.S. Pat.* 4,001,186, (to Upjohn Co.) (1977).
87. B.K. Onder, *U.S. Pat.* 4,021,412, (to Upjohn Co.) (1977).
88. W. Alvino and L. Edelman, *J. Appl. Sci.*, 19, 2961 (1975).
89. N. Ghatge and U. Mulik, *J. Polym. Sci., Poly. Chem. Ed.*, 18, 1905 (1980).
90. C.D. Hurd and A.G. Prapar, *J. Org. Chem.*, 24, 388 (1959).
91. F.J. Williams and P.E. Donahue, *J. Org. Chem.*, 42, 3414 (1977).
92. D.M. White, T. Takehoshi, and R.N. Schluenz, *J. Polym. Sci.: Poly. Chem. Ed.*, 19, 1635 (1981).
93. F.W. Harris and S.O. Norris, *J. Polym. Sci.: Polym. Chem. Ed.*, 11, 2143 (1973).
94. J.K. Stille, F.W. Harris, H. Mukamol, R.O. Rakutis, C.L. Schilling, G.K. Noren, and J.A. Reeds, *Adv. Chem. Ser.* 91, 628 (1969).
95. J.I. Jones, *J. Polym. Sci., C*, 22, 773 (1969).

96. A. Saiki, S. Hirada, T. Okubo, K. Mukai, T. Kimura, J. Electrochem. Soc.: Solid State Sci. Technol., 124, 1619 (1977).
97. A. Saiki, K. Mukai, S. Harada, Y. Miyadera, Preprints ACS Org. Coat. Plastic Chem., 43, 459 (1980).
98. Y. Harada, F. Matsumoto, T. Nakakado, J. Electrochem. Soc.: Solid State Sci. Technol., 130, 1, 133 (1983).
99. R.A. Dine-Hart, D.B.V. Parker, W.W. Wright, Br. Polym. J., 3, 222 (1971).
100. Y.K. Lee, J.D. Craig, and W.E. Pye, 1981 Proc. 4th Annual University/Government/Industry Microelectronics Symposium, Miss. State Univ., X-30 (May, 1981).
101. C.E. Diener and J.R. Susko in "Polyimides: Synthesis, Characterization, and Application," K.L. Mittal, ed., Vol. 1, Plenum Press, 1984, p. 353.
102. R.K. Agnihotri, Poly. Eng. Sci., 17, 366 (1977).
103. T.O. Herndon and R.L. Burke, Kodak Microelectronic Seminar, New Orleans, LA, 146 (Oct. 1979).
104. T. Nishida, A. Saiki, Y. Homma, K. Mukai, IEDA Tech. Digest, 552 (1982).
105. H.L. Leary, Jr. and D.S. Campbell in "Photon, Electron, and Ion Probes of Polymer Structure and Properties," D.W. Dwight, T.J. Fabish, and H.R. Thomas, eds., ACS Symp. Series, 162, American Chemical Society, Washington D.C., 1981.
106. F. Emmi, F. Egitto, R. Horwath, V. Vukanovic, Proc. Electrochem. Soc., 85, 193 (1985).
107. D.L. Goff, U.S. Pat. 4,416,973 (to DuPont) (1983).
108. O. Rohde, M. Riediker, A. Schaffner, and J. Bateman in "Advances in Resist Technology and Processing II," SPIE Vol. 539 (1985) p. 175.
109. R. Rubner, U.S. Pat. 4,040,831 (to Siemens) (1977).
110. J. Omote, K. Koseki, and T. Yamaoka, Polym. Eng. Sci., 29, 945 (1989).
111. G.C. Davis, Org. Coat. Appl. Polym. Sci., 48, 70 (1983).

112. W.D. Kray, U.S. Pat. 4,578,328 (to General Electric Co.) (1986).
113. S. Kubota, T. Moriwaki, T. Ando and A. Fukami, J. Appl. Polym. Sci., 33, 1763 (1987).
114. S. Kubota, T. Moriwaki, T. Ando, and A. Fukami, J. Macromol. Sci. Chem., A24, 1407 (1987).
115. S. Kubota, Y. Yamawaki, T. Moriwaki, and S. Eto, Polym. Eng. Sci., 29, 950 (1989).
116. P.M. Rentzepis and G.E. Busch, Mol. Photochem., 4, 353 (1972).
117. J.F. Rabek, "Mechanisms of Photophysical Processes and Photochemical Reactions in Polymers; Theory and Applications," John Wiley and Sons, New York (1987) p. 275.
118. A. Beckett and G. Porter, Trans. Faraday Soc., 59, 2038 (1963).
119. D. Braun and K.H. Becker, Angew. Makromol. Chem., 6, 186 (1969).
120. A.V. Buettner and J. Dedinas, J. Phys. Chem., 75, 187 (1971).
121. J. Dedinas, J. Phys. Chem., 75, 181 (1971).
122. A. Merlin, D.J. Loughnot, and J.P. Fouassier, Polym. Bull., 2, 847 (1980).
123. J.N. Pitts, Jr., R.L. Letsinger, R.P. Taylor, J.M. Patterson, G. Rectenwald, and R.B. Martin, J. Amer. Chem. Soc., 81, 1068 (1959).
124. G. Porter, and P. Suppan, Proc. Chem. Soc., 1964, 191.
125. G. Porter and F. Wilkinson, Trans. Faraday Soc., 57, 1686 (1961).
126. J. Saltiel, H.C. Curtis, and B. Jones, Mol. Photochem., 2, 331 (1970).
127. D.I. Schuster, and T.M. Weil, J. Amer. Chem. Soc., 94, 4091 (1973).
128. M.R. Topp, Chem. Phys. Lett., 32, 144 (1975).

129. C. Walling, and M.J. Gibian, J. Amer. Chem. Soc., 87, 3361 (1965).
130. J.C. Scaiano, J.C. Netto-Ferreira, A.F. Becknell, and R.D. Small, Polym. Eng. Sci., 29, 942 (1989).
131. H.R. Lee and Y. Lee, Journal of Polymer Science: Part A: Polymer Chemistry, 27, 1481 (1989).
132. J.V. Crivello, J.L. Lee, and D.A. Conlon, J. Polym. Sci.; Part A: Polym. Chem., 25, 3293 (1987).
133. D.N. Khanna and W.H. Mueller, Polym. Eng. Sci., 29, 954 (1989).
134. D.N. Khanna and W.H. Mueller, Proceedings of the 3rd International SAMPE Electronic Conference, 905 (1989).
135. F.F. Holob and J.T. Kobaki, German Pat. 1,922,339 (1970).
136. D.D. Perrin, W.L.F. Armarego, and D.R. Perrin, "Purification of Laboratory Chemicals," Pergamon Press, N.Y., 1980.
137. P.M. Hergenrother, N.T. Wakelyn and S.J. Havens, J. Polym. Sci.; Part A: Polym. Chem., 25, 1093 (1987).
138. P.M. Hergenrother and S.J. Havens, J. Polym. Sci.; Part A: Polym. Chem., 27, 1161 (1989).
139. J.E. McGrath, P.M. Sormani, C.S. Elsbernd, and S. Kilic, Makromol. Chem., Macromol. Symp. 1986, 6, 67-80; I. Yilgor and J.E. McGrath, Adv. Polym. Sci. 86, 1-88 (1988).
140. J.D. Summers, C.A. Arnold, R.H. Bott, L.T. Taylor, J.C. Ward, and J.E. McGrath, Polym. Prepr. 27(2), 403 (1986).
141. J.D. Summers, Ph.D. Thesis, VPI & SU, June 1988.
142. J.D. Summers, C.A. Arnold, R.H. Bott, L.T. Taylor, J.C. Ward and J.E. McGrath, SAMPE Symp. 32, 613 (1987).
143. J.D. Summers and J.E. McGrath, Polym. Prepr. 28(2), 230 (1987).
144. B.C. Johnson, I. Yilgor, and J.E. McGrath, Polym. Prepr., 25(2), 54 (1984); B.C. Johnson, Ph.D. Thesis, VPI & SU, 1984.

145. A.W. Levine, Division of Organic Coatings and Plastic Chemistry: Preprints, 185th National ACS meeting, 1983, pp. 287-291.
146. J.H. Lai, in "Polymers for Electronic Applications," J.H. Lai ed., CRC Press, Boca Raton, Florida (1989) p. 11.
147. K. Harada, T. Tamamura, and O. Kogure, J. Electrochem. Soc., 129, 2576 (1982).
148. C.A. Arnold, Y.P. Chen, M.E. Rodgers, J.D. Graybeal, and J.E. McGrath, 3rd International SAMPE Electronics Conference (1989) p. 198.
149. C.A. Arnold, J.D. Summers, Y.P. Chen, R.H. Bott, D. Chen and J.E. McGrath, Polymer (London), 30, 986 (1989).
150. M.J. Owen and J.C. Kendrick, Macromolecules, 3, 458 (1970).
151. M. Matzner, A. Noshay, L.M. Robeson, C.N. Merriam, R. Barclay, and J.E. McGrath, Applied Polym. Symp., 22, 143 (1973).
152. C.S.P. Sung, C.B. Hu, and E.W. Merrill, Polym. Prepr., 19, 20 (1978).
153. J.S. Riffle, Ph.D. Dissertation, VPI & SU, 1980.
154. R.L. Schmitt, J.A. Gardella, J.H. Magill, L. Salvati, and R.L. Chin, Macromolecules, 18(12), 2675 (1985).
155. W.S. Slempp, B. Santos-Mason, G.F. Sykes, and W.G. Witte Jr., AIAA Paper 85-0421, 23rd Aerospace Science Meeting, 1985.
156. L.J. Legen, J.T. Visentine, J.F. Kuminecz, and I.K. Spiker, AIAA Paper 85-0415, 23rd Aerospace Science Meeting, 1985.
157. R.H. Hansen, J.V. Pascale, J. Benedictis, and P.M. Rentzepis, J. Polym. Sci.: A-1, 2206 (1965).
158. L.B. Rothman, J. Electro. Chem. Soc., Solid State Sci. Technol., 127, 2219 (1980).
159. D.J. Belton and A. Joshi in "Molecular Characterization of Composite of Interfaces," H. Hatsuo and G. Kumar, eds., Plenum Press, New York, 1985, p. 187.
160. H.G. Linde, J. Polym. Sci.: Polym. Chem. Ed., 22, 1031 (1982).

161. A. Saiki and S. Hirada, J. Electrochem. Soc.: Solid State Sci. Technol., 129, 2278 (1982).
162. J.A. Deleo and M.R. Gupta, Proc. SPE Second Intl. Conf. on Polyimides, Ellenville, NY, 738 (Oct., 1985).
163. G.C. Davis, B.A. Heath, G. Gildenblat in "Polyimides: Synthesis, Characterization, and Applications," K.L. Mittel ed., Vol. II, Plenum Press, 1984, p. 847.
164. B. Chowdhury in "Polyimide Synthesis, Characterization, and Applications," K.L. Mittel, ed., Vol. I, Plenum Press, 1984, p. 401.
165. G.C. Davis and C.L. Fasoldt, Proc. SPE Second Intl. Conf. on Polyimides, Ellenville, NY, 153 (Oct., 1985).
166. A. Berger in "Polyimides: Synthesis Characterization and Applications," K.L. Mittel, ed., Vol. I, Plenum Press, 1984, p. 67.
167. "Polyimides: Materials, Chemistry and Characterization." C. Feger, M.M. Khojasteh and J.E. McGrath, Eds., Elseiver Publishing Co., (1989).

**The vita has been removed from
the scanned document**